
[All ETDs from UAB](#)

[UAB Theses & Dissertations](#)

2017

Connectivity Of The Striatal Resting-State Networks In Autism Spectrum Disorder

Thomas Patrick DeRamus
University of Alabama at Birmingham

Follow this and additional works at: <https://digitalcommons.library.uab.edu/etd-collection>



Part of the [Arts and Humanities Commons](#)

Recommended Citation

DeRamus, Thomas Patrick, "Connectivity Of The Striatal Resting-State Networks In Autism Spectrum Disorder" (2017). *All ETDs from UAB*. 1514.
<https://digitalcommons.library.uab.edu/etd-collection/1514>

This content has been accepted for inclusion by an authorized administrator of the UAB Digital Commons, and is provided as a free open access item. All inquiries regarding this item or the UAB Digital Commons should be directed to the [UAB Libraries Office of Scholarly Communication](#).

CONNECTIVITY OF THE STRIATAL RESTING-STATE NETWORKS IN AUTISM
SPECTRUM DISORDER

by

THOMAS P. DERAMUS

RAJESH K. KANA, CHAIR
MARK BOLDING
EDWIN W. COOK III
DAVID C. KNIGHT
SARAH O'KELLEY

A DISSERTATION

Submitted to the graduate faculty of The University of Alabama at Birmingham,
in partial fulfillment of the requirements for the degree of
Doctor of Philosophy

BIRMINGHAM, ALABAMA

2017

CONNECTIVITY OF THE STRIATAL RESTING-STATE NETWORKS IN AUTISM SPECTRUM DISORDER

THOMAS PATRICK DERAMUS

BEHAVIORAL NEUROSCIENCE

ABSTRACT

Social deficits and repetitive behaviors are core features of autism. Structural and functional alterations in the striatum, brain regions highly involved in movement planning, regulation, and motivation, may underlie these core features. However, few studies have examined functional connectivity (FC) of the striatum in autism; and fewer have examined anatomical connectivity despite hypotheses of structural alterations influencing FC in autism spectrum disorders (ASDs). To address these gaps, the current study examined FC of resting-state brain networks in the striatum in 19 typically developing and 19 children with autism (ages 7-17 years) from the Autism Brain Imaging Database Exchange II. The approach is unique in that it compares the traditional group analysis to a behavior-centric focus on repetitive behaviors and social motivation. These analyses were expanded upon using diffusion weighted imaging (DWI) measures of connectivity to examine the degree to which anatomical connectivity correlated with FC in the brain.

ASD participants displayed increased striatal-cortical FC in sensorimotor and default mode networks, but also striatal-cortical FC reductions in frontoparietal, dorsal attention, and default mode networks. Measures of social motivation were found to correlate with striatal-cortical FC in dorsal attention networks, while measures of stereotyped and compulsive behaviors were found to correlate with FC in sensorimotor and frontoparietal striatal-cortical networks respectively. FC between striatal and cortical regions typ-

ically associated with reward processing did not correlate with social motivation scores, in contrast to theories proposing dysfunction within these regions in ASD.

Very few anatomical connections were correlated with FC, and those that did were limited to default mode or frontoparietal networks that were not related to the initial TD vs ASD contrast or the behavior analysis. More data is needed to assess the influence of structural connectivity on functional connectivity given the constraints of the model used. The findings of this study seem to suggest that while there may be alterations in the striatum in ASD, those differences may be pronounced in brain regions associated with attention and cognitive control. Future work using behavior-and-anatomy-centric analyses in ASD may provide more insights into useful information processing models in a disorder where behavior is highly variable.

Keywords: autism; striatum; diffusion; functional connectivity; multimodal neuroimaging

ACKNOWLEDGMENTS

I would like to thank my mentor, Dr. Rajesh Kana, for his support for the last 6 years. Dr. Kana's mentoring and approach to science challenged me to constantly question methods and never blindly accept results, making me the scientist that I am today. Drs. Michael Friedlander, Laura and Mark Klinger, and Read Montague have my thanks for sparking my interests in neuroimaging. My time in Dr. Farah Lubin's lab taught me what it was like to work in neuroscience, how much I didn't know, and seeded my desire to learn more. Dr. Franklin Amthor has my sincerest thanks for taking a chance on accepting a Birmingham local with insatiable curiosity into the UAB Behavioral Neuroscience program, without which I would not have reached this point. I would also like to acknowledge Dr. David Clark for his trust and tutelage in techniques that I would only later realize how much I needed to understand.

I am indebted to my committee members, Dr. Sarah O'Kelley, Dr. Edwin Cook III, Dr. David Knight, and Dr. Mark Bolding for their valuable input and direction. I appreciate the valuable career, scientific, and personal advice I have received throughout my graduate career from Dr. Knight and Dr. Bolding. I am especially indebted to Dr. Deborah Kerr for her continued personal and professional support as I move forward in my academic career. Much of my goals would not be accomplished without her generous coaching and aid.

The UAB Roadmap Scholars (RMS) Program has my deepest thanks for their professional and financial support. I hope that someday the need for increased

representation of minorities and individuals with disabilities in academia is no longer necessary. I would also like to thank the Multimodal Neuroimaging Training Program (MNTP) at Carnegie Mellon University and University of Pittsburgh for an experience I will always cherish. Special thanks are due to Dr. Fang-Cheng Yeh, Thomas Kraynak, Cristina Roman, Dr. Rogers Silva, and Melissa Thye for their roles in teaching me to understand the techniques used for this project, as well as their continued friendships.

Special thank you are due to my former and current lab mates, Dr. Lauren Libero and Jose Omar Maximo for their friendship, feedback, and support throughout my research. Additional thanks are due to Tana Birky, Dr. Wesley Burge, Kevin Chang, Hrishikesh “Rishi” Deshpande, Terin Dupre, Dr. Joseph Griffis, Dr. Fred Guaraná Oliveria Souza, Nathaniel Harnett, Brandon Huffstetler, Dr. LaRita Jones, Jacob Knight, Samantha Lesniak, Dr. Angela Nietz, Delores Stacks, and Dr. Muriah Wheelock for their friendship during my graduate career.

I would also like to acknowledge initiatives such as Open-Science-Framework (OSF) and open-access learning platforms that promote well-informed, transparent research in the field. This project would not have been possible without the open-source Autism Brain Imaging Database Exchange (ABIDE), the institutions contributing to ABIDE, and the participants dedicating their valuable time to provide the data for ABIDE.

Finally, I would like to acknowledge my wife, Dr. Marci DeRamus, who has given me the strength and support needed to achieve my Ph.D., my daughter Ruby for her cheerful disposition, and my parents and in-laws for all their valuable help and support throughout this time. I truly could not have done it without all of you.

TABLE OF CONTENTS

	Page
ABSTRACT.....	ii
ACKNOWLEDGMENTS	iv
LIST OF TABLES	viii
LIST OF FIGURES	ix
LIST OF ABBREVIATIONS.....	x
OBJECTIVES.....	1
Aim Number 1	2
Aim Number 2	3
INTRODUCTION	4
The role of behavior and striatal connections in the brain	4
The Striatum and Connectivity in Autism	9
Novelty And Innovation	13
METHODS	15
Participant Data.....	15
Participant Data Exclusion Criteria	16
MRI Data Quality Assurance.....	17
Final Participant Count and Group Comparisons	19
Generation of Group Brain Template	20
Generation of ROIs for FC Analyses.....	24
Aim Number 1	26
MRI data collection and analysis	26
Data Preprocessing.....	27
Functional Connectivity Analysis.....	28
Potential Problems and Alternative Strategies.....	29
fMRI	29
Analytical	32
Aim Number 2	33
Functional Connectivity and Autism Symptoms	33

Restricted Repetitive Behavior Scale-Revised (RBS-R).....	34
Social Responsiveness Scale (SRS) Version 1.....	35
Functional Connectivity/Diffusion Analysis	36
DWI Processing and Extraction	36
Functional Connectivity/Anisotropy Analysis	37
Potential Problems and Alternative Strategies.....	39
Analytical	39
DWI.....	40
Mitigation of false-positives.....	41
Computational	41
RESULTS	44
Aim Number 1	44
Aim Number 2	49
Behavioral Correlates of FC	49
Anatomical Correlates of FC	54
Generalized Fractional Anisotropy	57
Normalized Quantitative Anisotropy	58
Assessments of Age and FSIQ.....	58
DISCUSSION.....	60
Aim Number 1	61
Aim Number 2	64
Correlations of FC with Behavioral Measures.....	64
Correlations with FC and Anisotropy Measures.....	67
FC with GFA.....	68
FC with NQA.....	69
Strengths, Limitations, and Future Directions	71
REFERENCES	78
APPENDICES	
Appendix A: tSNR by ROI and Correlations with Age, FSIQ, and QC metrics .	120
Appendix B: UAB IRB Exemption Form.....	125

LIST OF TABLES

<i>Tables</i>	<i>Page</i>
1 Tests for group differences in demographic and behavioral measures from sample	22
2 Tests for group differences in MRI data quality assurance pipelines	23
3 Regions of interest from the Choi/Yeo striatal parcellation yielding significant group differences in functional connectivity	48
4 Significant correlations between FC in Choi/Yeo networks with behaviors of interest	52
5 Significant correlations between FC of Choi/Yeo regions and generalized and quantitative anisotropy	56

LIST OF FIGURES

<i>Figure</i>	<i>Page</i>
1 Yeo et al. 2011 and Choi et al. 2012’s parcellation of the striatum and cortex coded into 7 networks: Visual, Somatosensory, Dorsal attention, Ventral attention, Limbic, Frontoparietal, and Default mode.....	6
2 Verstynen et al. 2012 (Figure. 1): Deterministic cortical-striatal tractography ending in the putamen seeded from cortical ROIs associated with specific functions from a single participant in Verstynen et al. 2012.	8
3 Flowchart describing the participant selection criteria	16
4 Participants in ABIDE Template by database and site. Volume and Surface renders of template constructed from ABIDE II T1s which passed quality assurance	20
5 The 107-ROI parcellation of the Yeo et al. 2011 and Choi et al. 2012 atlases in MNI normalized diffusion space, and example fiber-track streamlines based on QSDR reconstructed diffusion data	36
6 Connections with statistically significant group differences across networks.....	47
7 Connections with statistically significant correlations with RBS-R and SRS subscales	53
8 Regions in which FC is significantly correlated with generalized fractional or normalized quantitative anisotropy	55
9 Adapted figure from Figure 2 of DiMartino et al. 2017	75

LIST OF ABBREVIATIONS

ABIDE	Autism Brain Imaging Database Exchange
ACC	anterior cingulate cortex
ADC	apparent diffusivity coefficient
ADHD	attention deficit hyperactivity disorder
AFNI	Analysis of Functional NeuroImages
AMYG	amygdala
ANCOVA	Analysis of Covariance
ANTs	Advanced Normalization Tools
ASD	autism spectrum disorder
BG	basal ganglia
BNI	Barrow Neurological Institute
BOLD	blood oxygen level dependent
CI95	95% confidence interval
CNS	central nervous system
CSF	cerebrospinal fluid
DAN	dorsal attention network
DMN	default mode network
DS	dorsal striatum

DSM-IV	Diagnostic and Statistical Manual of Mental Disorders IV
DTI	diffusion tensor imaging
DWI	diffusion weighted imaging
EMC	Erasmus University Medical Center
EPI	echo planar image
ETH	Eidgenössische Technische Hochschule Zürich
FA	fractional anisotropy
FAST	FMRIB's Automated Segmentation Tool
FC	functional connectivity
FCP	1000 Functional Connectomes Project
FD	framewise displacement
FDR	false discovery rate
FG	fusiform gyrus
fMRI	functional magnetic resonance imaging
FOV	field of view
FPN	frontoparietal network
FSIQ	full-scale intelligence quotient
FSL	FMRIB Software Library
FSPGR	fast spoiled gradient echo
FWHM	full-width-half-maximum
GABA	gamma-aminobutyric acid
GFA	generalized fractional anisotropy
GQI	Generalized Q-Sampling Imaging

GU	Georgetown University
HIPAA	Health Insurance Portability and Accountability Act
ICA	independent component analysis
IFG	inferior frontal gyrus
INDI	International Neuroimaging Data-sharing Initiative
IP	Institut Pasteur
IPL	inferior parietal lobule
IRB	Institutional Review Board
IU	Indiana University
KKI	Kennedy Krieger Institute
KUL	Katholieke Universiteit Leuven
LMBC	limbic
LOC	lateral occipital cortex
MaxMun	Ludwig Maximilians University Munich
MDD	Major depressive disorder
MFG	middle frontal gyrus
MNI	Montreal Neurological Institute
mPFC	medial prefrontal cortex
MRI	magnetic resonance imaging
NAcc	nucleus accumbens
NQA	normalized quantitative anisotropy
NYU	New York University
OCD	obsessive compulsive disorder

ODF	orientation distribution function
OFC	orbital frontal cortex
OHSU	Oregon Health and Science University
ONRC	Olin Neuropsychiatry Research Center
PCC	posterior cingulate cortex
PDD-NOS	pervasive developmental disorder not otherwise specified
QA	quantitative anisotropy
QAP	Quality Assurance Protocol
QC	quality control
QSDR	Q-Space Diffeomorphic Reconstruction
rbs	Rank-Biserial Correlation Coefficient
RBS-R	Repetitive Behavior Scale-Revised
RMSD	root-mean-square deviation
ROI	region of interest
rsfMRI	resting-state functional magnetic resonance imaging
SAMN	somatomotor network
SDSU	San Diego State University
SEM	structural equation modeling
SFG	superior frontal gyrus
SMA	supplementary motor area
SN	substantia nigra
SNR	signal-to-noise ratio
SPM	Statistical Parametric Mapping

SRS	Social Responsiveness Scale
SyN	Symmetric Diffeomorphic Image Registration with Cross-Correlation
TCD	Trinity College Dublin
TD	typically developing
tDOF	temporal degrees of freedom
TE	echo time
TICV	total intracranial volume
ToM	theory-of-mind
TR	relaxation time
tSNR	temporal signal-to-noise ratio
UCD	University of California Davis
UCLA	University of California Los Angeles
UM	University of Michigan
UPSM	University of Pittsburgh School of Medicine
USM	Utah School of Medicine
VAN	ventral attention network
VIS	visual
vmPFC	ventral-medial prefrontal cortex
VS	ventral striatum
WASI-II	Wechsler Abbreviated Scale of Intelligence® second edition

OBJECTIVES

Autism Spectrum Disorders (ASDs) are a class of neurodevelopmental disorders affecting as many as 1 in 68 children between 3-17 years of age in the United States.¹ ASDs are characterized by social communication deficits, restricted interests and repetitive behaviors.^{2,3} Analyses of functional (temporal correlations in Blood Oxygen Level Dependent [BOLD] signal between brain regions) and structural white matter connections (measured through differences in the diffusion of water in the brain quantified using diffusion anisotropy) in individuals with ASDs have led to hypotheses that deficits in social cognition and language may be due to alterations in frontal-temporal brain connectivity.⁴⁻⁶ However, many of the symptoms related to repetitive behaviors⁷⁻⁹ and poor motivation for social stimuli¹⁰⁻¹⁴ in ASD have been attributed to alterations in striatum.

Prior work^{6,15-19} on resting-state functional connectivity (FC) suggests a trend of hyperconnectivity of subcortical structures with the rest of the brain in individuals with ASDs.^{6,15-17} However, no studies to date have examined the relationship of cortical-subcortical connectivity to repetitive behaviors or social motivation. Furthermore, diffusion weighted imaging (DWI) studies of the white matter report both increases and decreases in fractional anisotropy (FA) and diffusivity of frontal, temporal, and striatal white matter in individuals with ASDs.²⁰ The absence of behavior-specific, multimodal analyses of brain regions related to two core-features of ASD warrants further

exploration, especially in the context of developing translational models of brain structure/function relationships in ASD.

To address this gap, we utilized a combination of phenotypic, diffusion, and resting-state fMRI (rsfMRI) data from high-functioning ASD and typically developing (TD) children (ages 7-17 years) from the open-source Autism Brain Imaging Data Exchange II (http://fcon_1000.projects.nitrc.org/indi/abide/abide_I.html) (ABIDE-II). In addition, this project applies a novel, connectome-based²¹⁻²³ approach to examine the connectivity of striatal networks in individuals with ASD. Our goal was to examine whether FC differences in ASD is significantly influenced by, or independent of, behavioral measures of restricted-repetitive behaviors and social motivation in cortical-striatal resting-state networks in accordance with current models of the ASD phenotype. We also assessed the contribution of two measures DWI based diffusion anisotropy (fractional and quantitative) on FC between resting-state cortical-striatal brain regions to test the hypothesis that alterations in FC in ASD are driven by underlying white matter anomalies. Prior research using multimodal imaging techniques from our group has linked alterations in FC and brain morphology to facets of the ASD phenotype,^{4,5,24-30} making our research group well-equipped to further examine striatal circuitry in ASD.

AIM #1 Compare the functional connectivity of resting-state striatal brain networks in individuals with ASD and TD controls.

- *H1*: Resting-state functional connectivity of striatal structures with their cortical targets (e.g. nucleus accumbens, caudate, putamen to frontal and temporal cortex) will be greater in individuals with ASDs compared to TD controls.

AIM #2 Examine brain-behavior relationships by analyzing correlations between functional connections of resting-state striatal brain networks in individuals with ASDs with cognitive and behavioral factors (repetitive behaviors, social motivation scores) and structure-function relationships by correlating resting-state functional connections diffusion anisotropy.

- *H2*: Repetitive Behavior Scale-Revised (RBS-R)^{31,32} scores of stereotyped and compulsive behavior will correlate positively with functional connections between striatal structures such as the caudate and putamen and frontal motor and sensorimotor regions.
- *H3*: Social motivation scores from the Social Responsiveness Scale(SRS)³³ will correlate positively with functional connections between the nucleus accumbens and frontal regions of the brain.
- *H4*: Using connectome-based analysis of diffusion MRI, we propose that measures of diffusion anisotropy (generalized fractional and quantitative) will correlate with measures of FC in cortical-striatal networks.
- *H5*: RBS-R, SRS, and Anisotropy measures may explain group differences in FC between TD and ASD participants.

INTRODUCTION

The role of behavior and striatal connections in the brain

Human and animal studies have found that goal-orientated behaviors have distinct neural sub-components that recruit cortico-striatal structures. These components are modulated by GABAergic (Gamma-Aminobutyric Acid), glutamatergic, dopaminergic, oxytocin/vasopressin, and many other neurotransmitters and neuropeptides via frontal-striatal, nigral-striatal, cortical-limbic, and frontal limbic connections across the brain.^{12,34-45} Several mechanisms have been proposed to explain the complex interactions between striatal regions during positive and negative reinforcement paradigms in both human and animal literature, but a unifying feature among the findings is the role of the ventral striatum (VS) (of which the nucleus accumbens or NAcc is the primary structure) in modulating activity across several regions of the brain. The VS is the target of a number of cortical, limbic, and thalamic regions of the brain, and projects into the amygdala (AMYG), hypothalamus, nucleus basalis, and substantia nigra (SN).⁴⁶ These projections place the VS in a unique position to receive inputs from several brain regions while simultaneously being able to directly influence cortical and limbic areas.⁴⁶ A recent meta-analysis by Liu et al. (2012) on human neuroimaging studies of reward processing suggests that there are region-specific profiles of the human brain integral to certain components of reward processing. These include: *decision making* (NAcc, caudate, putamen, thalamus, ventral-medial prefrontal cortex [vmPFC], insula, anterior cingulate

cortex [ACC], medial prefrontal cortex [mPFC], inferior parietal lobule [IPL], and posterior cingulate cortex [PCC]), *anticipation* (ACC, insula, brainstem), and *reception* (being given an appetitive stimulus; NAcc, vmPFC, and AMYG).³⁵ The meta-analysis further suggests these regions are significantly influenced by the nature of the stimulus, with the vmPFC and PCC primarily associated with pleasant stimuli, and the ACC, insula, and mPFC with unpleasant stimuli.³⁵ However, it is a topic of debate whether striatal BOLD signal is primarily driven by the salience of the stimuli being presented, sensory stimulation, motor preparation, or whether the stimulus involves receiving a reward or avoiding punishment.⁴⁷⁻⁵¹ fMRI studies of connectivity have reported thalamus and insula activity influencing activity in the NAcc, and an increase in FC between the VS and vmPFC during aversive outcomes in TD individuals.^{52,53} Similar studies using Granger causality approaches to calculate FC argue that the VS receives input from the vmPFC and hippocampus (HIP), but can directly influence activity in the vmPFC.⁵⁴ Optogenetic stimulation of dopaminergic and glutamatergic hippocampal and amygdalar projections into the NAcc have been found to both produce hedonic affect and rescue depressive and anxious symptoms in rodents.^{55,56} The results from these experiments suggest that subcortical connections may influence motivation for receiving a reward or avoiding punishment over and above the frontal cortex, although this is relatively difficult to assess in human studies.

Basal ganglia (BG) structures (i.e. caudate, putamen, globus pallidus) that comprise the dorsal striatum (DS) have a separate, but somewhat overlapping role with VS structures. While the DS plays a role in reward processing, decision making, and learning similar to the VS,⁵⁷⁻⁵⁹ it is also actively involved in motor coordination and planning.

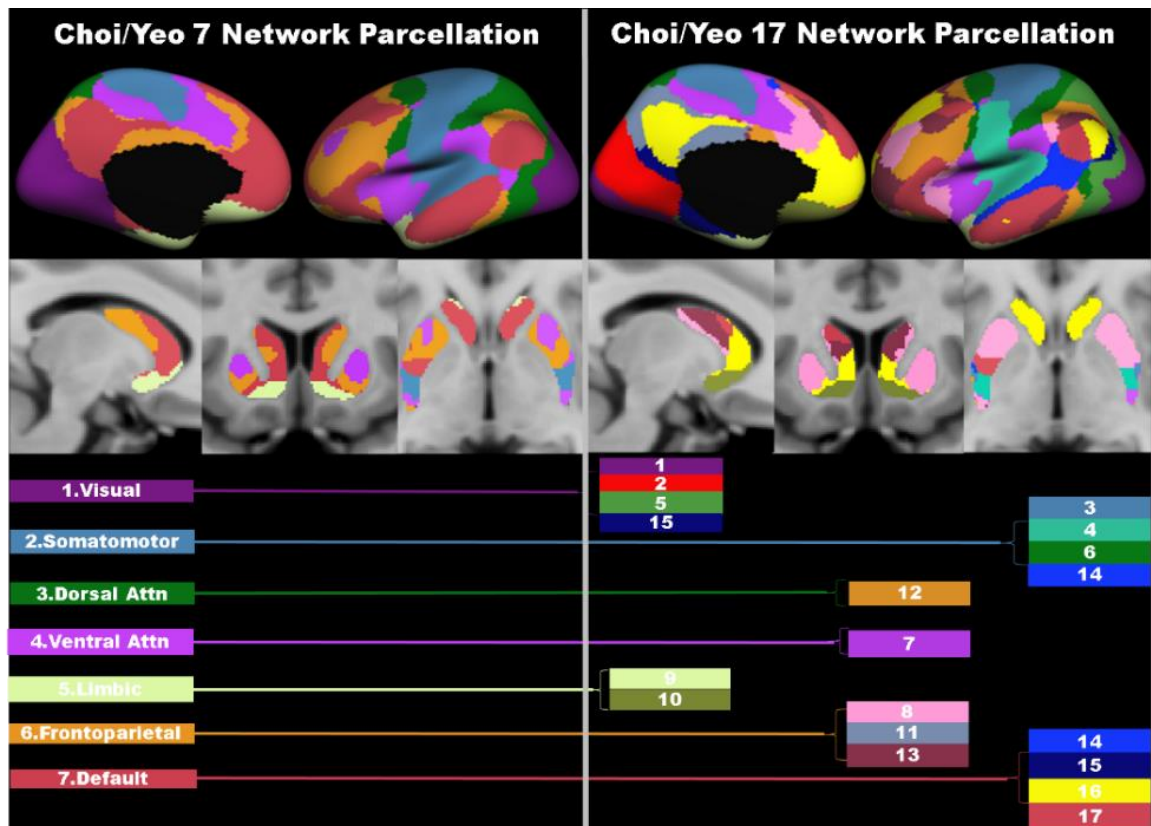


Figure 1. *Left:* Yeo et al. 2011 and Choi et al. 2012's parcellation of the striatum and cortex coded into 7 networks: Visual (Purple), Somatosensory (Blue), Dorsal attention (Green), Ventral attention (magenta), Limbic (Cream), Frontoparietal (Orange), and Default mode (Red). *Right:* 17 network parcellation from the Yeo et al. 2011 and Choi et al. 2012 atlases in which each network is divided into sub-networks (with some overlap between network types).

There is also evidence that the DS is heavily involved in the integration of sensory input to guide motor behavior and motor responses to stimuli through reciprocal connections with the thalamus and cortex.⁶⁰⁻⁶² The structure and common pathways of the BG relative to the striatum and cortex have been studied extensively in humans and primates,⁶³ with damage, lesions, and alterations within these areas associated with a number of movement disorders. Even in the absence of a task, structures within the striatum appear to display distinct FC with specific areas of the brain. In work by Choi et al., 2012,⁶⁴ striatal structures were grouped with resting-state cortical networks separated by function (e.g. Visual, Somatomotor, Dorsal/Ventral attention, Limbic, Frontoparietal, and Default mode) based on the highest correlation between striatal voxels with each cortical network

(See Figure 1). Some components of this parcellation have had connection profiles validated using tract-tracing in primates.^{64,65}

Despite this wealth of information, few studies have examined connections between regions encompassing the striatum using diffusion imaging techniques. One study found distinct white matter projections across VS to the vmPFC and uncus of the temporal pole⁶⁶ using a tensor-based DWI model⁶⁷ to perform tractography. A more recent study using Generalized Q-Sampling Imaging (GQI) reconstruction⁶⁸ found a number of projections between the striatum, lateral frontal cortex, and limbic structures, with the frontal projections alone numbering more than twice the amount of sensory and motor projections in the rostral aspects of the striatum.⁶⁹ Additionally, a recent study validated a known white matter tract connecting the NAcc and vmPFC,⁷⁰ referred to as the “accumbofrontal tract.”

Surprisingly however, there has been little research examining direct relationships between, BOLD-based FC and DWI-based anatomy measures. While there are experiments in the literature suggesting relatively high agreement between DWI based tractography and functionally connected resting-state brain networks,⁷¹⁻⁷⁴ this work has been limited to cortical-cortical connections. Furthermore, while there are several techniques available to integrate FC and DWI data such as Fusion ICA [<http://mialab.mrn.org/software/fit/index.html>], many of these techniques utilize tensor-based models to estimate diffusion. Compared to higher order diffusion models such as multi-tensors and orientation distribution functions (ODFs), tensors are more susceptible to partial volume effects (loss of contrast between adjacent tissues in an image)⁷⁵ and can produce artificially low fractional anisotropy (FA; the degree of anisotropy of water

diffusion in the brain) values in regions where there are multiple fibers at different orientations (as much as 60-90% of all white matter voxels according to some studies).⁷⁶ Given that subcortical-cortical projections are far more likely to have multiple fibers fanning, branching, or crossing white matter tracts, higher order ODF-based models would be far more useful to study subcortical-cortical connections such as those from the striatum to the cortex (See Figure 2 for a representative example from *Verstynen et al. 2012*). Exploring the relationship between structure and function of striatal connections in humans is important not only as a basic science question to validate known white matter architecture, but also due to the growing number of studies finding atypical striatal connections in patient populations.⁷⁷⁻⁷⁹

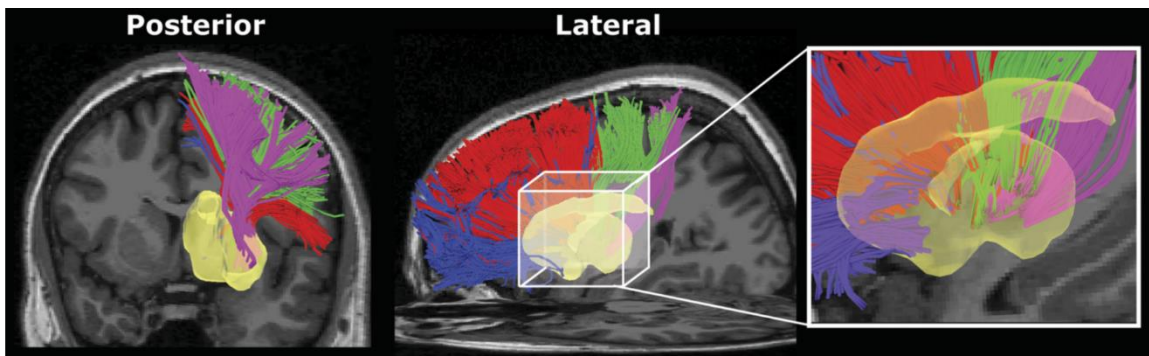


Figure 2. *Verstynen et al. 2012 (Figure. 1):* Deterministic cortical-striatal tractography ending in the putamen (yellow) seeded from cortical ROIs associated with specific functions from a single participant in Verstynen et al. 2012. These include: limbic (blue), prefrontal (red), motor (green), and somatosensory (purple) cortical ROIs.

The Striatum and Connectivity in Autism

Social deficits and repetitive behaviors that are hallmark features of ASD may be influenced by functional differences involving cortical and subcortical connections of the brain. Neuroimaging initiatives to study children and adults with ASDs have led to theoretical models proposing altered connections between brain areas in individuals with ASD. It has been suggested that alterations in FC may explain some of the social and language deficits common to ASD.^{4,5,24,26,80-83} An increasing number of studies using both traditional neuroimaging analyses and machine learning approaches to data analysis propose that alterations in brain connections may serve as promising markers for ASD.^{30,84-89}

Recently, there has been increased interest in the NAcc in ASD in the context of the social motivation hypothesis, which posits that deficits in social processing in ASD stem from a decreased motivation to seek out social stimuli.^{10,12,102,103} Some support for social motivation theory has been found through ASD-specific alterations in BOLD signal in the NAcc in response to monetary,^{13,14,104,105} object,¹⁴ and social rewards.^{13,104,105} However, the concept of social motivation may be inherently convoluted by multiple underlying mechanisms. These include: the role of learning in motivation, whether social cognition pre-empts social motivation, its domain specificity, and the observation that certain clinical populations (e.g. ADHD, major depression [MDD], anxiety) that are highly comorbid in ASD display similar deficits.¹² Alterations in striatal development and function are frequently listed as potential sources of restricted interest and repetitive behaviors in ASD,^{9,106,107} However, the few published studies have examined volumetric

MRI and tensor-based diffusion MRI measures rather than BOLD-based functional striatal-cortical connections.

Disruptions in frontal-striatal, nigral-striatal, cortical-limbic, and frontal-limbic dopaminergic and oxytocin/vasopressin pathways (all of which relate to motivation, salience, and reward) have been reported in individuals with ASD.^{108–110} Volumetric studies of regions associated with reward processing in ASD using voxel-based morphometry and post-mortem tissue studies report ASD-related volumetric alterations within the caudate,^{111–113} putamen,¹¹³ hippocampus (HIP),^{114–116} AMYG,^{113,115,116} vmPFC,^{117,118} and NAcc.¹¹³ Volumetric alterations of the caudate and putamen correlate with repetitive behaviors in ASD in some published work.¹⁰⁶ Studies using reward tasks report reductions in activity within the striatal and prefrontal regions, and those using rsfMRI report alterations in FC in ASD in these same regions.^{13,14,17,34,104,105,107,119–121} Considering these findings, the interaction of subcortical striatal structures with the cortex in ASD may provide a unifying framework for better understanding the ASD phenotype.

Unifying models or “biomarkers” are difficult to develop for individuals with autism however, largely due to the complexity and clinical heterogeneity within this population. For example, ADHD, obsessive compulsive disorder (OCD), Tics/Tourette’s syndrome, anxiety disorders, and depression are frequently comorbid with ASD.^{122–137} Subgroups within ASD and common comorbid conditions can also display overlap on clinical and screening with one another.^{130,138} In addition, many comorbidities common to ASD have been associated with alterations in BOLD signal and FC, particularly within subcortical structures, in absence of ASD.^{138–157} This confound is not novel in behavioral

and clinical studies of individuals with ASDs, but it is only recently beginning to be addressed in neuroimaging literature. Studies have linked alterations in connectivity to behavioral measures of ASD severity.¹⁵⁸ However, many of these results are from post-hoc correlations on results of TD vs ASD contrasts. This practice carries two risks: One, any mechanistic interpretations of group differences become less generalizable, as the models are not examining the relationship of the behavior to the brain, but rather how strongly it relates to results from a previous contrast in which the test itself is designed to separate the two groups. This may in turn, lead to gross oversimplifications of brain regions with multi-dimensional functions.^{138,159} Second, if not properly addressed, such practices can lead to artificially inflated effect sizes.¹⁶⁰⁻¹⁶² As such, relating fMRI-based brain function to clinical measures and behavior early in the analytical process is critical to the development of informed models of cognition in patient groups.

Perhaps the most critical factor, yet to be addressed regarding connectivity-based hypotheses of ASD, is the relationship between structural and functional connections. Just et al., (2004; 2007) originally proposed that alterations in FC are likely influenced by alterations in underlying white matter. With the exception of a single paper using a multi-modal data-driven analytical technique combining resting state, diffusion, and voxel-based morphometry,¹⁶³ the literature on the structure/function connections in ASD have either been domain specific analyses (i.e. either FC or diffusion analyses), or have implemented post-hoc correlations when significant group differences were already reported in either FA or FC.⁴ While many studies have found significant correlations between measures of FC and diffusion indices, such as FA in TD populations,^{71,72,164,165} many FC/DWI results from some studies in ASD have been task-specific. In studies

where alterations in FC are task specific, additional behavioral and/or clinical data are necessary before inferences about the relationship of FC to FA can be considered.¹⁶⁶

When such relationships are not identified, the validity of conclusions such as *brain architecture influencing FC and behavior* are significantly reduced.¹⁶⁷ Furthermore, this approach, if performed incorrectly, also carries risks of artificial inflation of the correlations between diffusion and FC.^{160–162,168–170}

Connectome analyses based on apriori-parcellations of the human cortex^{21,22} such as those implemented by the HCP and graph-theoretical connectivity approaches have the potential to simultaneously analyze FC and DWI metrics of connectivity. While this approach has been applied to both FC^{171–173} and diffusion-based^{174–176} measures of brain connectivity in isolation, studies examining these measures relative to one another using non-correlative methods¹⁷⁷ are rare, with those incorporating behavioral/clinical measures even more so. Establishing the relationships between structural and functional connections are integral not only for understanding how communication between specific regions of relation to cognition and behavior, but also how such connections can vary at individual level. Exploring the structural and functional connectivity, relative to clinical measures meant to be interpreted as part of a “spectrum” of behaviors, has been the focus of many brain imaging studies. Behavior-centric approaches should be similarly applied to clinical populations as opposed to the widely used dichotomous “patient or not” approaches which may be less sensitive to heterogeneity.

As a first step towards this goal, we propose a focused analysis on resting-state striatal networks (via the Yeo et al., 2011 and Choi et al., 2012 network parcellations) in a well-matched sample of TD and ASD children retrieved from the ABIDE-II database. This

analysis will focus on functional connections of striatal regions, believed to be specific to reward processing and restrictive, repetitive behaviors in ASD. Analyses conducted will focus on 2 main research goals: 1) the degree to which diffusion anisotropy correlates with resting-state FC between cortical-striatal brain regions; and 2) assess establish brain-behavior relationships with FC and clinical measures specific to social motivation and repetitive behaviors in ASD and TD individuals This will be the first in a set of multiple studies aimed at examining the FC/behavior relationships of the striatum in ASD.

Novelty and Innovation

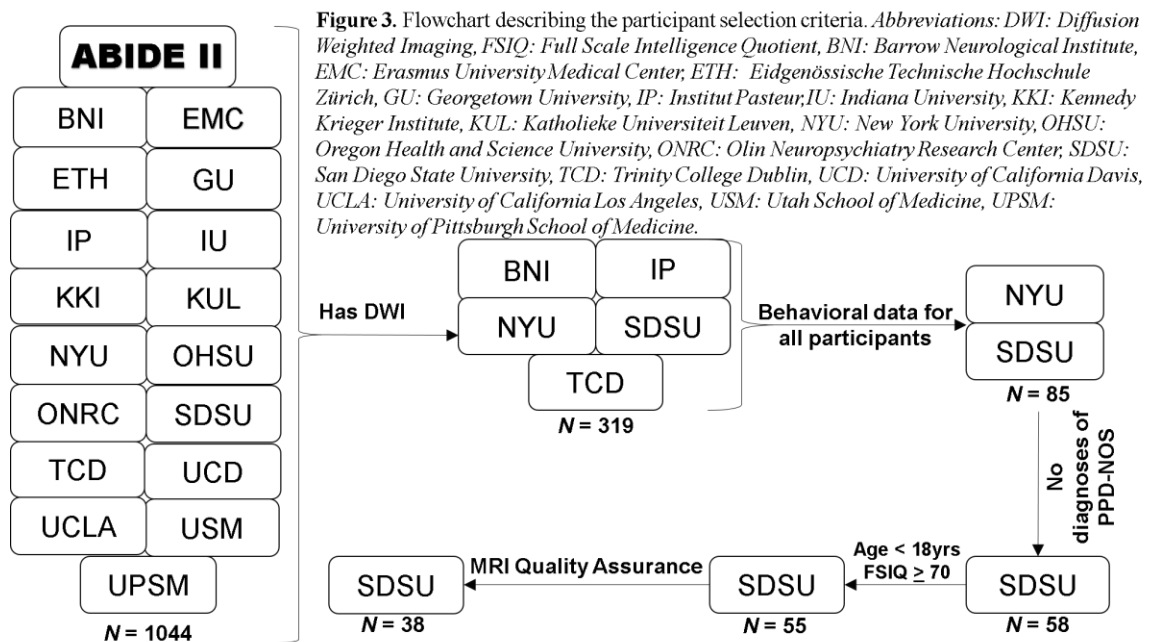
This study is novel in both its theoretical and analytical approach about studying the striatum in ASD: This proposal is the first, to our knowledge, to directly assess the contribution of striatal FC to behavioral symptoms (repetitive behaviors, social motivation) in ASD participants. In addition, it will also be the first study to relate measures of white matter connectivity to cortical-striatal, striatal-striatal, and cortical-cortical FC based on network-specific (e.g. somatomotor, reward) parcellations in participants with ASD. Relating behavior to measures of brain function is important given the breadth of connections and behaviors influenced by the exchange of information across cortical and subcortical regions. Doing so is especially important in clinical populations as group differences in fMRI measures may be better explained by these measures (e.g. motivation, individual clinical symptoms, salience). The latter is critical given the high comorbidity ASD has with other disorders that can also influence brain regions implicated as “biomarkers” for ASD.^{77,120,140,147,148,178–183} This research question is the beginning of what will be many future studies, aimed at moving the field

towards neuroimaging studies which utilize a multi-dimensional behavioral and clinical approaches to understand the neurobiology of ASD.

Finally, there have been significant advances in DWI, with orientation distribution function (ODF) modeling techniques such as GQI,⁶⁸ and Q-Space Diffeomorphic Reconstruction (QSDR),¹⁸⁴ which are increasingly able to address discrepancies in crossing and neighboring white matter tracts that share voxels compared to apparent diffusivity coefficients (ADCs) calculated by the typical tensor.¹⁸⁵ ODF based reconstruction offers the advantage of increased spatial information and orientation information at the voxel-level over and above the typical tensor, in addition to less sensitivity to artifacts that affect the typical tensor; and greater reliability compared to the traditional FA measures (unpublished data). In addition, tractography in *DSI Studio*¹⁸⁶ utilizes quantitative anisotropy (QA) for fiber tracking. Briefly summarized, QA is the amount of anisotropic spins that diffuse along a fiber orientation, and defined at the peak for each orientation of spin distribution function. QA scales with spin density and the isotropic component of the spin distribution function is discarded, whereas regular ODF does not scale with spin density and is often min-max scaled to 0-1. The net result is a considerable reduction in the generation of false fibers.¹⁸⁶ This proposal will be the first, to our knowledge, to utilize ODF/QA based tractography specific to striatal connections in ASD, adding to a growing literature of advanced diffusion analyses in ASD.

METHODS

Participant Data: The data for this proposal is obtained from the Autism Brain Imaging Data Exchange dataset 2 (ABIDE-II). ABIDE-II contains MRI images and phenotypic data from 487 individuals with ASD and 557 TD control participants (age range: 5-64 years) across 17 institutions coordinated by Dr. Adriana Di Martino and supported by two NIMH R21 grants (http://fcon_1000.projects.nitrc.org/indi/abide/abide_II.html for more details). Of the 17 imaging centers contributing to ABIDE-II, four provide diffusion data (Barrow Neurological Institute in Phoenix Arizona, New York University Langone Medical Center, San Diego State University, Trinity Center for Health Sciences at Trinity College Dublin), creating a total pool of 263 participants (105 TD, 158 ASD) with structural, resting state, and diffusion MRI data. Images from these 263 participants were filtered by participant clinical data and MRI data quality assurance protocols and the criteria described below. See Figure 3 for a summary of the participant data selection workflow.



Participant Data Inclusion/Exclusion Criteria: MRI data submitted to ABIDE-II came from participants under the age of 18 years at time of scan, report Wechsler Abbreviated Scale of Intelligence® second edition (WASI-II)^{187,188} full-scale intelligence quotients (FSIQs) greater than 70, either no reported diagnosis (for TD participants), or a diagnosis of Autism or Asperger’s syndrome, but not a diagnosis of pervasive developmental disorder not otherwise specified (PDD-NOS), and scores from the stereotype and compulsive behaviors of the RBS-R (Repetitive Behavior Scale-Revised) and social motivation from the SRS (Social Responsiveness Scale). Participants who did not meet these criteria were excluded from the analyses. Applying these exclusion criteria dropped the number of usable participant data from all sites of interest (BNI, NYU, and TCD) except SDSU, leaving a total of 55 participants (25 TD M/F: 23/2, 30 ASD M/F: 25/5, age 7.4-17.8 years [M: 13.01±3.06]) with the adequate combination of phenotypic data for the final analysis.

MRI Data Quality Assurance: Images for the analysis were selected based on a 4-step process: 1) Multiple Data types per participant: each participant with rs-fMRI data needed matching DWI data for individual-subject pairing. 2) Available phenotypic data: participants with missing age (in years), FSIQ, RBS-R, and SRS-Motivation scores were excluded from the analysis. 3) Automated quality assurance: pipelines for identifying motion, signal-to-noise, and variability between images during MRI sequences were utilized to identify outliers in the MR signal that may artificially create significant group differences or correlations with behaviors of interest. 4) Visual quality assurance: images were visually inspected by the experimenters for artifacts not identified by the automated pipeline as an additional quality check. Step 1 identified five different sites (BNI, IP, NYU, SDSU) with DWI data. However, DWI acquisition parameters differed, with NYU utilizing two 64 direction diffusion tensor imaging (DTI) sequences with isotropic (3x3x3mm) voxels with an optional field-map for image correction. However, while the NYU data has isotropic DWI data and the most phenotypic data, the NYU sample was reduced to 26 TD and 11 ASD participants based on the data exclusion criteria from the participant data step. Thus, using this sample by itself would result in underpowered analyses (based on both a small, Cohen's $f^2 = 0.02$, and medium, Cohen's $f^2 = 0.15$ effect size based on 80% statistical power at an $\alpha = 0.05$). DWI data from BNI were excluded due to skewed voxel resolutions (1.406x1.406x3mm), which are not appropriate for tractography-based analyses. The remaining centers with DWI data include TCD and SDSU. While both sites differ in diffusion weighting (TCD; $b=1000$, SDSU; $b\sim 1500$), and both have non-isotropic voxel dimensions (1.938x1.938x2mm and

1.875x1.875x2mm respectively) both datasets use a 61-direction diffusion sequence. Step 2 found that as described in the *Participant Data Exclusion Criteria* section, only SDSU collected phenotypic data (RBS-R and SRS) for all participants (TCD only collected these measures for ASD participants). As a result, only participants from SDSU were used in the analysis. For step 3, each of the 55 SDSU participants' T1, DWI, and rsfMRI images (30 ASD, 25 TD) underwent quality assessment using the Quality Assurance Protocol (QAP) developed as part of the Preprocessed Connectomes Project (PCP) of the 1000 Functional Connectomes Project (FCP) and International Neuroimaging Data-sharing Initiative (INDI) (<http://preprocessed-connectomes-project.org/quality-assessment-protocol/index.html>). Diffusion data quality was also assessed using an additional pipeline adapted from workflow developed at University of Pennsylvania Perelman School of medicine (<http://upenncmroi.wpengine.com/qascripts/>).¹⁸⁹ Quality control (QC) metrics were z-scored for all participant images across each modality (T1, echo planar images [EPI], and DWI), and those with z-values greater than 3 were flagged as univariate outliers. Participant EPI images were analyzed for motion spiking using *ArtDetect* (<http://gablab.mit.edu/index.php/software>) via the *CONN* toolbox (version 17.e).¹⁹⁰ If more than 20% of a participant's total EPI volumes were flagged by root-mean-square-deviation (RMSD) motion greater than 2mm and/or standardized global signal intensity-by-volume exceeding a z-scored threshold of 3, then the participant was excluded from the analysis. As the fourth and final step, visual QC examining data quality for artifacts not detectable by automated means (i.e. Gibbs ringing, ghosting, motion not detected by framewise displacement) were performed by the PI and tests for

group differences across QC metrics were assessed prior to the calculation of FC values (see Table 2).

Final Participant Count and Group Comparisons: Of the remaining 55 participant datasets from SDSU, one participant was excluded from the analysis due to a lack of DWI data (sub-28852), five participants were removed due to more than 20% of their total EPI volumes corrupted by motion (sub- 28862, sub- 28875, sub- 28887, sub- 28892, sub-28907), one participant (sub-28872) was removed due to an abnormally high temporal signal-to-noise-ratio (tSNR) value in their DWI data driven by a hyperintensity artifact in the participant's vmPFC, another four were removed due to DWI data acquired with parameters significantly different from the rest of the participants in the study (0.94x0.94x2mm vs 1.88x1.88x2mm), one participant was discarded due to a T1 image with dimensions that differed from the standard acquisition for the dataset (1.2x1x1mm vs 1x1x1mm), and one participant was discarded due to an aberrantly large inherent smoothness in their T1 image (sub-28888).

This left a final sample of 38 participants (19 TD M/F:17/2, 19 ASD M/F:16/3, age 8-17.8 years [M: 13.16 SD: 3.03]). For the final participant count, group differences in demographic information (Age, FSIQ), clinical measures of ASD (RBS-R subsets, SRS social motivation), and QC metrics for T1, EPI, and DWI data were assessed using either a two-tailed student's t-test (assuming unequal variance), or a Wilcoxon rank-sum test^{191,192} dependent upon the results of an Anderson-Darling test¹⁹³ for normality in MATLAB© 2016a.¹⁹⁴ The results of these analyses are described below in Tables 1, and 2 respectively.

Generation of Group Brain Template: It has been widely acknowledged that

normalization of MRI data from pediatric populations to adult brain templates and the use of adult-brain tissue priors can negatively impact the results and conclusions of MRI based analyses.^{195–200}

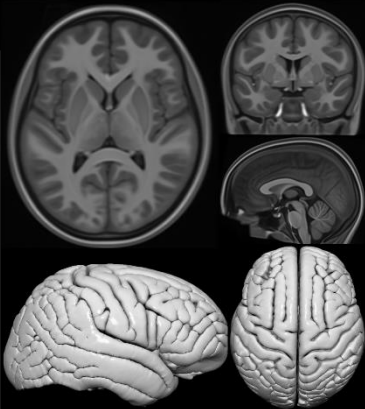
ABIDE I TD/ASD	ABIDE II TD/ASD	
<ul style="list-style-type: none"> • KKI 9/3 • MaxMun 3/0 • NYU 39/26 • ONRC 2/1 • UPSM 0/1 • SDSU 6/2 • TCD 11/3 • UCLA 23/24 • UM 10/6 • USM 0/2 • Yale 3/1 	<ul style="list-style-type: none"> • GU 31/13 • IP 2/5 • NYU 23/9 • SDSU 10/15 • TCD 13/12 • UCD 5/8 • UCLA 7/4 	
Totals: 197/135		
M/F: 178/19, 124/11		
Mean Age: 12.38±2.87/12.89±3.10		
Mean IQ: 113.55±12.62/106.71±14.44*		

Figure 4. *Left:* Participants in ABIDE Template by database and site. *Right:* Volume and Surface renders of template constructed from ABIDE I T1s which passed quality assurance. *Significantly different at $p < 0.05$

To address this concern, a custom preprocessing pipeline was generated which attempted to minimize any biases that may have been introduced through preprocessing methods informed by adult brain templates such as the standard SPM preprocessing pipeline. First, we generated a group template using Advanced Normalization Tools (ANT)s’ (<http://stnava.github.io/ANTs/>) Multivariate Template Construction workflow (<https://github.com/stnava/ANTs/blob/master/Scripts/antsMultivariateTemplateConstruction.sh>) utilizing T1 images from ABIDEI and ABIDEII databases. QAP data readouts for 2,324 individual T1 images were obtained from ABIDEI and ABIDEII databases and concatenated into a single data file. Participants were removed if their ages were greater than or equal to 18 years or their FSIQ scores were less than 70, leaving 834 participants. The remaining T1 data was then z-scored across all QC dimensions, and any participant with a z-score greater than 3 across any dimension or a “fail” mark by any one of the 3 independent raters from the ABIDE initiative were discarded, leaving approximately 621

T1s. Visual examination of the 621 remaining images was performed for artifacts not identified by automated QC (i.e. subtle motion, Gibbs ringing), and discarded if any such artifacts were identified. This left a total of 332 brains (197 TD, M/F 178/19; age 5.9-17.8 years [M: 12.37 ± 2.87], FSIQ 83-144 [M: 113.55 ± 12.62], 135 ASD, M/F 124/11; age 5.2-17.9 years [M: 12.90 ± 3.10], FSIQ 78-149 [M: 106.71 ± 14.44]) for template generation. The template and additional information regarding selection by site and group differences are described in Figure 4.

Table 1. Tests for group differences in demographic and behavioral measures from sample

Demographic Information	Mean TD	Median TD	StdDevTD	Mean ASD	Median ASD	StdDevTD	t-value	Z-value	df	ranksum	Hedges' g	r _b	Pvalue	95% Confidence Interval
Age at Scan		13.00	2.91		13.40	3.21		0.01		371.50		0.00	0.99	[-0.34,0.32]
Edinburgh Handedness Scores		100.00	51.82		100.00	69.22		0.37		382.50		0.06	0.71	[-0.37,0.27]
WASI FSIQ	105.16		11.19	101.58		14.84	0.84		33.47		0.27		0.41	[-5.09,12.25]
WASI VIQ	107.00		8.67	96.53		17.39	2.35		26.44		0.75		*0.03	[1.32,19.63]
WASI PIQ	103.32		15.23	106.68		17.34	-0.64		35.41		0.20		0.53	[-14.11,7.38]
SRS Social Motivation Raw Score		4.00	2.65		18.00	4.85		-5.26		190.00		0.87	0.00	[0.87,0.87]
RBS-R 6 Stereotyped Behaviors		0.00	0.67		2.00	3.80		-4.56		220.50		0.75	0.00	[0.58,0.89]
RBS-R 6 Compulsive Behaviors		0.00	2.71		2.00	5.45		-3.65		249.50		0.60	0.00	[0.36,0.81]

* $p < 0.05$

Table 2. Tests for group differences in MRI data quality assurance pipelines.

Quality Assurance Metric	Mean ID	Median ID	StDev ID	Mean ASD	Median ASD	StDev ASD	t-value	Z-value	df	ranksum	Hedges' g	r _b	P-value	95% Confidence Interval
Number of Valid Images	173.00	173.00	4.24	172.00	172.00	6.48	0.88	0.88	401.00	401.00	0.15	0.38	0.15	[-0.46,0.18]
Temporal DOF	48.20	48.20	1.39	47.90	47.90	2.12	0.88	0.88	401.00	401.00	0.15	0.38	0.15	[-0.46,0.18]
Max RMSD Motion	0.50	0.50	0.51	0.58	0.58	1.16	-1.14	-1.14	331.00	331.00	0.19	0.25	0.19	[-0.14,0.49]
Mean RMSD Motion	0.09	0.09	0.05	0.08	0.08	0.04	-0.55	-0.55	351.00	351.00	0.09	0.58	0.09	[-0.24,0.42]
Max Global Signal	4.05	4.05	2.64	5.20	5.20	5.30	-0.58	-0.58	350.00	350.00	0.10	0.56	0.10	[-0.23,0.42]
Mean Global Signal	0.86	0.86	0.05	0.85	0.85	0.15	-0.06	-0.06	368.00	368.00	0.01	0.95	0.01	[-0.33,0.35]
T1 Contrast to Noise Ratio	7.75	7.75	0.66	7.45	7.45	0.75	1.32	1.32	35.53	35.53	0.42	0.19	0.42	[-0.16,0.77]
T1 Signal to Noise Ratio	15.49	15.49	1.37	14.98	14.98	1.17	1.22	1.22	35.12	35.12	0.39	0.23	0.39	[-0.33,1.34]
T1 Percent Artifact Voxels	0.27	0.27	0.04	0.27	0.27	0.02	0.14	0.14	35.65	35.65	0.05	0.89	0.05	[-0.02,0.03]
T1 Entropy Focus Criterion	0.41	0.41	0.03	0.41	0.41	0.02	0.05	0.05	35.65	35.65	0.02	0.96	0.02	[-0.02,0.02]
T1 Smoothness of Voxels	3.02	3.02	0.14	3.06	3.06	0.23	-0.35	-0.35	358.00	358.00	0.06	0.73	0.06	[-0.27,0.39]
T1 Foreground to Background Energy Ratio	1241.07	1241.07	221.61	1267.43	1267.43	252.14	-0.34	-0.34	35.42	35.42	0.11	0.73	0.11	[-182.64,129.91]
T1 Cortical Contrast	0.37	0.37	0.03	0.37	0.37	0.02	0.25	0.25	34.42	34.42	0.08	0.80	0.08	[-0.01,0.02]
EPI Signal-to-noise Ratio	15.94	15.94	0.65	15.83	15.83	0.80	0.45	0.45	34.51	34.51	0.14	0.66	0.14	[-0.37,0.59]
EPI Entropy Focus Criterion	0.40	0.40	0.02	0.40	0.40	0.02	-0.66	-0.66	35.63	35.63	0.21	0.51	0.21	[-0.02,0.01]
EPI Smoothness of Voxels	2.80	2.80	0.11	2.75	2.75	0.16	0.98	0.98	32.26	32.26	0.31	0.33	0.31	[-0.05,0.14]
EPI Foreground to Background Energy Ratio	63.39	63.39	6.58	63.80	63.80	6.29	-0.26	-0.26	361.00	361.00	0.05	0.79	0.05	[-0.28,0.37]
EPI Ghost to Signal Ratio	0.01	0.01	0.00	0.01	0.01	0.00	2.06	2.06	35.52	35.52	0.66	*0.05	0.66	[0.00,0.00]
EPI DVARS	1.11	1.11	0.11	1.13	1.13	0.13	-0.27	-0.27	34.66	34.66	0.09	0.79	0.09	[-0.09,0.07]
EPI 3dToutcount Outliers	0.00	0.00	0.00	0.00	0.00	0.01	-1.52	-1.52	318.00	318.00	0.25	0.13	0.25	[-0.07,0.55]
EPI Global Correlation	0.04	0.04	0.02	0.05	0.05	0.01	-1.31	-1.31	325.00	325.00	0.22	0.19	0.22	[-0.11,0.53]
EPI Median Distance Index	0.00	0.00	0.00	0.00	0.00	0.00	-0.61	-0.61	349.00	349.00	0.10	0.54	0.10	[-0.23,0.41]
DWI Temporal Signal-to-noise Ratio	6.82	6.82	0.41	6.72	6.72	0.50	0.68	0.68	34.70	34.70	0.22	0.50	0.22	[-0.20,0.40]
DWI Maximum voxel intensity outlier count	1168.00	1168.00	2840.56	2532.00	2532.00	2984.59	-1.33	-1.33	324.50	324.50	0.22	0.18	0.22	[-0.10,0.52]
DWI Mean voxel intensity outlier count	360.49	360.49	273.53	442.66	442.66	183.61	-1.52	-1.52	318.00	318.00	0.25	0.13	0.25	[-0.07,0.56]
DWI Signal-to-Noise Ratio	5.91	5.91	2.52	7.42	7.42	2.37	-0.06	-0.06	368.00	368.00	0.01	0.95	0.01	[-0.32,0.34]
DWI Entropy Focus Criterion	0.42	0.42	0.02	0.42	0.42	0.01	-0.93	-0.93	32.62	32.62	0.29	0.36	0.29	[-0.01,0.01]
DWI Smoothness of Voxels	2.06	2.06	0.07	2.06	2.06	0.10	0.85	0.85	400.00	400.00	0.14	0.40	0.14	[-0.46,0.18]
DWI Foreground to Background Energy Ratio	11.12	11.12	10.20	13.62	13.62	11.03	-0.09	-0.09	367.00	367.00	0.02	0.93	0.02	[-0.32,0.34]
DWI Ghost to Signal Ratio	0.04	0.04	0.02	0.04	0.04	0.03	0.20	0.20	378.00	378.00	0.04	0.84	0.04	[-0.37,0.29]
DWI Mean Frame-wise-displacement	0.58	0.58	0.63	0.61	0.61	0.71	-0.44	-0.44	355.00	355.00	0.07	0.66	0.07	[-0.26,0.39]
DWI Volumes with displacement greater than .20	4.00	4.00	9.90	4.00	4.00	11.39	-0.34	-0.34	358.50	358.50	0.06	0.74	0.06	[-0.27,0.37]
DWI DVARS	1.04	1.04	0.02	1.04	1.04	0.03	0.00	0.00	371.00	371.00	0.00	1.00	0.00	[-0.34,0.33]
DWI 3dToutcount Outliers	0.02	0.02	0.00	0.02	0.02	0.00	-0.88	-0.88	340.00	340.00	0.15	0.38	0.15	[-0.18,0.46]
DWI Global Correlation	0.48	0.48	0.03	0.47	0.47	0.03	0.38	0.38	33.98	33.98	0.12	0.70	0.12	[-0.02,0.02]
DWI Median Distance Index	0.06	0.06	0.01	0.07	0.07	0.01	-1.15	-1.15	33.87	33.87	0.36	0.26	0.36	[-0.01,0.00]

* $p < 0.05$

Generation of ROIs for FC Analyses: The cortical parcellation used for generating regions of interest (ROIs) is the Choi et al., 2012's 17-network parcellation of the striatum with the cerebral cortex from 1,000 participants' (500 to derive parcellation and 500 to validate) resting state connectivity profiles.⁶⁴ In this parcellation, striatal voxels were assigned to cortical regions from the Yeo et al., 2011 cortical parcellation, informed by a combination of task-based functional connectivity,^{64,201} histological tracings of cortical connections in macaque monkeys,^{202,203} and the confidence intervals of resting-state seed-to-voxel correlations in the participant pool.^{64,65} The parcellation and the methods are described in detail in the respective *Freesurfer*^{204–208} documentation page and publication (http://www.freesurfer.net/fswiki/StriatumParcellation_Choi2012).

The parcellation includes 7 networks involving multiple domains (*visual, somatomotor, limbic, frontoparietal, dorsal attention, ventral attention, and default mode*) across the cortex split into subdomains (totaling 17 networks). However, not all subcortical voxels were strongly correlated with each of the 17 cortical regions of the cortical parcellation. For example, there were minimal correlations between the putamen and the visual cortex. In addition, the original parcellation used a surface-based method for analysis, while the atlas is published in a 1x1x1mm isotropic volume of the MNI 152 brain in FSL(FMRIB Software Library).²⁰⁹ Furthermore, each of the cortical and subcortical regions were grouped by their confidence-interval-based clustering of highest functional connectivity. This is problematic for the proposed analysis as no protocols for separating networks into distinct brain regions are available from the developers.

To address this limitation, we created individual masks of each network using Analysis of Functional NeuroImages (AFNI)'s²¹⁰ clustering algorithm to separate each

cortical and subcortical network into distinct brain regions based on grouping by clusters in conservative estimates of functionally connected regions from the Yeo et al., 2011 and Choi et al. 2012 atlases. Voxels that did not fall into individual clusters and small clusters were grouped into larger regions based on Euclidean distance from neighboring clusters (~ 3-4mm or less from a larger cluster typically elicited grouping while larger distances were considered individual regions) and if sides, edges, or corners of an unassigned voxel or small cluster flanked those of a larger cluster. This process was repeated for all networks. Once complete, each cluster-based ROI was resampled to a 2mm isotropic mask, and all cluster-based ROIs that did not survive this interpolation (i.e. reported 0 for cluster size and volume after resampling, reflecting sub-voxel interpolation) were discarded from subsequent analyses. This left a total of 107 individual cortical and subcortical brain regions in the atlas, corresponding to 10 sub-networks of interest (derived from somatomotor, limbic, frontoparietal, dorsal attention, ventral attention, and default mode regions) from the atlas. Each ROI derived from clustering was dilated between 3-12mm and multiplied by a binarized mask of the liberal definition of the cortical surface from the each of the Choi et al. 2012 and Yeo et al. 2011 network parcellations to form a “loose” mask including grey and white matter for diffusion tractography analyses. The “loose” atlas was then masked by the more conservative definition of the cortical surface (containing only grey matter) for the FC analyses described in the aims and results sections.

AIM #1

Compare the functional of connectivity resting-state striatal brain networks in individuals with ASD and TD controls.

MRI data collection and analysis: The images for each participant include: one T1 weighted 3D-(fast spoiled gradient echo) FSPGR anatomical image (TR/TE: 11.08/4.3ms, FOV: 256mm, 256×256 matrix, 176 slices, 1mm² isotropic voxels, flip angle: 45°), 180 individual T2-weighted EPI images stacked across 6 minutes of resting state MRI (TR/TE: 2000/30ms, 3.4mm slice thickness, in-plane resolution: 3.48x3.48x3.4 mm², number of slices: 39-40) and a set of single-shot echo-planar diffusion weighted images TR/TE: 11000/91ms, FOV: 240mm, 128×128matrix, 2mm slice thickness, 68 axial slices) using a single-shell paradigm with two diffusion weighting values ($b = 0$ and 1000 s/mm^2) in 61 non-linear directions. Informed assent and consent was obtained from all participants and their caregivers in accordance with the University of California, San Diego, and San Diego State University Institutional Review Board (IRB), and the datum were anonymized (protected health information such as participant names, dates of birth, and facial features were removed from MRI scans) prior to the submission of the data to ABIDE-II in accordance with HIPAA guidelines and 1000 FCP/INDI protocols. The removal of protected health information and open-access nature of the MRI datum from the ABIDE and ABIDE-II databases qualified the proposed analyses for IRB exemption (no individual IRB protocol for data collection or participant information storage required). The exemption status of the project was issued on March 22, 2017 following a

full review conducted in accordance with UAB's Assurance of Compliance and approved by the Department of Health and human Services.

Data Preprocessing: Functional EPIs were processed through a customized pipeline including routines from Statistical Parametric Mapping 12 (SPM 12; Wellcome Trust Centre for Neuroimaging) implemented in the *CONN* toolbox (version 17.b),¹⁹⁰ in MATLAB©,²¹¹ *AFNI*,²¹⁰ and *ANTs* (<http://stnava.github.io/ANTs/>). The preprocessing pipeline utilized a 6 step process. 1) Realignment and Unwarping to estimate and correct subject motion. Field maps have already been applied to the data by SDSU researchers prior to submission to ABIDE-II. 2) Co-registration to N4Bias corrected (*ANTs*' N4BiasFieldCorrection)²¹² and skullstripped (via *AFNI*'s 3dSkullStrip https://afni.nimh.nih.gov/pub/dist/doc/program_help/3dSkullStrip.html) anatomical T1 images for each participant via *ANTs*' Symmetric Diffeomorphic Image Registration with Cross-Correlation (*SyN*: antsRegistrationSyN).²¹³ 3) Segmentation using FSL's²⁰⁹ FAST (<https://fsl.fmrib.ox.ac.uk/fsl/fslwiki/FAST>) to generate grey matter, white matter, and cerebral spinal fluid tissue images. 4) Registration of the participant T1 (and accompanying segmented tissue-types) and co-registered EPI using *ANTs*' *SyN* registration. 5) Signal and motion outlier detection at the participant level using ArtDetect (<http://gablabs.mit.edu/index.php/software>) to serve as nuisance regressors for motion-related changes in BOLD signal. 6) Each participant's EPI timeseries data was smoothed to 6mm full-width-half-maximum (FWHM),^{214,215} prior to data analysis.

Functional Connectivity Analysis: Tissue-type and smoothed EPI images, normalized to the ABIDE group template, for each participant were loaded into the *CONN* toolbox (version 17.e),¹⁹⁰ in MATLAB©²¹¹ for denoising and signal extraction for the FC analyses. *CONN* utilizes an aCompCor²¹⁶ principal-component-based denoising strategy which includes the removal of effects related to tissue types (white matter, cerebrospinal fluid [CSF]) and data correction procedures (realignment and scrubbing with 1st order temporal derivatives for each) of the EPI data. Following the identification and regression of nuisance variables (CSF, white matter, motion, and motion-derivatives), the data were band-pass filtered from 0.01–0.08Hz, which was recently found to reduce differences in FC between high and low motion groups and mean absolute correlations between FC and RMSD motion compared to the standard 0.01–0.1 Hz filter for rsfMRI data.²¹⁷ After which, the EPI timeseries data is linearly detrended and for first-level analyses of the functional data. Following this process, FC values were extracted from each pairwise combination of ROIs within each network of the clusterized Choi/Yeo atlas to be used as the dependent variable in subsequent analyses.

Prior to each ROI pair by group comparison, measures of FC were checked for univariate normality using the Anderson-Darling test.¹⁹³ If values were found to be non-normally distributed, a non-parametric Wilcoxon-rank sum^{191,218} test was used to compare group differences in lieu of a student's t-test. A 5% false-discovery rate (FDR) correction²¹⁹ was used at the level of all ROI pairs (628 total) for comparisons of FC between ROI pairs to reduce false positives. Effect sizes for parametric tests (Hedge's *g*),²²⁰ non-parametric tests (rank-biserial correlations),²²¹ and confidence intervals for all results are also computed (using Harald Hentchke's measures-of-effect-size-toolbox;

<https://www.mathworks.com/matlabcentral/fileexchange/32398-hhentschke-measures-of-effect-size-toolbox> in MATLAB[®]) and reported as measures of utility, reliability, and for future power calculations.

Potential Problems and Alternative Strategies:

fMRI: As described in the **METHODS: MRI Data Quality Assurance** section, images were quality checked visually by the researchers and scores from the QAP pipeline (<http://preprocessed-connectomes-project.org/quality-assessment-protocol/>). Scores on QAP data quality measures were tested for any significant differences between diagnostic groups (TD vs ASD) to assess the potential of these measures as possible confounding variables. Motion artifact is a potential confound for all fMRI analyses, but is a much greater risk for studies with smaller brain regions such as the NAcc ($k \approx 1000\text{mm}^3$). Subcortical and some cortical regions (such as the OFC) are highly susceptible to signal dropout. To evaluate any potential group difference in ROI signal, tSNR was calculated by dividing the mean EPI time-series for each subject (slice time corrected, unwarped, and realigned) and then dividing the mean ROI image signal by the standard deviation of the ROI time-series signal. Each of the 25 subcortical (bilateral NAcc and subregions of the caudate and putamen) and 2 cortical OFC ROIs were mapped back to individual subject space using the inverse transforms generated by ANTs (<http://stnava.github.io/ANTs/>). Anderson Darling tests¹⁹³ were conducted for tSNR values for each ROI and either a student's t-test or a Wilcoxon rank-sum test^{191,192} was conducted depending on the normality of the data. This approach identified an ROI in the left hemisphere of a default mode subnetwork (network 16, corresponding to regions of the head of the caudate and putamen) that displayed a large ($g = 0.7$) and statistically

significant ($t(35) = 2.21$, $p = 0.03$, CI95 1.34,31.52) reduction in tSNR in the ASD group. A univariate outlier was also identified in the right hemisphere of the frontal cortex in “limbic” subnetwork 10 (corresponding to the OFC) in sub-28853. Removal of this participant did not result in a significant group difference in tSNR of the OFC, so the participant’s data was retained. Results from this ROI are interpreted in the **RESULTS** section with this finding noted and Appendix Table 1 contains a summary of these analyses. Two ROIs in the tail of the right putamen and one in the left posterior body of the putamen (in networks 8, 13, and 14 respectively) did not survive interpolation back to native space.

Group differences between TD and ASD participants in mean/max motion, total volumes excised following outlier detection (see ArtDetect below), and final temporal degrees of freedom (tDOF) following ArtDetect and aCompCorr corrections, were performed prior to the final analyses and are reported in Table 2. No significant group differences in RMSD motion or tDOF were found. However, a significant ($t(36) = 2.06$, $p < 0.05$, CI95 0.00003,0.0035) and large ($g = 0.66$) group difference in ghost-to-signal ratio (GSR)²²² was identified, indicating that TD children were more likely to exhibit ghosting in brain regions prone to ghosting artifacts compared to individuals with ASD (TD, [M:0.010±0.002]; ASD, [M=0.008±0.003]) based on the phase-encoding direction.

As of July 2017, there were two publications examining the test-retest reliability and differences in results regarding noise mitigation pipelines in resting state fMRI.^{223,224} These papers cite two main areas of concern from previous literature when measuring resting-state FC: 1) correlations between connectivity results and measures of motion (such as framewise displacement [FD] and RMSD) and 2) distance-dependence

artifact.²²⁵ The former assesses if FC results are significantly influenced by measures of head motion in the scanner. Previous work has identified motion in fMRI data can artificially reduce FC values in some networks (e.g. frontoparietal and default mode), and while artificially increasing FC in other regions (e.g. somatomotor regions).^{223,224,226–228} Distance-dependence analyses address the phenomenon that motion in fMRI data significantly increases proximal (short range) FC results while reducing distal (medium to long-range) FC results.^{223,224,226–229} Distance-dependence is concerning given that many current theories of FC in ASD are centered on reduced long-range and enhanced short-range functional connections in the brain.^{4,26,225,230,231} It has also been suggested aCompCorr has the potential to exacerbate distance-dependence.^{223,224}

To address these concerns, FC-motion correlations were performed using Spearman's ρ^{232} for each FC result of interest. This analysis revealed a total of 39 of the 628 pairwise connections that significantly correlated with motion. These include 3 pairs in somatomotor network regions, 3 pairwise connections in ventral attention network regions, 9 pairs in frontoparietal network regions, 12 pairs in dorsal attention network regions, and 12 pairwise combinations of default mode network regions. It should be noted however, that none of these comparisons survived FDR correction for multiple comparisons.²¹⁹ Following the motion-FC correlations, the Euclidean distance between the center of gravity for each pair of ROIs of interest (in template space) were correlated with the motion-FC correlations using a Spearman's ρ^{232} to determine if any FC results were also influenced by distance-dependence artifact.^{224,226–229} Results from this inspection revealed a small but significant ($\rho(626) = -0.08, p < 0.05$) relationship between FC-motion correlations and Euclidean distance, with ROIs closer to one another

exhibiting higher FC-motion correlations and ROIs further from one another exhibiting lower FC-motion correlations. This finding is in line with previous cautionary reports of reduced correlations relative to Euclidian distance between ROIs.^{224,226–229} Given this finding, results from all analyses should be considered relative to RMSD motion.

Analytical: Given the relatively smaller sample size (and thus, lower power) for this study, the results of these analyses may not generalize to the larger population, and would require replication with a larger sample size. As such, all possible attempts were made to control for false positives, adjust for smaller sample size, and estimate effect sizes for power calculations for future analyses. Collinearity between demographic factors were expected (e.g. Age and IQ), but only PIQ displayed a significant relationship with age ($\rho(36) = -0.36, p = 0.03$), with reduction in PIQ as a function of age in the final UCSD sample. Despite the lack of collinearity in these variables, the number of observations relative to variables of interest limit the ability to effectively model and study interaction effects of age and FSIQ relative to TD vs ASD and as a result, pairwise t and Wilcoxon-rank-sum tests were chosen as opposed to general linear models (i.e. ANCOVA). However, considering the finding of little collinearity, results are compared to those of general-linear-model approaches to address the impact these variables may have on the results.

Age, and WASI®-II¹⁸⁸ FSIQ scores have the potential to display effects much larger than that of group considering the range of the participant sample (7.4-17.8 years and 77-130 respectively). To address this, we performed correlative analyses on the effects of age and IQ on all connections of interest prior to all planned analyses. Increases in FC relative to age were found in 18 pairs of frontal-parietal ROIs, 6 pairs of dorsal attention

network ROIs, and 3 pairs of default mode network ROIs. Reductions in FC with increase in age were noted in 4 frontoparietal, 2 dorsal attention, and 8 default mode network ROIs. Significant increase in FC relative to FSIQ scores were found in 7 ventral attention network ROIs, 3 pairs of frontoparietal ROIs, and 6 pairs of default mode network ROIs. Significant decreases in FC relative to FSIQ were found in 3 pairs of somatomotor ROIs, 2 pairwise combinations each for dorsal attention network and ventral attention network ROIs, 2 frontoparietal, and 4 pairs of default mode regions. These results are summarized in Appendix Table 2. However, it should be noted that none of these results survived 5% FDR correction for multiple comparisons.

AIM #2 Examine brain-behavior relationships by analyzing correlations between functional connections of resting-state striatal brain networks in individuals with ASDs with cognitive and behavioral factors (repetitive behaviors, social motivation scores) and anatomical connections of the striatum.

Functional Connectivity and Autism Symptoms: The effects of clinical measures derived from subdomains of ASD symptom severity measures such as the RBS-R and SRS (described below) will be conducted as a second-level analysis on FC values between striatal ROIs and associated networks. The goal of both analyses is to establish if clinical measures can predict or relate to FC across striatal ROIs and their respective networks.

Restricted Repetitive Behavior Scale-Revised (RBS-R): The RBS-R²³³ is a 43-item scale spread across 5 or 6 subdomains (depending on factor interpretation) designed to assess the severity of items across the restricted interest and repetitive behaviors that were core features of ASDs under the DSM-IV.²³⁴ The authors have chosen the 6-factor solution of the measures, which include: stereotyped behaviors (apparently purposeless movements or actions that are repeated in a similar manner), self-injurious behaviors (movements or actions that have the potential to cause redness, bruising, or other injury to the body, and that are repeated in a similar manner), compulsive behaviors (behaviors repeated and performed according to rules, or involves things being done “just so”), ritualistic behaviors (performing activities of daily living in a similar manner), sameness (resistance to change, insisting that things stay the same), restricted behaviors (limited range of focus, interest or activity). Each of these domains contain 4-11 items that are rated by an informant on a 0-3 Likert scale representing the presence and severity (behavior does not occur: 0, behavior is a mild problem: 1, behavior is a moderate problem; 2, and behavior is a severe problem: 3) of the behavior in the last month. Higher scores indicate greater severity within the respective domain.

In accordance hypotheses proposing “disrupted connectivity” alterations in the striatum contributing to repetitive behaviors, FC between brain regions associated with somatomotor and cognitive control should be significantly related to restricted-repetitive behaviors in ASD. To that end, we propose two analyses: 1) Correlating raw scores for Stereotyped behaviors (6 items) with somatomotor networks (3, 4, and 14) in the Yeo et al. 2011/Choi et al. 2012 due to their association with sensory/motor integration.⁶⁴ 2) Correlating raw scores for compulsive (8 item) behaviors with FC between Yeo et al.

2011/Choi et al. 2012 frontoparietal network (8 and 13) regions due to the relationship frontoparietal regions share with inhibition and cognitive control.^{235,236} FC values which correlate with either of these two metrics may be indicative of alterations in brain communication that lead to increases in the incidence and intensity of repetitive behaviors.

Social Responsiveness Scale (SRS) Version 1: The SRS³³ is a 65 item questionnaire completed by an informant (e.g. parent, teacher, significant other) that is rated on a 1-4 point Likert scale for each behavior (Not true: 1, Sometimes true: 2, Often true: 3, Almost always true: 4). Scoring of the SRS is broken down into a total raw score for all questions (0-199), but can also be separated into 5 subdomains: Social Awareness (0-21), Social Cognition (0-32), Social Communication (0-55), Social Motivation (0-32), and Autistic Mannerisms (0-36), with higher scores representing greater impairment in each. SRS has been interpreted as measures of “social impairment” in individuals with ASDs, but the authors have also noted that repetitive behaviors, communication deficits, and symptoms that are not exclusive to an ASD diagnosis are also included in this questionnaire.²³⁷⁻²⁴⁰ For the purposes of this proposal, the authors will be utilizing the Social Motivation subscale raw scores as a proxy for attention towards and the desire to engage in social situations when exploring the hypothesis that social motivation influences connectivity between striatal subregions such as the NAcc. FC between the limbic (primarily NAcc to OFC) of the Yeo et al. 2011/Choi et al. 2012 parcellation and social motivation raw scores are explored in accordance with “social motivation hypotheses” of ASD. However, the researchers believe the role of attention in “social motivation hypotheses”

of ASD warrants exploration of regions associated dorsal attention network and ventral attention network within the Yeo et al. 2011/Choi et al. 2012 parcellation.

Functional Connectivity/Diffusion Analysis: To further examine claims by brain connectivity accounts of ASD positing that alterations in FC are driven by alterations in the underlying white matter, correlations between FC and DWI derived measures of connectivity were performed within the sample of TD and ASD participants. The 3-step analyses outlined below aim to 1) identify anatomical connections within resting-state

parcellations, 2) determine if there are any significant relationships between measures of diffusion velocity (GFA) or spin density (NQA) and FC

where tracts may be present.

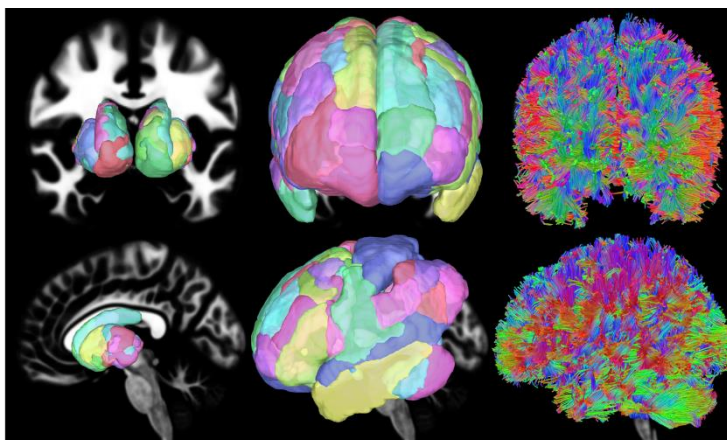


Figure 5. The 107 “loose” ROI parcellation of the Yeo et al. 2011 and Choi et al. 2012 atlases in MNI normalized diffusion space (left and center), and example fiber-track streamlines based on QSDR reconstructed diffusion data (right, 100000 tracts displayed for visualization purposes).

DWI Processing and Extraction: DWIs were eddy-current corrected and reconstructed in *DSI Studio*^{68,186} using QSDR¹⁸⁴ with a path length of 1.2 and no r^2 weighting. These parameters were found to have the highest test-retest reliability in QSDR¹⁸⁴ from work performed with the PI’s Multimodal Neuroimaging training program (MNTP) training cohort under Fang-Cheng Yeh, M.D., Ph.D. (unpublished data). As part of QSDR,¹⁸⁴ each b0 volume was co-registered to the skull-stripped and bias corrected T1 to use as a guide for constrained diffeomorphic mapping to normalize the diffusion data to a T2-

weighted MNI template. Once normalized to the MNI template, whole-brain deterministic tractography utilizing a Euler method⁶⁷ for building tracts were performed using *DSI Studio*^{68,186} for each participant's normalized images with a total fiber count of 1 million. Tracking parameters include: QA threshold of $0.6 \times$ Otsu's threshold for the image, max turning angle randomly selected from $15-90^\circ$ for each tract grown, step size randomly selected from a 0.1-3 (2mm) voxel distance, propagation from 0-95% ratio between incoming and subsequent direction during tracking. After which, mean generalized fractional, normalized quantitative anisotropy (GFA and NQA respectively), and total streamline count that passes through each ROI-to-ROI pair in the "loose" mask from the *Freesurfer* based Yeo et al. 2011/Choi et al. 2012 parcellation were extracted for each participant (See Figure 5).

Functional Connectivity/Anisotropy Analysis: Following whole-brain tractography for each participant, ROI pairs within networks of interest were extracted and fiber counts were thresholded to minimize false fibers (using $[\text{max fiber count} \times 0.001]$ for the minimum count needed for anisotropy), and ROI pairs reporting more than 75% of the total participants with streamline counts greater than participant-level fiber maximas were kept for subsequent analyses, while pairs in which less than 75% of all participants reported streamlines below threshold were discarded. Previously published work has proposed using probabilistic group thresholds in which $\frac{1}{4}$ either report at least one streamline connecting ROIs²⁴¹ or at least $\frac{1}{2}$ of the participants report a probability threshold for tracts based on a group map of 0.5 or greater,²⁴² which were considered conservative, in order to filter out false fibers for sample sizes smaller than those for our

analysis (32 and 10). However, since QA based deterministic fiber tracking is more robust to accidental identification of false fibers,^{184,186} we chose to use a conservative threshold of 75% of participants due to the large number of ROIs across a small number of subjects and the quality of the data. Subsequent FC/anisotropy analyses between ROIs were only conducted for ROI pairs that reported streamlines and anisotropy values above threshold.

For the remaining ROIs with streamlines and anisotropy values, normality was assessed across both the first-level FC results produced by *CONN*²⁴³ and the anisotropy values from *DSI Studio*^{68,186} using an Anderson-Darling test.¹⁹³ The next step of the analysis assesses the size of the correlation between FC and RMSD motion, and framewise displacement in the DWI data by participant and anisotropy measures (NQA and GFA). The final step performs either a Pearson's r for normally distributed data or a Spearman's ρ ²³² for non-normally distributed data. However, if RMSD is found to significantly correlate with FC, or if mean framewise displacement is found to correlate with anisotropy, or both FC and anisotropy correlate with their respective motion measures, a partial correlation between FC and anisotropy is instead performed in an attempt to account for one or both respective measures of motion. Separate correlations were run for GFA and NQA with the intention of examining the relationship between separate ODF-based diffusion measures that provide different information about diffusion data (velocity for GFA, and quantitative spin distribution for NQA) and FC between any pair of ROIs. For each analysis run, the correlations, p-values, and motion/DV correlations were saved and the results were multiple-comparison corrected using a 5% FDR for the total number of tests in each type of anisotropy.

Potential Problems and Alternative Strategies:

Analytical: Ideally, interactions between diagnostic groups (ASD vs TD) would be included in the model and mediation analyses that would be performed between measures of SRS, RBS-R, NQA and GFA on measures of FC, should the interaction effects be statistically significant. We acknowledge that the statistical power for the analysis is relatively low, limiting any multi-dimensional conclusions that could be drawn from regression models should they be present. As such, interaction terms were not modeled for the diffusion indices, nor were moderation analyses performed. Spearman ρ rank correlations²³² performed on the independent variables of interest (RBS-R, SRS, GFA and NQA) to assess multicollinearity revealed that raw motivation scores from the SRS and stereotyped and compulsive behaviors from the RBS-R are highly correlated with one another ($\rho(36) = 0.67$, $\rho(36) = 0.61$, and $\rho(36) = 0.71$, all $p < 0.0001$ respectively). Anisotropy measures were equally highly correlated with one another across brain regions which reported tracts ($\rho(7218) = 0.45$, $p < 0.00001$), despite the information conveyed by GFA and NQA being theoretically distinct from one another. The combination of these results supports our decision to use separate models for each to avoid variance inflation within a single model.

A recent publication assessing data quality in the Human Connectome Project (HCP) discovered that many demographic variables (e.g. age, FSIQ, weight, and psychiatric diagnosis scales) may strongly correlate with motion-related measures from MRI data.²⁴⁴ As a check against this potential confound, mean RMSD motion was correlated with RBS-R stereotyped behaviors, RBS-R compulsive behaviors, and SRS-

motivation raw scores. No significant correlations between any SRS or RBS-R variables of interest were identified.

DWI: The tSNR and maximum voxel value of each DWI were calculated using automated shell code (<https://www.med.upenn.edu/cmroi/qascripts.html>).¹⁸⁹ After which, analyses were performed to assess group differences in tSNR and maximum voxel displacement, which based on discriminatory data quality studies using machine learning, are the most influential data quality measure which separates good from excellent and good from poor data quality respectively.¹⁸⁹ Motion differences in DWIs between each group were assessed using QAP's measures of framewise displacement, in addition to other measures of potential artifact (see: <http://preprocessed-connectomes-project.org/quality-assessment-protocol/>). Correlations between FD and the extracted diffusion measures (count, NQA, GFA) were performed as part of each analysis to assess any contributions of motion to the data. While RMSD motion and mean framewise displacement in DWIs were found to highly correlate with one another ($\rho(36) = 0.38$, $p = 0.02$), 36 ROI pairs required a correction for both across all anisotropy measures. No significant differences were identified in any diffusion-based quality metrics between TD and ASD individuals prior to the FC/DWI correlations. Registration accuracy to the MNI template is available as part of QSDR reconstruction. As an additional check, template registration accuracy (measured by the R^2 value of DWI data to the template) was also correlated with variables of interest and are assessed as potential sources of artifact.

Previous research indicates that surface-based parcellations display less reliability compared to volume-based parcellations due to the absence of white matter regions in these parcellations.²⁴⁵ To mitigate this problem as much as possible, the “loose” mask of

the Yeo et al. 2011/Choi et al. 2012 was used as there is partial volume overlap with white and grey matter in this less-conservative parcellation. However, in theory, whole-brain tractography mitigates this to a degree as the seeding parameters are asking the program to identify up to 1 million tracts within a mask of the entire brain as opposed to building streamlines between specific grey matter ROIs where tractography may be suspect.

Mitigation of false-positives: Psychological research has come under increased scrutiny due to findings that many published research studies may contain numerous false positives.^{246,247} The authors acknowledge that the low sample size, which both reduces the statistical power and likelihood of obtaining a representative sample for the analysis risks producing such false positives.²⁴⁸ FDR corrections²¹⁹ with a 5% false-positive rate for each group of tests (628 for TD vs ASD group FC, 446 for FC/behavior correlations, 190 for both GFA and NQA correlations with FC) to attempt to limit false-positives. Should no results survive FDR correction, uncorrected results will be reported with the caveat that they do not survive multiple comparisons. Additionally, the extracted participant data and code for the analytical pipeline are made openly available on the Open Science Framework (<https://osf.io/>)^{249,250} for replication and meta-analyses.

Computational: The authors acknowledge the connectome does not fully represent white-matter tract profiles in the human brain. Diffusion tractography is, by nature, a second order reconstruction of the flow of water throughout the human brain, which is then used to model what is assumed to be white-matter fiber tracts. Such models do not fully represent the microstructural resolution and nature of white-matter fiber bundles, is susceptible to many subject and scanner artifacts, and should be interpreted as

approximations at best when analyzed. Furthermore, the connectome approach applied here addresses structural connectivity on a very binary level, meaning it assumes that any 2 regions in the connectome are or are not structurally connected. On a biological level, a single tract or set of tracts may pass through several regions in the brain, carrying information to one or all brain regions upon which axons and dendrites synapse. Additionally, many functional connections may stem from 2nd or 3rd order communication from brain regions not physically connected by a single white matter tract. Tract verification programs are available in most popular diffusion analysis packages to attempt to address the former. However, these are difficult to implement in connectome-based analyses due to the number of tracts generated across the entire brain. For the latter, higher-order modeling may be used (e.g. ICA, SEM, homology), but to our knowledge, these have currently only been applied to tensors and not higher-order diffusion data.^{251,252} Further research will be required to implement such models for higher-order spherical deconvolution diffusion modeling.

We have made attempts in the past to grow tracts in between individual ROIs, but this approach may be influenced by several other variables including but not limited to: inter-subject variability in total intracranial volume (TICV) and ROI size relative to seed count, voxel-count differences in seed-to-ROI locations relative to seed count, total-fiber count relative to TICV, and maximum allowable tract minimum and maximums relative to TICV determined ROI distances. While weighting tractography algorithms by such factors are theoretically possible, no clear guidelines for doing so have been published to date to our knowledge. Additionally, performing such weighting would not only be highly experimental, but also computationally intensive. As such, the authors have

chosen to normalize the diffusion images to a standard MNI template and perform tractography across the whole brain with the same settings for each participant and apply the 75% or more tract-present analysis for diffusion analyses to be performed. The authors have also chosen to measure group differences using normalized quantitative anisotropy (NQA), which scales the maximum QA value of a subject to 1 in lieu of QA so measures may be more comparable participants. In theory, these steps will minimize the influence of individual differences in head size and diffusion morphometry and reduce the likelihood of analyzing false tracts, but there are still many more experiments that must be performed to test the reliability and accuracy of connectomes before inferences drawn from them can be interpreted as real-world representations (see Maier-Hein et al., 2016 for limitations).²⁵³

RESULTS

AIM #1 Compare the functional connectivity of resting-state striatal brain networks in individuals with ASD and typically developing controls.

No significant group differences were found following an FDR correction for the total number of tests (628). Additionally, there were only a few significant group differences in striatal-cortical connectivity even at an uncorrected statistical threshold of $p < 0.05$ for each test (see Table 3 for summary). Regarding frontoparietal network 8, there were reductions in FC in ASD between the sections of the body and head of left and right putamen with the right precentral gyrus region ($t(36) = 2.16, p = 0.04, g = 0.69, CI95 0.007, 0.23$; $t(28) = 2.24, p = 0.03, g = 0.71, CI95 0.01, 0.20$), and the left putamen tail and contralateral IPL ($t(36) = -2.41, p = 0.02, g = 0.77, CI95 0.02, 0.21$). An increase in FC in ASD between the medial body of the left caudate and a region containing the ipsilateral middle and inferior temporal gyri (MTG, ITG) corresponding to frontoparietal network 13 ($t(31) = -2.04, p < 0.05, g = 0.65, CI95 -0.21, -0.0003$). Both left and right aspects of dorsal attention network corresponding to the tail of the putamen displayed reduced FC with a right medial aspect of the cingulate gyrus in ASD compared to TD participants ($t(36) = 2.50, p < 0.02, g = 0.80, CI95 0.04, 0.35$; $t(36) = 2.98, p = 0.005, g = 0.95, CI95 0.05, 0.26$). A medial aspect of the body of the left putamen (corresponding to somatomotor network 14) displayed increased FC in ASD compared to TD participants with bilateral aspects inferior frontal gyrus (IFG)/OFC ROI bordering the insula (left:

$t(36) = -2.12, p < 0.05, g = 0.68, CI95 -0.25, -0.006$; right: $t(36) = -2.51, p < 0.02, g = 0.80, CI95 -0.24, -0.025$). Only one subcortical ROI pair in the default mode network ROIs displayed altered connectivity, with ASD individuals displaying increased FC between a right dorsal-medial aspect of the caudate and a temporal ROI containing aspects of the middle, superior, and inferior temporal gyrus corresponding to default mode network 17 in the parcellation ($t(34) = -2.14, p < 0.04, g = 0.68, CI95 -0.24, -0.006$). No group differences in cortical-subcortical connections were found in ventral attention network or limbic networks.

Multiple cortical-cortical connections within the ventral attention, frontoparietal, and default mode regions, and one pair within the dorsal attention network, displayed significantly reduced FC (all $p < 0.05, g > 0.4$) in individuals with ASD. In contrast, the connection between the insula and MTG/lateral occipital cortex (LOC; part of ventral attention network), the connection between the ACC/superior frontal gyrus (SFG) and IPL (part of frontoparietal network 8), and the connection between the IPL and SFG/middle frontal gyrus (MFG; part of default mode network 17) were significantly greater in individuals with ASD compared to TD individuals. The complete results of the group-level analysis with the relevant test statistics, effect sizes, and confidence intervals are reported in Table 3. Figure 6 displays t and Z values of group differences by connection. However, it should be noted that none of these results survive FDR correction for multiple comparisons and should be interpreted with caution.

Of the 27 uncorrected results from group level comparisons, three of the connections were identified as having a strong correlation with FSIQ (right insula:right MTG/LOC, right insula:right IPL, right insula:left MTG) and another connection

displayed a significant relationship with age (right IPL:left SFG/MFG). When age or FSIQ were accounted for using ANCOVAs, all FC results except for FC between the right insula and right IPL retained a significant effect of group.

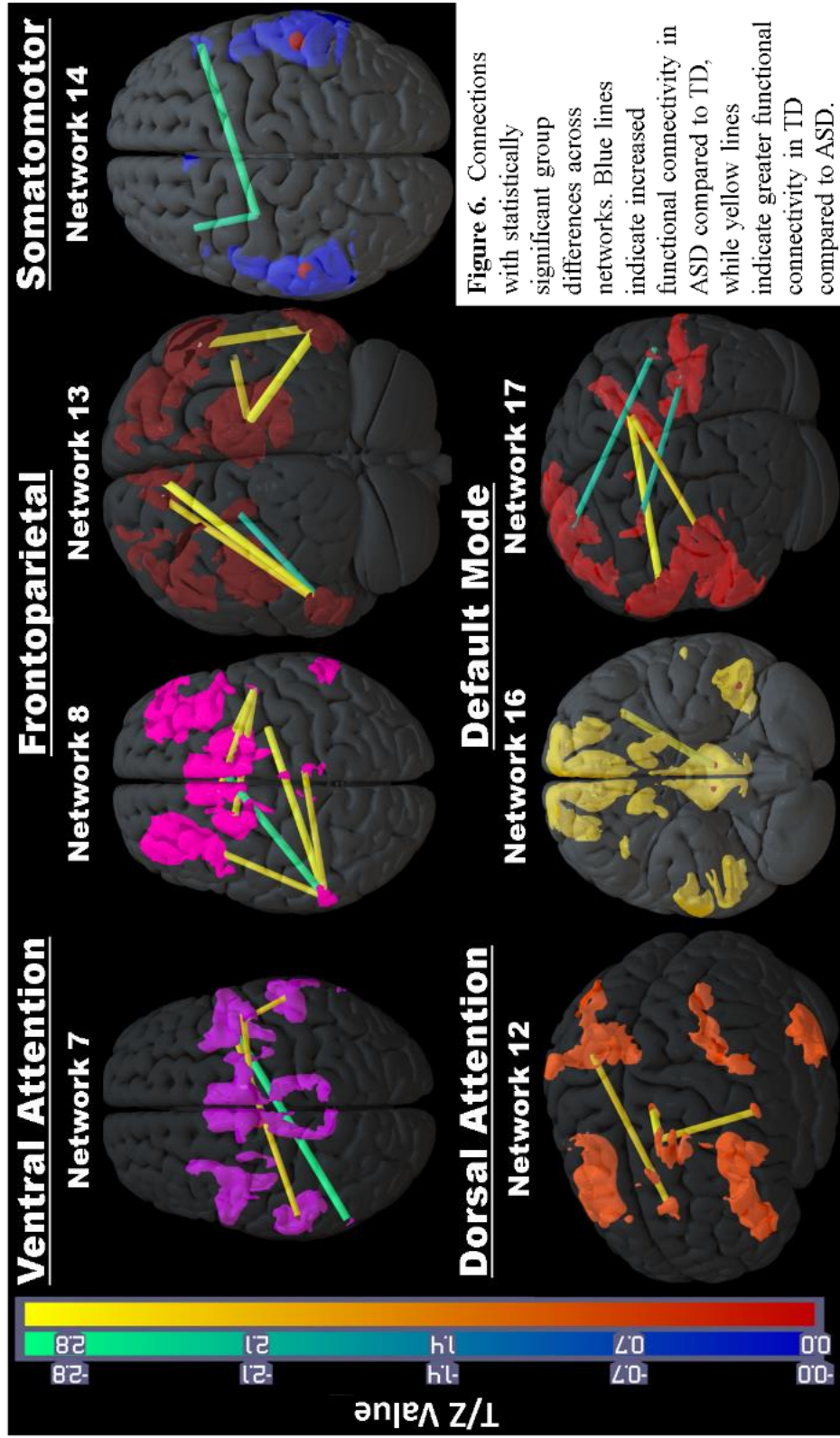


Figure 6. Connections with statistically significant group differences across networks. Blue lines indicate increased functional connectivity in ASD compared to TD, while yellow lines indicate greater functional connectivity in TD compared to ASD.

Table 3. Regions of interest from the Choi/Yeo striatal parcellation yielding significant group differences in functional connectivity.

Connection	Mean TD	Median TD	SD	ASD	Mean ASD	Median ASD	SD	r-value	Z-value	df	ranksum	Hedges' g	F _b	P-value	FDR-Pvalue	95% Confidence Interval
Yeo Right 7 ACC SMA Para	0.37	0.23	0.23	0.19	0.12	0.18	0.26	2.23	35.57	0.71	0.03	0.99	[0.02,0.34]			
Yeo Right 7 Preccn Postccn	-0.08	0.23	0.18	0.12	0.18	0.23	0.18	-2.97	35.66	0.94	0.01	0.99	[-0.34,-0.06]			
Yeo Right 7 MTG LOC	0.54	0.27	0.23	0.38	0.27	0.22	0.22	2.04	34.61	0.65	0.05	0.99	[0.00,0.33]			
Yeo Right 7 Insula Oper	0.35	0.21	0.18	0.18	0.23	0.23	0.23	2.34	35.45	0.74	0.03	0.99	[0.02,0.31]			
Yeo Right 7 Insula Oper	0.13	0.10	0.10	0.02	0.18	0.18	0.18	2.24	27.90	0.71	0.03	0.99	[0.01,0.20]			
Choi Right 8 Putamen body	0.00	0.15	0.15	-0.11	0.14	0.14	0.14	2.41	35.85	0.77	0.02	0.99	[0.02,0.21]			
Choi Right 8 Putamen tail	0.13	0.17	0.17	0.02	0.17	0.17	0.17	2.16	35.99	0.69	0.04	0.99	[0.01,0.23]			
Choi Left 8 Putamen body	-0.03	0.28	0.28	0.15	0.18	0.18	0.18	-2.41	30.95	0.76	0.02	0.99	[-0.34,-0.03]			
Yeo Right 8 ACC SFG	0.24	0.23	0.23	0.08	0.26	0.26	0.26	2.04	35.23	0.65	0.05	0.99	[0.00,0.32]			
Yeo Right 8 PCC ACC	0.06	0.22	0.22	-0.09	0.22	0.22	0.22	2.09	35.97	0.66	0.04	0.99	[0.00,0.29]			
Yeo Right 8 Precentral	0.14	0.20	0.20	0.01	0.20	0.20	0.20	2.04	35.98	0.65	0.05	0.99	[0.00,0.26]			
Yeo Left 8 IPL	0.22	0.16	0.16	0.06	0.16	0.16	0.16	2.98	35.98	0.95	0.01	0.99	[0.05,0.26]			
Choi Right 12 ACC	0.16	0.25	0.25	-0.03	0.22	0.22	0.22	2.50	35.52	0.80	0.02	0.99	[0.04,0.35]			
Choi Left 12 Putamen tail	0.28	0.20	0.20	0.15	0.15	0.15	0.15	2.33	33.93	0.74	0.03	0.99	[0.02,0.25]			
Choi Right 12 OFG	-0.05	0.18	0.18	0.06	0.12	0.12	0.12	-2.04	31.46	0.65	0.05	0.99	[-0.21,0.00]			
Yeo Right 13 FP	0.19	0.15	0.15	0.04	0.24	0.24	0.24	2.39	29.60	0.76	0.02	0.99	[0.02,0.29]			
Yeo Left 13 Caudate body	0.33	0.19	0.19	0.12	0.26	0.26	0.26	2.87	32.76	0.91	0.01	0.99	[0.06,0.36]			
Yeo Right 13 IFG	0.50	0.20	0.20	0.32	0.21	0.21	0.21	2.62	35.83	0.83	0.01	0.99	[0.04,0.31]			
Yeo Right 13 ITG MTG	0.16	0.20	0.20	-0.01	0.17	0.17	0.17	2.78	34.86	0.88	0.01	0.99	[0.05,0.29]			
Yeo Left 13 ITG MTG	0.37	0.21	0.21	0.20	0.27	0.27	0.27	2.22	35.98	0.71	0.03	0.99	[0.01,0.33]			
Choi Left 13 SFG	-0.09	0.18	0.18	0.04	0.14	0.14	0.14	-2.51	33.66	0.80	0.02	0.99	[-0.24,-0.02]			
Choi Left 14 Putamen body	0.03	0.18	0.18	0.16	0.16	0.16	0.16	-2.13	35.91	0.68	0.04	0.99	[-0.25,-0.01]			
Choi Left 14 Putamen body	0.06	0.18	0.18	-0.07	0.20	0.20	0.20	2.08	35.32	0.66	0.04	0.99	[0.00,0.25]			
Yeo Left 16 PCC Precuneous	-0.16	0.15	0.15	-0.04	0.20	0.20	0.20	-2.14	33.67	0.68	0.04	0.99	[-0.24,-0.01]			
Choi Left 17 Caudate	0.74	-0.07	0.19	0.06	0.20	0.20	0.20	-2.22	294.00	0.37	0.03	0.99	[0.05,0.65]			
Yeo Right 17 IPL	0.17	0.19	0.19	0.56	0.17	0.17	0.17	3.02	35.40	0.96	<0.005	0.99	[0.06,0.29]			
Yeo Right 17 OFC PP	0.17	0.23	0.23	0.07	0.17	0.17	0.17	3.02	35.40	0.96	0.02	0.99	[0.06,0.29]			
Yeo Right 17 OFC PP	0.17	0.23	0.23	0.07	0.17	0.17	0.17	3.02	450.00	0.38	0.02	0.99	[-0.64,-0.08]			

AIM #2 Examine brain-behavior relationships by analyzing correlations of functional connections striatal networks in individuals with ASDs with by cognitive and behavioral factors (repetitive behaviors, social motivation scores) and anatomical connections of the striatum.

Behavioral Correlates of FC:

Group comparisons on the three subscales confirmed significantly higher scores in the ASD group (RBS-R-Stereo, $Z = 221$, $p < 0.001$, $r^{bs} = 0.75$, CI95 0.58, 0.89; RBS-R-Compulsive, $Z = 250$, $p < 0.001$, $r^{bs} = 0.75$, CI95 0.36,0.81, SRS-Motivation, $Z = 190$, $p < 0.001$, $r^{bs} = 0.88$, CI95 0.868,0.871), suggesting that these measures distinguish TD from ASD participants at a within this sample. Only two ROI pairs from somatomotor network 14 were found to have significant and positive correlations with RBS-R measures of stereotyped behavior. These were the medial aspect of the body of the left putamen with two bilateral IFG/OFC regions bordering the insula reported previously in the ASD vs TD group comparisons (left: $\rho(36) = 0.33$, $p = 0.04$; right: $\rho(36) = 0.39$, $p = 0.02$). RBS-R compulsive behaviors on the other hand was found to correlate with 13 different pairs of ROIs in the frontoparietal networks. FC in 2 of the 3 subcortical connections (both in frontoparietal network13) between the left caudate and cortex (contralateral IFG and IPL) were related to increases in RBS-R compulsivity scores (IFG: $\rho(36) = 0.39$, $p = 0.02$; IPL: $\rho(36) = 0.33$, $p = 0.04$), while the third connection between the right putamen tail and contralateral IPL in frontoparietal network 8 was associated with reductions in FC as RBS-R compulsivity scores increased ($\rho(36) = -0.34$, $p < 0.03$). The remaining significant correlations for RBS-R compulsivity were between the right

frontal pole, (with bilateral ITG/MTG and SFG/MFG regions respectively), right IFG-left ITG/MTG, right IPL-right ITG/MTG, and left and right ITG/MTG-right Paracingulate/SFG. All cortical-cortical results within frontoparietal network 13 displayed reductions in FC as RSBR-compulsive scores increased. The left IPL in frontoparietal network 8 displayed a significant positive correlation with both a right ACC/SFG ROI ($\rho(36) = 0.33, p < 0.04$) and a significant negative correlations with the left FP/OFC ROI ($\rho(36) = -0.39, p < 0.02$).

No significant correlations were identified between any ROIs within the limbic of the Choi/Yeo parcellation (network 10) and SRS-motivation scores. FC in ventral attention network and dorsal attention network, however, displayed relationships with SRS measures of social motivation. Both the left and right tail of the putamen relative to the right ACC displayed significant negative relationships with SRS social motivation scores (left: $\rho(36) = -0.33, p < 0.05$, right: $\rho(36) = -0.40, p = 0.01$) not unlike what was seen in the ASD vs TD comparisons. However, FC between the right tail of the putamen and the IFG/MFG in network 12 displayed a significant positive relationship with SRS-motivation ($\rho(36) = 0.33, p < 0.05$). The remaining significant correlations with SRS-motivation in dorsal attention network and ventral attention network are cortical-cortical, with the FC between the right OFC in and 3 other regions (right IFG/MFG, right IPL, left ACC) in dorsal attention network displaying significant negative correlations with SRS motivation (IFG/MFG: $\rho(36) = -0.37, p = 0.02$, IPL: $\rho(36) = -0.34, p = 0.04$, ACC: $\rho(36) = -0.35, p < 0.03$). Results within the ventral attention network revealed similarly negative relationships in FC and SRS-motivation between the right insula and bilateral IPL ROIs (left: $\rho(36) = -0.35, p = 0.03$; right: $\rho(36) = -0.40, p < 0.01$), and the right

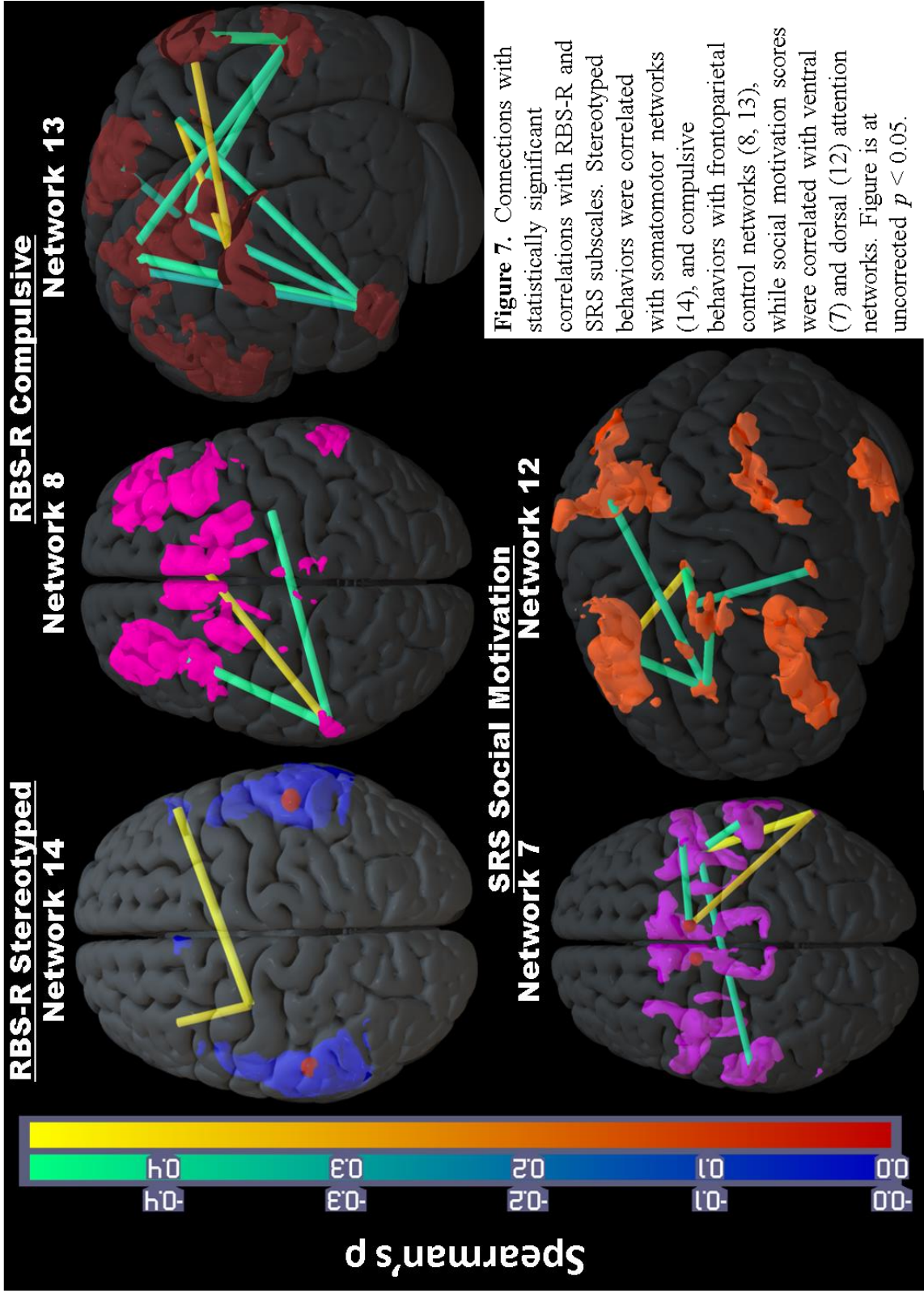
ACC/supplementary motor area (SMA) and an ROI containing precentral/postcentral gyrus ($\rho(36) = -0.36, p < 0.03$). An ROI containing the MTG/LOC and parts of the fusiform however, displayed significantly positive relationships with SRS-motivation and FC with the right ACC/SMA ($\rho(36) = 0.32, p < 0.05$) and insula ($\rho(36) = 0.43, p = 0.007$).

Correlations with behavior at an uncorrected threshold are summarized Table 4 and Figure 7. It should be noted that of all 446 comparisons conducted as part of the behavioral/FC correlation analysis, none survived a 5% FDR correction for multiple comparisons. As such, all results should be interpreted with caution given the low statistical power of this experiment. Additionally, FC within 3 ROI pairs (right insula-right MTG/LOC; right insula-right IPL; and left posterior body of the putamen and right IFG) were found to significantly correlate with FSIQ. Follow-up partial Spearman's ρ^{232} correlations found a stronger relationship between right insula and right MTG/LOC FC with increasing social motivation deficits when controlling for FSIQ ($\rho(35) = 0.50, p < 0.002$), and a similar but slightly weaker relationship between the putamen and IFG ($\rho(25) = -0.36, p = 0.03$). The insula-IPL connection however, resulted in an inversion of the relationship, with FC decreasing as social motivation impairments increased ($\rho(35) = -0.37, p = 0.02$) when accounting for FSIQ.

Table 4. Significant correlations between FC in Choi/Yeo networks with behaviors of interest.

	Connection		ρ	PValue	FDR-Pvalue
RBS-R 6 Stereotyped	Choi Left 14 Putamen body	Yeo Right 14 IFG	0.39	0.02	0.74
	Choi Left 14 Putamen body	Yeo Left 14 OFC	0.33	0.04	0.74
RBS-R 6 Compulsive	Choi Left 13 Caudate body	Yeo Right 13 IFG	0.35	0.03	0.74
	Choi Left 13 Caudate body	Yeo Right 13 IPL	0.37	0.02	0.74
	Yeo Right 13 FP	Yeo Right 13 ITG MTG	-0.41	0.01	0.74
	Yeo Right 13 FP	Yeo Left 13 ITG MTG	-0.37	0.02	0.74
	Yeo Right 13 FP	Yeo Right 13 SFG MFG	-0.34	0.04	0.74
	Yeo Right 13 IFG	Yeo Left 13 ITG MTG	-0.40	0.01	0.74
	Yeo Right 13 IPL	Yeo Right 13 ITG MTG	-0.47	<0.003	0.74
	Yeo Right 13 ITG MTG	Yeo Right 13 SFG Paracingulate	-0.40	0.01	0.74
	Yeo Left 13 ITG MTG	Yeo Right 13 SFG Paracingulate	-0.44	0.01	0.74
	Yeo Left 13 ITG MTG	Yeo Left 13 SFG	-0.32	0.05	0.74
	Choi Right 8 Putamen tail	Yeo Left 8 IPL	-0.37	0.02	0.74
	Yeo Right 8 ACC SFG	Yeo Left 8 IPL	0.34	0.04	0.74
	Yeo Left 8 FP OFC	Yeo Left 8 IPL	-0.39	0.02	0.74
SRS Social Motivation Raw Score	Choi Right 12 Putamen tail	Yeo Right 12 ACC	-0.40	0.01	0.74
	Choi Right 12 Putamen tail	Yeo Right 12 IFG MFG	0.33	0.05	0.74
	Choi Left 12 Putamen tail	Yeo Right 12 ACC	-0.33	0.05	0.74
	Yeo Right 12 IFG MFG	Yeo Right 12 OFG	-0.37	0.02	0.74
	Yeo Right 12 IPL	Yeo Right 12 OFG	-0.34	0.04	0.74
	Yeo Left 12 ACC Cingulate	Yeo Right 12 OFG	-0.35	0.03	0.74
	Yeo Right 7 ACC SMA Para	Yeo Right 7 MTG LOC	0.32	0.05	0.74
	Yeo Right 7 ACC SMA Para	Yeo Right 7 Preccn Postccn	-0.36	0.03	0.74
	Yeo Right 7 Insula Oper	Yeo Right 7 MTG LOC	0.43	0.01	0.74
	Yeo Right 7 Insula Oper	Yeo Right 7 Oper IPL	-0.40	0.01	0.74
	Yeo Right 7 Insula Oper	Yeo Left 7 IPL	-0.35	0.03	0.74

Somatomotor (RBS-R Stereotyped), Frontoparietal (RBS-R Compulsive), Limbic, Dorsal and Ventral Attention (SRS Social Motivation) networks.



Anatomical Correlates of FC:

The fiber count threshold required that at least 28 of the 38 participants in the analysis report tract streamline counts above threshold (set by image data quality by participant) between any pair of ROIs. This reduced the number of pairwise combinations of ROIs from 628 to 190. While all networks of interest in the parcellation had streamlines between at least 1 pair of ROIs, certain networks within the parcellation contained more tracts than others. Most streamlines surviving the threshold were cortical-cortical (176), but less than half as many connections were subcortical- cortical (133) and subcortical-subcortical (18) were also identified. Most of the streamlines were between frontoparietal ROIs (39%), which is not surprising considering that it is the largest network within the parcellation. This was followed by default mode network (31%), and dorsal/ventral attention networks (23%), with somatomotor (4%) and limbic (3%) networks accounting for the lowest number of tracts. The limbic network however, had the largest number of streamlines relative to possible combinations between ROI pairs at 100%, likely due to the lower number of possible combinations in the network (6) and their proximity (24-40 mm³ in MNI space) to one another. Summary statistics of streamline counts and results by network are displayed below in Table 5 and Figure 8.

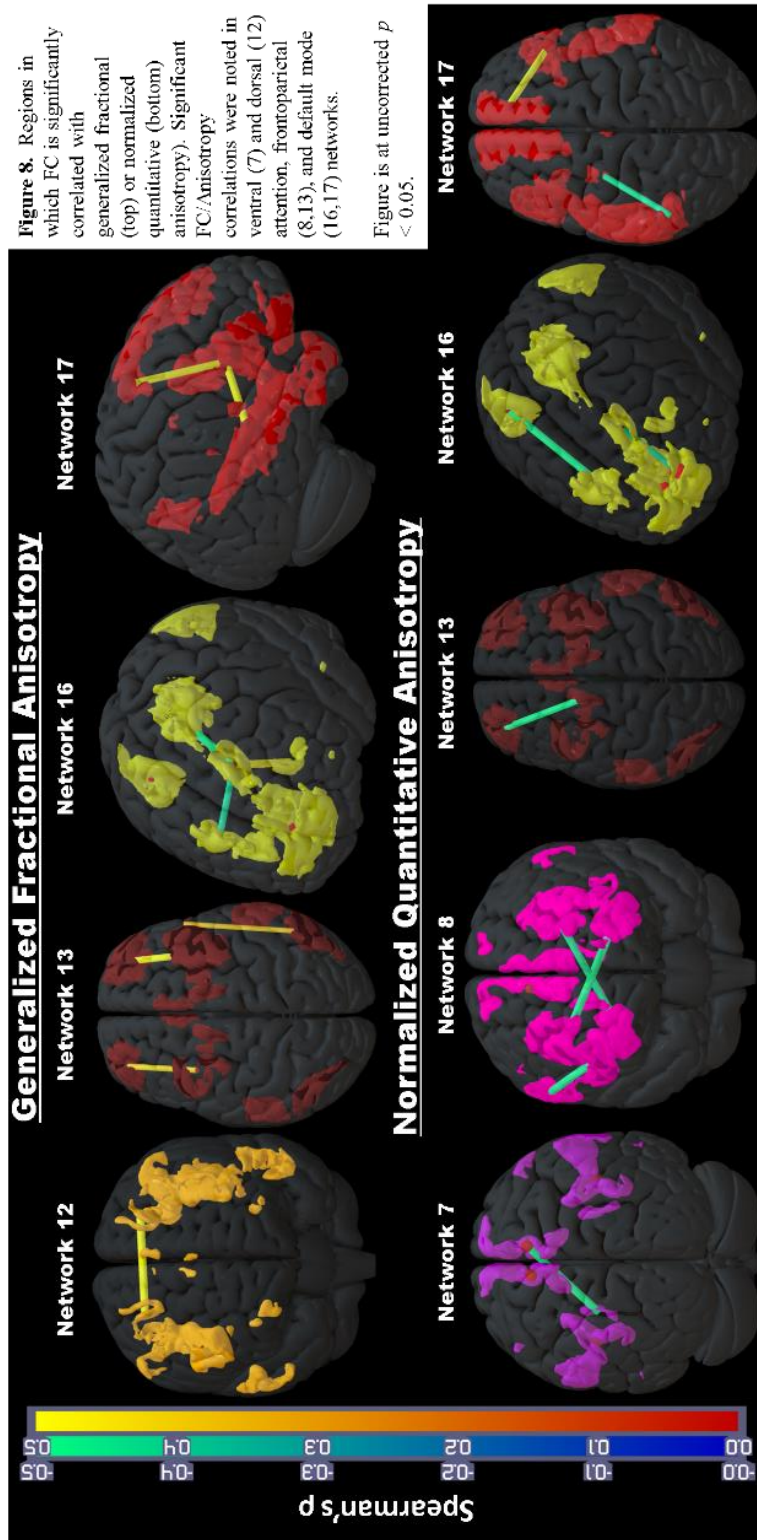


Table 5. Significant correlations between FC of Choi/Yeo regions and generalized and quantitative anisotropy.

	Connection	Motion Correction	p	% of Participants below threshold	PValue	FDR-Pvalue	
GFA	Yeo Right 12 SFG MFG	None	0.36	13.16	0.02	0.61	
	Yeo Right 13 FP	Yeo Right 13 SFG MFG	0.53	2.63	<0.001	0.14	
	Yeo Right 13 IFG	Yeo Right 13 IPL	0.38	13.16	0.02	0.56	
	Yeo Left 13 FP	Yeo Left 13 SFG MFG	0.44	5.26	0.01	0.56	
	Choi Left 16 Caudate head	Yeo Left 16 SFG	0.40	0.00	0.01	0.56	
	Yeo Right 16 FP MFG	Yeo Left 16 SFG	-0.35	2.63	0.03	0.74	
	Yeo Right 16 PCC Precuneous	Yeo Left 16 SFG	-0.42	23.68	0.01	0.56	
	Choi Left 17 Putamen tail	Yeo Left 17 FP OFC	0.39	5.26	0.02	0.56	
	Yeo Left 17 FP OFC	Yeo Left 17 MFG	0.36	0.00	0.03	0.61	
	NQA	Choi Left 7 Putamen tail	None	-0.35	2.63	0.03	0.75
		Choi Right 8 Caudate	Yeo Left 8 MFG	-0.34	7.89	0.04	0.75
		Choi Left 8 Putamen body	Yeo Right 8 FP MFG	-0.37	23.68	0.02	0.75
		Yeo Right 8 IPL	Yeo Right 8 OFC Insula	-0.37	5.26	0.02	0.75
		Choi Left 13 Caudate body	Yeo Left 13 FP	-0.50	0.00	<0.002	0.33
Yeo Right 16 LOC IPL		Yeo Right 16 MTG STG	-0.41	0.00	0.01	0.75	
Yeo Left 16 FP ACC		Yeo Left 16 SFG	-0.34	5.26	0.04	0.75	
Choi Left 17 Putamen tail		Yeo Left 17 IPL	-0.35	7.89	0.03	0.75	
Yeo Right 17 FP SFG		Yeo Right 17 OFC FP	0.40	0.00	0.02	0.75	

Motion correction indicates partial correlations were performed accounting for motion in BOLD or DWI scans. Participants below threshold describes the percentage of the 38 participants with streamline values of 0 due to counts below their respective false-fiber threshold.

Generalized Fractional Anisotropy: Of the 190 connections analyzed as part of the GFA analysis, 9 ROI pairs returned statistically significant at uncorrected p -values of $p < 0.05$ for each analysis. Four default mode, 3 frontoparietal, and 1 dorsal attention network ROI pair displayed statistically significant correlations between FC and GFA. Subcortical-cortical connections were limited to default mode network between the left head of the caudate and ipsilateral SFG ($\rho(35) = 0.40, p = 0.01$), and the left tail of the putamen with an ROI consisting of parts of the ipsilateral frontal pole and OFC ($\rho(35) = 0.39, p = 0.02$). These results required correction for DWI framewise displacement and mean RMSD motion respectively. The remaining results cortical-cortical relationships, with positive correlations between FC and GFA in interhemispheric MFG/SFG ROIs, left and right frontal pole ROIs with their ipsilateral MFG/SFG regions, right IFG with ipsilateral IPL, and a left frontal pole/OFC ROI with the ipsilateral MFG. Two default mode network connections however, displayed negative relationships with FC and GFA, with increasing FC between the right MFG and contralateral SFG, and right PCC and contralateral SFG associated with reduced GFA. Correlation values, types, motion/measure relationships, and uncorrected p -values are reported in Table 5. Of note, none of the statistically significant ROI pairs correspond to any regions of the (uncorrected) statistically significant group differences within AIM 1 of the analysis. Additionally, while many of the statistically significant correlations range from medium to large (0.33-0.50), half of the results displayed positive relationships between FC and GFA while others displayed negative relationships between FC and GFA. Additionally, these 9 results do not survive 5% FDR multiple comparison corrections.

Normalized Quantitative Anisotropy: Of the 190 connections analyzed as part of the NQA analysis, 8 ROI pairs displayed statistically significant negative relationships between FC and NQA at an uncorrected threshold of $p < 0.05$ for each test, with only one displaying a positive relationship. Four default mode, 4 frontoparietal, and 1 ventral attention network displayed significant correlations with FC at this threshold. Most of the frontoparietal connections were frontal-striatal, with connections from the caudate and putamen to contralateral medial frontal regions and ipsilateral frontal pole. Additional correlations between frontal-striatal FC and GFA were located between the left body of the putamen and an ACC/SMA ROI within the dorsal attention network, and the left putamen tail with the ipsilateral IPL in the default mode network. The remaining cortical-cortical connections were frontal-parietal, cingulofrontal, and interfrontal (which displayed increases in FC relative to increases in NQA) in default mode network, with the insula-IPL connection in the frontoparietal network. These results similarly did not survive a 5% FDR correction for multiple comparisons.

Assessments of Age and FSIQ: No significant correlations were identified between any of the clinical measures of interest (RBS-R & SRS) and age or FSIQ. However, FC and GFA measures between some ROIs were identified as correlating with age, some results were found to correlate with registration accuracy of the DWI data to the template, and age was found to be highly correlated with framewise displacement in diffusion data ($\rho = 0.44, p = 0.005$). Given this observation, 6 of the statistically significant correlations between GFA and these variables were re-analyzed using partial correlations to account for age, FSIQ, registration, and motion metrics as necessary. Once these variables were

included accounted for in the partial correlations, the ipsilateral frontal pole to MFG, right IFG to IPL, and right frontal pole to left SFG results were no longer significant (see Appendix Table 3).

DISCUSSION

Much of the attention of neuroimaging research in individuals with ASD has been either on the use of fMRI to confirm or expand the prevalent hypotheses in ASD-related behaviors (e.g. ToM deficits, alterations in perceptual processing streams, neural correlates of goal-oriented behavior), or in discovering MRI based “biomarkers” or “neural signatures” unique to individuals with ASD, or some combination of these. While several studies have proposed that FC may be a useful tool to identify the “neural fingerprints” unique to ASD, much of the work in the field has focused on cortical-cortical brain connections. While hippocampal²⁵⁴ and amygdalar^{98,101,254–257} connections have been frequently studied in the ASD/FC literature, the striatum (including the NAcc, caudate, and putamen) have received relatively little attention in individuals with ASD. This is surprising considering the findings proposing striatal dysfunction may be major contributors to stereotyped or compulsive behaviors and social reward processing in ASD.^{8,11,14,15,34,105,106,108,119,258–260} Additionally, the disrupted connectivity account of ASD propose that anomalies in FC stem from underlying alterations in white matter connections. While there is support for these hypotheses in the literature, many of the published results are more or less limited to a single domain of investigation (structural MRI, FC, or DWI) with post-hoc correlations calculated after TD/ASD group differences are identified. Additionally, many recent studies (including those in children and adults with ASD) have discovered that spurious group differences in FC and DWI may arise

from analytical strategies that do not adequately control for head motion.^{217,223–225,227,261}

The current study attempted to address these limitations and their effects by using both a traditional group-level analysis for FC and a novel, clinical-focused and FC/DWI analyses (embedded with multiple data quality assurance steps) to mitigate the impact of motion artifacts.

AIM 1

Contrary to our hypotheses of increased FC within the striatum and its targets in ASD, no group differences were found after a 5% FDR correction was applied. Even at the uncorrected level, very few cortical-striatal connections (a total of 9) differed between TD and ASD individuals. Increases in striatal-cortical connections from the left body of the putamen with the left OFC and right IFG in sensorimotor network 14 provides some support for our original hypothesis of increased connectivity with frontal ROIs in ASD. Similarly, increases in two subregions of the left caudate with the ipsilateral ITG/MTG in frontoparietal network 13 and right temporal pole in default mode network 17 are also in line with our original hypothesis derived from previous findings. However, many bilateral connections with the left and right putamen to a right precentral gyrus and left IPL in default mode network 8, and the right ACC in the dorsal attention network were found to be reduced in ASD, which provides less support for our original hypotheses. These findings appear relatively novel, as analytical approaches similar to ours parcellating the striatum into subregions¹⁷ have reported the inverse in precentral areas, and little mention of FC alterations in the putamen with and IPL. Alterations in FC for parietal areas has been reported previously in the caudate but not the putamen.¹⁷ Whether

these results stem from fundamentally different methods of analysis (e.g. ROI-vs-voxel based, single vs multi-level parcellation of the striatum), sample variability (previous studies had a smaller age range),¹⁷ or reflect a genuine relationship with compulsive behaviors is difficult to say with the current limitations in statistical power.

The remaining 18 results at an uncorrected statistical threshold (see Table 3) were cortical-cortical connections between temporal, frontal, parietal, and cingulate areas, primarily favoring reductions in individuals with ASDs (15/18). These were almost exclusively within frontoparietal regions, which are typically associated with cognitive control.^{235,236} The remaining 7 comprise frontal-parietal or cingulo-frontal ventral attention (3), dorsal attention (1), or intrahemispheric frontal-frontal or cingulo-parietal default mode (3) connections. Cortical-cortical, especially frontal-parietal “long distance” connections are frequently reported in both the task and resting-state literature in individuals with ASD and multiple review papers are available discussing their consistency and implications.^{82,83,158,230,262} However, our results noted 3 exceptions to this trend in increased connectivity between the right insula to right MTG/LOC, right ACC/SFG to left IPL, and right IPL to left SFG/MFG (corresponding to the ventral attention, frontoparietal network 8, and default mode network 17 respectively). The insula-MTG/LOC result is interesting considering the role of the MTG/LOC in object recognition.

The lack of ASD/TD group differences in cortical-striatal regions typically associated with reward (NAcc and OFC) does not seem to support the theories of general dysfunction within reward circuitry in ASD. Results in attention networks may suggest that disruption in attentional streams may possibly play a greater role than those of

reward. However, it is worth noting that there are considerably greater numbers of combinations of cortical and subcortical connections across the regions in both dorsal and ventral attention networks compared to the limbic ROIs (171 to 6 respectively) typically associated with reward processing. Statistically significant alterations (mostly reductions in ASD) in FC between frontoparietal regions were frequent (12/27 results) and large ($g = 0.65-0.91$), suggesting that FC between brain regions associated with cognitive-control^{235,236} may be significantly altered in ASD. However, frontoparietal network pairs (constituting half of the significant group differences may also have a bias in this parcellation as this network contains 227 pairwise combinations (~36% of all possible combinations) and may be more likely to be statistically significant due to chance. As such, claims of disruptions in the connectivity of brain regions associated with cognitive control will require additional experiments using inhibition tasks. However, group differences in default mode ROIs were present but sparse despite a similarly large representation within the parcellation (182 pairs or 30% of the parcellation) and subcortical-cortical somatomotor regions were greater in individuals with ASDs despite constituting a relatively low percentage of the total possible combinations (~7%) with relatively large effect sizes ($g \geq 0.6$). Alterations in subcortical-cortical somatomotor regions, if replicated, could provide important insights into repetitive behaviors in ASDs.

AIM 2

Correlations of FC with Behavioral Measures:

There was considerable overlap between the results of FC/behavioral correlations and the results of group comparisons, with 16 of the 26 correlations between behavioral measures present in the same ROI pairs that were significant in the TD vs ASD group comparisons. This is not surprising given that these measures were developed to categorize the presence or absence of behaviors within individuals with ASDs. The results from the sensorimotor networks are a good example, with increasing incidence of stereotyped behavior correlating with increased FC between the left posterior body of the putamen and frontal regions such as the OFC and IFG. This supports the initial hypothesis of a relationship between stereotyped behaviors and sensorimotor FC.

Interestingly, there were 11 ASD/TD group differences that did not correspond to any correlations between FC and clinical measures, and 10 correlations between FC and clinical measures that were not present within the group analysis. These differences were primarily driven by additional FC/behavioral correlations with frontoparietal and attention networks and an absence of default mode results in FC/behavioral correlations. There was data available in the literature to suggest default networks would be correlated with the subscales of interest. For example, increases in FC between the caudate and contralateral ROIs near the IFG and IPL, were associated with a greater incident of compulsive behaviors, identified as part of the behavioral correlation analysis but not the group comparisons. Coincidentally, similar putamen ROIs in the group analysis which displayed reductions in FC do not correlate with these behaviors in post-hoc brain-behavior correlations in the ASD-only group. Attention networks correlating FC with

SRS-motivation similarly mirrored the ASD vs TD comparisons, with 7 pairs of ROIs replicating across group and behavioral analyses, but 4 pairs on each analysis producing results unique to the other. General results seem to indicate a reduction in putamen tail to ACC and frontal-parietal FC when there is greater motivation to engage in social stimuli in a participant. The exception to this is the right putamen tail and right IFG/MFC, which displays increasing FC with greater impairment in social motivation. This result was not present in the initial analysis for ASD vs TD. Interestingly, as social motivation impairment increases, FC between a right MTG/LOC ROI containing parts of the LOC and right insula, ACC/SMA, the latter of which was not present in the ASD vs TD analysis. Like the frontoparietal network results, none of the attention network results unique to the ASD group was significantly correlated with SRS-motivation measures.

Analyses from this behavior-centric framework seem to result in reduced connectivity between frontal and temporal ROIs with increasingly severe compulsive behaviors, and reductions in FC with decreasing social motivation impairment in inter-frontal (ACC:SFG and SFG:OFC), frontal-parietal, cingulo-frontal, and subcortical-cingulo connections. The findings of increased FC between subcortical to cortical IFG/MFG and frontal and cingulate regions with an area comprising the fusiform is of note given the role the former plays in communication and language and the latter in face processing. Both the IFG and fusiform responses are frequently described as atypical in both BOLD signal^{101,263,264} and FC^{256,265} in the ASD literature. The prospect that FC between cortical and subcortical ROIs is increased with social motivation impairment may provide insights into the role of communication and perception in social motivation with relevant behavioral experiments in the future. Nevertheless, caution is advised in

generalizing the current model considering none of the results survived corrections for multiple comparisons. Additionally, the finding that at least one behavioral result had a directional change once FSIQ was accounted for (Right Insula to right IPL in the ventral attention network with SRS-Motivation) in the analysis suggests that these variables may exert greater influence on FC than we were able to assess with our sample; in addition, previous work on subcortical structures suggests this may be the case.^{266,267} It is also possible that our sample is highly variable (9 of the ASD participants were medicated with antipsychotic, stimulant, anticonvulsant, or antiadrenergic medication) despite our attempts to match on age and FSIQ. However, multivariate approaches to assess contributions of such developmental factors such as age and IQ in a much larger sample are needed for adequate statistical power for such generalizations.

The combination of the behavioral/FC correlations seem to indicate that analyses of brain-behavior relations in ASD are capable of both providing the same information as an analysis of group differences, but also additional regions relative to behaviors of interest with the bonus of providing directional effects of FC relative to the behaviors of interest. The correlations were also relatively strong even at an uncorrected statistical threshold ($\pm 0.32-0.47$ based on a medium effect of ≥ 0.30 and a large effect ≥ 0.50). This behavior-centric approach to fMRI analyses of brain function fits well with the NIH RDoC initiative urging symptom-based studies across diagnoses to develop better models of brain function. This is especially relevant to research within the ASD population since so many individuals with ASD express comorbid conditions that overlap with ASD symptoms. Any of which has the potential to be mediating or moderating variables on a specific behavioral domain. Leveraging large datasets like ABIDE and ADHD-200 have

the potential to identify brain regions associated with behavioral or clinical domains. Some research groups and brain parcellations have already begun this line of research.²⁶⁸ Such models would be extremely useful for studying the mechanisms of brain function or diagnostic subdomains within a given clinical population, but the heterogeneity in behavioral questionnaires and data collection practices severely limit the possibility of such research in the future. Should these practices improve, inclusion of these variables using multivariate techniques could lead to informative models of how the brain functions in individuals with ASDs.

Correlations with FC and Anisotropy Measures:

The relatively low number of streamlines between ROIs in the parcellation (190 of 628 original pairs) is not surprising given the limitations of the pairwise approach to diffusion streamlines used for the analysis. It however, highlights 2 important features worth considering when implementing multi-modal MRI data analysis techniques: 1) Any analysis proposing that FC may be a result of underlying neuroanatomy may wish to perform tractography first to establish anatomical connections between ROIs of interest. 2) If connections span multiple brain regions, higher order models (2nd...nth order connections) may be necessary to examine structure-function relationships. Graph theory techniques may have the potential to address higher order connections (in which connectivity between 2 or more regions is moderated by FC or physical connections between a third region) in these types of analyses. Q-based,^{72,269} and persistent homological^{252,270} graph theory approaches have been utilized previously to address such

questions, but our current ODF-based diffusion model does not lend itself well to such techniques. As such, it is a venue of future development.

FC with GFA:

Contrary to our initial hypotheses, only a handful of ROI pairs exhibited significant correlations between FC and GFA even at uncorrected statistical thresholds. This is surprising considering several previous studies report relatively high correlations between default mode regions and FA. The finding that more than half of the results were in default mode regions however, coincides with this previous work. Also, in contrast to our hypothesis, only one GFA/FC correlation overlapped with a previous behavior/FC result. This relationship found increases in FC between the right frontal pole and right SFG/MTG associated with decreases in RBS-R scores and increases in GFA. However, when correlated with each other, RBS-R scores did not exhibit significant correlations with GFA between these regions ($\rho(36) = -0.24, p = 0.15$). Also surprising is the lack of sensorimotor results within the analysis considering that much of the parcellation was derived from a combination of functional connections between motor regions and anatomical tract tracings in macaque monkeys.⁶⁴ Most of the FC/GFA correlations display positive relationships between GFA and FC between intra-frontal, frontal-parietal, and frontal-striatal connections, with frontal-posterior-cingulo and intra-frontal MFG to SFG as the exception. However, once considering the finding that a third of the results are no longer significant once potential effects of age or registration accuracy are addressed, the default mode ipsilateral FP to MFG, contralateral FP to SFG, and frontoparietal IFG to IPL results should be interpreted with caution.

FC with NQA:

The finding that all but one of the significant results at an uncorrected threshold displayed small to moderate (0.34-0.50) negative relationships with NQA comes in stark contrast to our initial hypothesis, the implications of which are concerning. Given that QA/NQA is theoretically more robust to false fibers and artifacts from crossing fibers as it is calculated at the level of the fiber and not the voxel,¹⁸⁶ the method should be more representative of the underlying anatomy compared to GFA. The fact that the results of GFA and NQA analyses do not overlap seems to support the idea that each are providing different information. However, the finding that FC decreases with increasing NQA seems to suggest that increases in functional connections are associated with “less dense” underlying white matter. To our knowledge, our group is the first to use this measure relative to FC, and future work to explain it will be required, but given that relatively few ROI pairs had NQA/FC correlations, it would appear that measures of white matter tractography have little to do with FC without the use of higher order models.

In summary, our analyses do not seem to support our initial hypotheses of alterations in FC between brain regions typically associated with reward (limbic) ASD influencing social motivation. However, an uncorrected trend of reduced striatal-cortical connectivity reductions in ASD subcortical-cortical FC in dorsal attention regions which correlate negatively with SRS motivation scores (larger scores mean more impairment) may imply that alterations in brain regions associated with attention may contribute more to dysfunctions in social motivation than reward regions. This would be an inversion of the social motivation hypothesis (which proposes that the lack of reward drives attention), and would imply that attentional systems for the preparation and response for

goal-directed behaviors (aka: task positive).^{201,271} It could easily be argued that social stimuli fall under this umbrella, and may reflect difficulty with communication or social navigation in such situations. The subcortical-cortical relationships between frontoparietal and somatomotor is interesting, as frontoparietal is associated with cognitive control^{235,236} and seems to display a general reduction in FC in ASD and general increases in subcortical-cortical FC with incidences of compulsive behaviors. In contrast, FC between subcortical-cortical somatomotor regions were higher in ASD and associated with greater incidences of compulsive behaviors. The cortical-cortical results mirrored these trends, with primarily reductions in FC between frontoparietal regions in ASD associated with greater incidences of compulsive behaviors, but added some alterations in ventral attention regions that were primarily associated decreases in FC with increasing social motivation impairments. The exception to the ventral attention network results being connections between the MOG (which is heavily involved in object processing) and ACC/insula regions. These may highlight imbalances between inhibition from control networks (via frontoparietal regions), difficulty filtering and reorienting to relevant stimuli (via dorsal attention and ventral attention networks), and overactivity of somatomotor regions in ASD. Caution is advised however, as these conclusions are highly reverse-inferential and will require task-based experiments to assess the validity of such conclusions, and many of the cortical-cortical results may be subject to the potential effects of distance-dependence.

Strengths, Limitations, and Future Directions:

We made considerable efforts to mitigate participant and MRI based artifacts within our sample, and constrain our analyses to participants with relevant behavioral and quality diffusion data to study structure-function and brain-behavior relationships within ASD. This has given us confidence that our results are minimally artifact-driven. Unfortunately, these practices limited our number of viable participants, reducing the power of the analysis to detect a significant effect (should it be present) to 64% (based on a β/α ratio of 4 [.80/.05]) assuming an effect size of Cohen's $f^2 = 0.15$ as calculated from a compromise power analysis in G*Power^{272,273} before the mass-univariate nature of MRI analyses are considered. This is an unfortunate limitation that the authors acknowledge stemming from heterogeneous phenotypic data-collection practices across ABIDE-II centers. It should also be noted that a small but statistically significant difference was identified for distance-dependence artifact across all ROI pairs of interest ($\rho(626) = -0.08, p < 0.05$), which may affect measures of “long distance” connections. Comparisons of RMSD motion between the did not find significant differences in median RMSD in TD compared to ASD groups ($Z = 351, p = 0.60, r^{bs} = 0.09, CI95 -0.24,0.42$). The lack of significant group differences in motion may suggest that group differences in mean RMSD motion are not a concern in the analysis. However, much of the literature suggests this artifact may occur even in minimal (typically not flagged for scrubbing) differences in motion, which is worth considering in studies of pediatric populations in which thresholds for motion are typically less conservative. Follow up correlations with mean RMSD did not reveal any significant relationships with FC in any group level ROI pair, leading the authors to conclude any such relationships have been mitigated to the best

possible degree. Similarly, DWI data was normalized to an adult template, which is typically not suggested for a pediatric population. The T1 weighted co-registration prior to normalization should have aided in addressing potential confounds related to this issue, but there are studies in the literature that have reported artefactual results in age-related studies as a function of extensive warping from smaller brains to a larger template.^{195,196,198,274,275} We are exploring methods to minimize such artifacts, including weighting results by Euclidean distance in native space, weighting tractography counts by total intracranial volume, or treating total intracranial volume as a covariate in future analyses. However, further research is necessary to establish the effects of distance and image warping in populations in which these parameters are typically high.

The discrepancy in the FC/Anisotropy results in this study compared to others may stem from heterogeneity in tractography approaches. While much of the previous work similarly utilizes whole-brain tractography, previous work has used smaller numbers of ROIs,²⁷⁶ native-space tracking,^{71,74,276} and many have used lower resolution diffusion data except for Honey et al. 2009, which used a higher-order diffusion scheme not yet available on ABIDE-II. However, none of these studies, to date, have utilized higher-order tensors or ODF based models to guide tractography. This is surprising given the number of advancements in tractography algorithms in the last decade and research suggesting that anywhere from 60-90% of white matter voxels in the brain contain fiber crossings.⁷⁶ While we are unsure if this may be why the results are inconsistent, it is widely accepted that FA and GFA are more susceptible to partial volume effects, reductions from crossing fibers, and FA is defined at the voxel rather than the fiber level (QA is defined at the level of the fiber). While we have made every attempt to ensure

that results are not driven by artifact (i.e. motion, SNR, registration errors), more work is needed to assess the validity and reliability of these different approaches with higher-resolution data. Our choice of a “connectivity threshold” to filter out potentially false fibers, in theory, should have aided with accuracy, but given that these thresholds can be subject-specific and may relate to other data quality metrics, it could have introduced biases into the analyses.

Many of the models proposed for the role of the striatum in human and animal behavior note the relationship between learning and reward within these subcortical circuits. Unfortunately, the cortical parcellation chosen for our analysis did not include any functional connections between the striatum and hippocampus or amygdala. This is not an insignificant limitation given the number of functional and structural connections between the hippocampus and amygdala with the striatum and cortex frequently noted in human and animal literature. However, mapping individual subregions of the striatum to subregions of the HIP and AMYG would be an enormous scientific undertaking. Ideally future research will explore voxelwise FC with cortical-limbic regions such as those performed by Choi et al., 2012. Identifying such relationships and relating them back to the striatum is important considering limbic areas have the strong potential to be moderators for frontal-striatal networks (e.g. NAcc, HIP, vmPFC connections for goal oriented behavior). Additionally, many other subcortical regions (e.g. subthalamic nucleus and SN) are greatly involved in the behavior of the striatum but are not easy to resolve using MRI without specific protocols designed for their acquisition. We intend to re-visit limbic-to-striatal connections, and how they related to the cortex, as such parcellations improve with the literature. Open source MRI initiatives, increased

structural resolution, and novel analytical techniques move the field towards this goal with each development. However, it should be noted that the approach taken by the authors and the atlas developers is not inconsequential given that much of the striatal parcellation was validated in a large sample (1000 individuals), is based on previous work in somatomotor network, and tract tracing in primates. However, while the organization and topology of the striatum from the atlas may be accurate, developmental shifts in these locations are possible within pediatric samples, which is outside the framework of the current study.

Most importantly, the authors acknowledge that the analysis above is based upon resting-state FC with networks associated with specific tasks. While there is evidence to support task-based network topology is preserved in resting-state paradigms,^{64,277} task-based fMRI analyses are currently still the best tool for identifying neural correlates when a task is performed or a psychological state is inferred (with appropriate controls). The authors intend to explore neural correlates of cortical-striatal networks associated with reward processing and motor planning in the future, attempting to link cortical-striatal BOLD signal and tractography to subsets of the ASD phenotype using a behavior-first approach proposed as part of continued work stemming from the results proposed in this document. Behaviorally relevant neural correlates of ASD are critical given the heterogeneous nature of the ASD phenotype.

One unavoidable confound of the current experiment is the influence of medication effects on BOLD signal and diffusion within our patient population. Three participants were actively taking central antiadrenergic medication during the scan, which has the potential to affect global BOLD signal. At least five were taking some form of

dopaminergic CNS stimulant or antipsychotic, three were on serotonergic antidepressants, and at least one participant was on a GABA-based anticonvulsant. Most of these medications impact the circuitry of interest in some form (particularly striatal reward circuitry). However, all the participants on medication were children with ASD, and removing these participants from the analysis would have resulted in only 10 ASD participants. The lack of statistical power due to the small sample size has been noted multiple times throughout the document. While the participants needed to be retained to prevent severe skewing of the sample, it is possible that medication may have blunted group differences or behavioral relationships with BOLD signal.

Worth noting however, is that many individuals with ASD have additional diagnoses beyond ASD (e.g. ADHD, MDD, OCD, Anxiety, Tics) that have the potential to affect striatal, control, sensorimotor, and other networks or combinations of networks. Many individuals on the spectrum, including children, are typically on one or more forms

of psychotropic medication for ASD or a comorbid

condition.²⁷⁸ A

recent work

analyzing the

potential effects

of medication on

connectivity

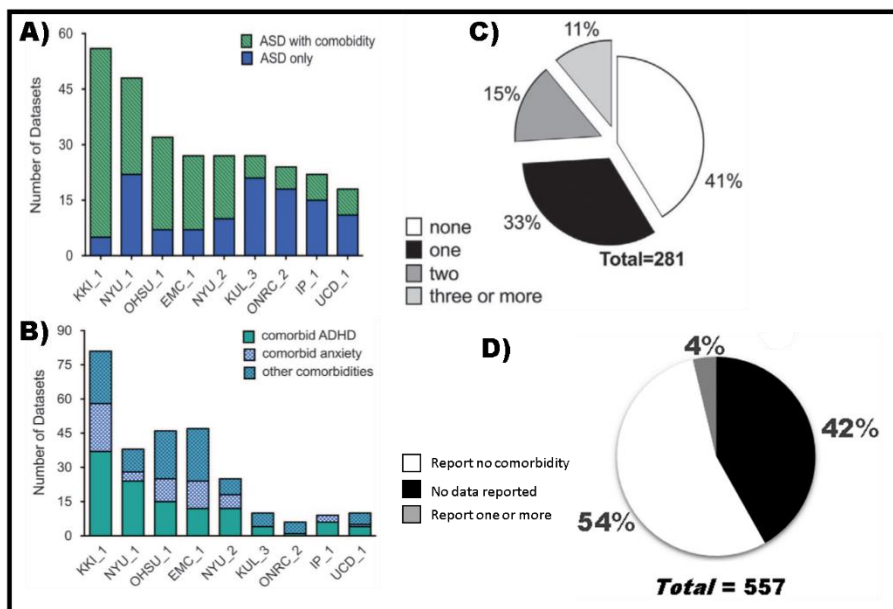


Figure 9. Adapted figure from *Figure 2 of DiMartino et al. 2017*. A) Distribution of the 9 ABIDE datasets where comorbidities with ASD are reported. B) Distribution of most common comorbidities (ADHD and anxiety). C) Distribution of total participants with ASD with and without comorbid conditions from sites in A. D) Distribution of ASD participants from phenotypic data file for ABIDE-II users in which comorbidities, no comorbid conditions, or no data from participants collected.

(including striatal-cortical and cortical-cortical) suggested that individuals with ASDs that are on such medications have cortical-cortical and striatal-cerebellar alterations in FC compared to individuals with ASD that are not on such medications.²⁷⁹ What is worth noting however, is that few if any studies, to date, have assessed the contribution of any of these conditions to brain function in ASD. This is despite the numerous findings that relatively few individuals with ASD report no comorbidities.^{124,126,129,135,137} As such, there is considerable uncertainty that alterations in FC are driven by the psychotropic medication itself or the condition(s) that it is designed to treat within individuals with ASDs.

The ABIDE database notes that a large majority of the participants in the samples have comorbid conditions, with 60% of ASD participants reporting one or more comorbid psychiatric diagnoses. ADHD and anxiety disorders are the most frequently reported (see DiMartino Figure 9),²⁸⁰ but few of the data sets (9 of the now 26 sites) have collected such information. We propose that future analyses and data collection initiatives collect not only data on comorbid conditions from individuals with ASD, but also measures of commonly occurring comorbidities (e.g. ADHD and anxiety measures), or large-scale tests such as the Structured Clinical Interview for DSM (S.C.I.D.) or M.I.N.I. International Neuropsychiatric Interview (M.I.N.I.) to analyze the contribution of such measures. Additionally, it is strongly advised that future research focus on neural correlates of behaviors of interest in individuals with ASD (similar to RDoC criteria), as our results suggest that a focus using this approach not only preserves results similar to those identified by group contrasts, but also may identify brain regions unique to such behaviors. Given the overlap many ASD symptoms share with other diagnoses, and the

high rate of comorbidities in ASD, it is becoming clearer that ASD is a multifactorial disorder that will require multifactorial, not dichotomous, solutions.

Neuroimaging as a field is heterogeneous, even across similar modalities of imaging. Inconsistencies in results even within similar datasets or paradigms could stem from a number of factors, including: 1) non-standardized definitions of results and measures of structural and functional connectivity,¹⁵⁸ 2) variability in data processing, filtering, and analytical approaches to studying connectivity,^{6,158,281,282} 3) a lack of robustness (lack of similarity of results across participants, different scan parameters and data acquisition techniques),^{281,283} and 4) the influence of other factors such as development,^{6,284} or clinical heterogeneity⁶ on measures of functional and structural connectivity. Initiatives such as HCP and INDI have been attempting to address some of these issues to a degree through standardized preprocessing protocols, but effect sizes specific to scanner type and field strength can not only be significantly different from one another,²⁸⁵⁻²⁸⁷ but also influenced by other factors such as age of the participants,^{288,289} which may eclipse the effects specific to diagnosis. Adequate considerations and corrections to data acquired from different scanners can aid in the former, and informed participant recruitment strategies and criteria can help mitigate the latter. However, to truly address these concerns, consistency across scan parameters and protocols such as those implemented by HCP will be required.

REFERENCES

- 1 Christensen DL, Baio J, Braun KVN, Bilder D, Charles J, Constantino JN, *et al.* Prevalence and Characteristics of Autism Spectrum Disorder Among Children Aged 8 Years - Autism and Developmental Disabilities Monitoring Network, 11 Sites, United States, 2012. *MMWR Surveill Summ* 2016;**65**:1–23. <https://doi.org/10.15585/mmwr.ss6503a1>.
- 2 Control C for D. Estimated Prevalence of Autism and Other Developmental Disabilities Following Questionnaire Changes in the 2014 National Health Interview Survey. *Natl Health Stat Report* 2015:1–21.
- 3 American Psychiatric Association. *DSM-5*. 2013.
- 4 Just MA, Cherkassky VL, Keller TA, Kana RK, Minshew NJ. Functional and anatomical cortical underconnectivity in autism: Evidence from an fmri study of an executive function task and corpus callosum morphometry. *Cereb Cortex* 2007;**17**:951–61. <https://doi.org/10.1093/cercor/bhl006>.
- 5 Kana RK, Libero LE, Moore MS. Disrupted cortical connectivity theory as an explanatory model for autism spectrum disorders. *Phys Life Rev* 2011:410–37. <https://doi.org/10.1016/j.pprev.2011.10.001>.
- 6 Picci G, Gotts SJ, Scherf KS. A theoretical rut: revisiting and critically evaluating the generalized under/over-connectivity hypothesis of autism. *Dev Sci* 2016;**19**:524–49. <https://doi.org/10.1111/desc.12467>.

- 7 Hollander E, Anagnostou E, Chaplin W, Esposito K, Haznedar MM, Licalzi E, *et al.* Striatal volume on magnetic resonance imaging and repetitive behaviors in autism. *Biol Psychiatry* 2005;**58**:226–32.
<https://doi.org/10.1016/j.biopsych.2005.03.040>.
- 8 Langen M, Schnack HG, Nederveen H, Bos D, Lahuis BE, de Jonge M V., *et al.* Changes in the Developmental Trajectories of Striatum in Autism. *Biol Psychiatry* 2009;**66**:327–33. <https://doi.org/10.1016/j.biopsych.2009.03.017>.
- 9 Langen M, Bos D, Noordermeer SDS, Nederveen H, Van Engeland H, Durston S. Changes in the development of striatum are involved in repetitive behavior in autism. *Biol Psychiatry* 2014;**76**:405–11.
<https://doi.org/10.1016/j.biopsych.2013.08.013>.
- 10 Dawson G, Meltzoff AN, Osterling J, Rinaldi J, Brown E. Children with autism fail to orient to naturally occurring social stimuli. *J Autism Dev Disord* 1998;**28**:479–85.
- 11 Dawson G, Osterling J, Rinaldi J, Carver L, McPartland J. Brief Report: Recognition Memory and Stimulus-Reward Associations: Indirect Support for the Role of Ventromedial Prefrontal Dysfunction in Autism. *J Autism Dev Disord* 2001;**31**:337–41. <https://doi.org/10.1023/A:1010751404865>.
- 12 Chevallier C, Kohls G, Troiani V, Brodtkin ES, Schultz RT. The social motivation theory of autism. *Trends Cogn Sci* 2012:231–8.
<https://doi.org/10.1016/j.tics.2012.02.007>.
- 13 Dichter GS, Richey JA, Rittenberg AM, Sabatino A, Bodfish JW. Reward circuitry function in autism during face anticipation and outcomes. *J Autism Dev Disord*

- 2012;**42**:147–60. <https://doi.org/10.1007/s10803-011-1221-1>.
- 14 Dichter GS, Felder JN, Green SR, Rittenberg AM, Sasson NJ, Bodfish JW. Reward circuitry function in autism spectrum disorders. *Soc Cogn Affect Neurosci* 2012;**7**:160–72. <https://doi.org/10.1093/scan/nsq095>.
- 15 Abrams D a, Lynch CJ, Cheng KM, Phillips J, Supekar K, Ryali S, *et al*. Underconnectivity between voice-selective cortex and reward circuitry in children with autism. *Proc Natl Acad Sci U S A* 2013;**110**:12060–5. <https://doi.org/10.1073/pnas.1302982110>.
- 16 von dem Hagen EAH, Stoyanova RS, Baron-Cohen S, Calder AJ. Reduced functional connectivity within and between ‘social’ resting state networks in autism spectrum conditions. *Soc Cogn Affect Neurosci* 2013;**8**:694–701. <https://doi.org/10.1093/scan/nss053>.
- 17 Di Martino A, Kelly C, Grzadzinski R, Zuo XN, Mennes M, Mairena MA, *et al*. Aberrant striatal functional connectivity in children with autism. *Biol Psychiatry* 2011;**69**:847–56. <https://doi.org/10.1016/j.biopsych.2010.10.029>.
- 18 Nair A, Carper RA, Abbott AE, Chen CP, Solders S, Nakutin S, *et al*. Regional specificity of aberrant thalamocortical connectivity in autism. *Hum Brain Mapp* 2015;**36**:4497–511. <https://doi.org/10.1002/hbm.22938>.
- 19 Cerliani L, Mennes M, Thomas RM, Di Martino A, Thioux M, Keyzers C. Increased Functional Connectivity Between Subcortical and Cortical Resting-State Networks in Autism Spectrum Disorder. *JAMA Psychiatry* 2015;**72**:1–11. <https://doi.org/10.1001/jamapsychiatry.2015.0101>.
- 20 Travers BG, Adluru N, Ennis C, Tromp do PM, Destiche D, Doran S, *et al*.

- Diffusion tensor imaging in autism spectrum disorder: a review. *Autism Res* 2012;**5**:289–313. <https://doi.org/10.1002/aur.1243>.
- 21 Sporns O, Tononi G, Kötter R. The human connectome: A structural description of the human brain. *PLoS Comput Biol* 2005:0245–51. <https://doi.org/10.1371/journal.pcbi.0010042>.
- 22 Sporns O. The human connectome: A complex network. *Ann N Y Acad Sci* 2011:109–25. <https://doi.org/10.1111/j.1749-6632.2010.05888.x>.
- 23 Yeh F-C, Vettel J, Singh A, Poczos B, Grafton S, Erickson K, *et al*. Local Connectome Fingerprinting Reveals the Uniqueness of Individual White Matter Architecture. *bioRxiv* 2016:43778.
- 24 Kana RK, Keller TA, Cherkassky VL, Minshew NJ, Just MA. Atypical fronto-posterior synchronization of theory of mind regions in autism during mental state attribution. *Soc Neurosci* 2009;**4**:135–52. <https://doi.org/10.1080/17470910802198510>.
- 25 Just MA, Keller TA, Malave VL, Kana RK, Varma S. Autism as a neural systems disorder: A theory of frontal-posterior underconnectivity. *Neurosci Biobehav Rev* 2012:1292–313. <https://doi.org/10.1016/j.neubiorev.2012.02.007>.
- 26 Cherkassky VL, Kana RK, Keller TA, Just MA. Functional connectivity in a baseline resting-state network in autism. *Neuroreport* 2006;**17**:1687–90. <https://doi.org/10.1097/01.wnr.0000239956.45448.4c>.
- 27 Kana RK, Liu Y, Williams DL, Keller TA, Schipul SE, Minshew NJ, *et al*. The local, global, and neural aspects of visuospatial processing in autism spectrum disorders. *Neuropsychologia* 2013;**51**:2995–3003.

- <https://doi.org/10.1016/j.neuropsychologia.2013.10.013>.
- 28 Libero LE, Maximo JO, Deshpande HD, Klinger LG, Klinger MR, Kana RK. The role of mirroring and mentalizing networks in mediating action intentions in autism. *Mol Autism* 2014;**5**:50. <https://doi.org/10.1186/2040-2392-5-50>.
- 29 Murdaugh DL, Shinkareva S V, Deshpande HR, Wang J, Pennick MR, Kana RK. Differential Deactivation during Mentalizing and Classification of Autism Based on Default Mode Network Connectivity. *PLoS One* 2012;**7**:e50064. <https://doi.org/10.1371/journal.pone.0050064>.
- 30 Libero LE, DeRamus TP, Lahti AC, Deshpande G, Kana RK. Multimodal neuroimaging based classification of autism spectrum disorder using anatomical, neurochemical, and white matter correlates. *Cortex* 2015;**66**:46–59. <https://doi.org/10.1016/j.cortex.2015.02.008>.
- 31 Bodfish JW, Symons FJ, Lewis MH. The repetitive behavior scales (RBS). *West Carolina Cent Res Reports* 1999.
- 32 Bodfish JW, Symons FJ, Parker DE, Lewis MH. Varieties of repetitive behavior in autism: Comparisons to mental retardation. *J Autism Dev Disord* 2000;**30**:237–43. <https://doi.org/10.1023/A:1005596502855>.
- 33 Constantino JN, Gruber C. The Social Responsiveness Scale Los Angeles. 2002. *Calif West Psychol Serv* n.d.
- 34 Schmitz N, Rubia K, Van Amelsvoort T, Daly E, Smith A, Murphy DGM. Neural correlates of reward in autism. *Br J Psychiatry* 2008;**192**:19–24. <https://doi.org/10.1192/bjp.bp.107.036921>.
- 35 Liu X, Hairston J, Schrier M, Fan J. Common and distinct networks underlying

- reward valence and processing stages: A meta-analysis of functional neuroimaging studies. *Neurosci Biobehav Rev* 2011;1219–36.
<https://doi.org/10.1016/j.neubiorev.2010.12.012>.
- 36 Haber SN, Knutson B. The reward circuit: linking primate anatomy and human imaging. *Neuropsychopharmacology* 2010;**35**:4–26.
<https://doi.org/10.1038/npp.2009.129>.
- 37 Elliott R, Elliott R, Friston KJ, Dolan RJ. Dissociable neural responses in human reward systems. *J Neurosci* 2000;**20**:6159–65.
<https://doi.org/20/16/6159> [pii].
- 38 Ernst M, Nelson EE, Jazbec S, McClure EB, Monk CS, Leibenluft E, *et al*. Amygdala and nucleus accumbens in responses to receipt and omission of gains in adults and adolescents. *Neuroimage* 2005;**25**:1279–91.
<https://doi.org/10.1016/j.neuroimage.2004.12.038>.
- 39 Cauda F, Cavanna AE, D’agata F, Sacco K, Duca S, Geminiani GC. Functional Connectivity and Coactivation of the Nucleus Accumbens: A Combined Functional Connectivity and Structure-Based Meta-analysis. *J Cogn Neurosci* 2011;**23**:2864–77. <https://doi.org/10.1162/jocn.2011.21624>.
- 40 McClure SM, York MK, Montague PR. The Neural Substrates of Reward Processing in Humans: The Modern Role of fMRI. *Neurosci* 2004;**10**:260–8.
<https://doi.org/10.1177/1073858404263526>.
- 41 O’Doherty JP. Reward representations and reward-related learning in the human brain: Insights from neuroimaging. *Curr Opin Neurobiol* 2004:769–76.
<https://doi.org/10.1016/j.conb.2004.10.016>.

- 42 Delgado MR. Reward-related responses in the human striatum. *Ann N Y Acad Sci* 2007;**1104**:70–88. <https://doi.org/10.1196/annals.1390.002>.
- 43 Apicella P, Ljungberg T, Scarnati E, Schultz W. Responses to reward in monkey dorsal and ventral striatum. *Exp Brain Res* 1991;**85**:491–500. <https://doi.org/10.1007/BF00231732>.
- 44 Emson PC, Waldvogel HJ, Faull RLM. Chapter 4 – Neurotransmitter Receptors in the Basal Ganglia. *Handb. Behav. Neurosci.*, vol. 20. 2010. p. 75–96.
- 45 Lovinger DM. Neurotransmitter roles in synaptic modulation, plasticity and learning in the dorsal striatum. *Neuropharmacology* 2010;**58**:951–61. <https://doi.org/http://dx.doi.org/10.1016/j.neuropharm.2010.01.008>.
- 46 Haber SN. Neuroanatomy of Reward: A View from the Ventral Striatum. In: Gottfried JA, editor. *Neurobiol. Sensat. Reward*, vol. 5. Boca Raton (FL); 2011. p. 1–24.
- 47 Zink CF, Pagnoni G, Martin-Skurski ME, Chappelow JC, Berns GS. Human striatal responses to monetary reward depend on saliency. *Neuron* 2004;**42**:509–17. [https://doi.org/10.1016/S0896-6273\(04\)00183-7](https://doi.org/10.1016/S0896-6273(04)00183-7).
- 48 Knutson B, Adams CM, Fong GW, Hommer D. Anticipation of increasing monetary reward selectively recruits nucleus accumbens. *J Neurosci* 2001;**21**:RC159. <https://doi.org/20015472> [pii].
- 49 Cooper JC, Knutson B. Valence and salience contribute to nucleus accumbens activation. *Neuroimage* 2008;**39**:538–47. <https://doi.org/10.1016/j.neuroimage.2007.08.009>.
- 50 Jensen J, McIntosh AR, Crawley AP, Mikulis DJ, Remington G, Kapur S. Direct

- activation of the ventral striatum in anticipation of aversive stimuli. *Neuron* 2003;**40**:1251–7. [https://doi.org/10.1016/S0896-6273\(03\)00724-4](https://doi.org/10.1016/S0896-6273(03)00724-4).
- 51 Guitart-Masip M, Fuentemilla L, Bach DR, Huys QJ, Dayan P, Dolan RJ, *et al.* Action dominates valence in anticipatory representations in the human striatum and dopaminergic midbrain. *J Neurosci* 2011;**31**:7867–75. <https://doi.org/10.1523/JNEUROSCI.6376-10.2011>.
- 52 Cho YT, Fromm S, Guyer AE, Detloff A, Pine DS, Fudge JL, *et al.* Nucleus accumbens, thalamus and insula connectivity during incentive anticipation in typical adults and adolescents. *Neuroimage* 2013;**66**:508–21. <https://doi.org/10.1016/j.neuroimage.2012.10.013>.
- 53 Camara E, Rodriguez-Fornells A, Münte TF. Functional connectivity of reward processing in the brain. *Front Hum Neurosci* 2008;**2**:19. <https://doi.org/10.3389/neuro.09.019.2008>.
- 54 Lopez-Paniagua D, Seger CA. Interactions within and between Corticostriatal Loops during Component Processes of Category Learning. *J Cogn Neurosci* 2011;**23**:3068–83. https://doi.org/10.1162/jocn_a_00008.
- 55 Ramirez S, Liu X, MacDonald CJ, Moffa A, Zhou J, Redondo RL, *et al.* Activating positive memory engrams suppresses depression-like behaviour. *Nature* 2015;**522**:335–9. <https://doi.org/10.1038/nature14514>.
- 56 Stuber GD, Sparta DR, Stamatakis AM, van Leeuwen WA, Hardjoprajitno JE, Cho S, *et al.* Excitatory transmission from the amygdala to nucleus accumbens facilitates reward seeking. *Nature* 2011;**475**:377–80. <https://doi.org/10.1038/nature10194>.

- 57 Owen AM, McMillan KM, Laird AR, Bullmore E, Maia TV, Zald DH, *et al.* The role of the dorsal striatum in reward and decision-making. *J Neurosci* 2003;**14**:8161–5. <https://doi.org/10.1002/mrm.25535>.
- 58 Balleine BW, Delgado MR, Hikosaka O. The role of the dorsal striatum in reward and decision-making. *J Neurosci* 2007;**27**:8161–5. <https://doi.org/10.1523/JNEUROSCI.1554-07.2007>.
- 59 O’Doherty J, Dayan P, Schultz J, Deichmann R, Friston K, Dolan RJ. Dissociable Role of Ventral and Dorsal Striatum in Instrumental Conditioning. *Science* (80-) 2004;**304**:452–4. <https://doi.org/10.1126/science.1094285>.
- 60 Reig R, Silberberg G. Multisensory Integration in the Mouse Striatum. *Neuron* 2014;**83**:1200–12. <https://doi.org/10.1016/j.neuron.2014.07.033>.
- 61 McFarland NR, Haber SN. Organization of thalamostriatal terminals from the ventral motor nuclei in the macaque. *J Comp Neurol* 2001;**429**:321–36. [https://doi.org/10.1002/1096-9861\(20000108\)429:2<321::AID-CNE11>3.0.CO;2-A](https://doi.org/10.1002/1096-9861(20000108)429:2<321::AID-CNE11>3.0.CO;2-A).
- 62 McFarland NR, Haber SN. Thalamic relay nuclei of the basal ganglia form both reciprocal and nonreciprocal cortical connections, linking multiple frontal cortical areas. *J Neurosci* 2002;**22**:8117–32. <https://doi.org/22/18/8117> [pii].
- 63 Alexander GE, Crutcher MD. Functional architecture of basal ganglia circuits: neural substrates of parallel processing. *Trends Neurosci* 1990;**13**:266–71.
- 64 Choi EY, Yeo BT, Buckner RL. The organization of the human striatum estimated by intrinsic functional connectivity. *J Neurophysiol* 2012;**108**:2242–63. <https://doi.org/10.1152/jn.00270.2012>.

- 65 Thomas Yeo BT, Krienen FM, Sepulcre J, Sabuncu MR, Lashkari D, Hollinshead M, *et al.* The organization of the human cerebral cortex estimated by intrinsic functional connectivity. *J Neurophysiol* 2011;**106**:1125–65.
<https://doi.org/10.1152/jn.00338.2011>.
- 66 Lehericy S, Ducros M, Van De Moortele PF, Francois C, Thivard L, Poupon C, *et al.* Diffusion Tensor Fiber Tracking Shows Distinct Corticostriatal Circuits in Humans. *Ann Neurol* 2004;**55**:522–9. <https://doi.org/10.1002/ana.20030>.
- 67 Basser PJ, Pajevic S, Pierpaoli C, Duda J, Aldroubi A. In vivo fiber tractography using DT-MRI data. *Magn Reson Med* 2000;**44**:625–32.
[https://doi.org/10.1002/1522-2594\(200010\)44:4<625::AID-MRM17>3.0.CO;2-O](https://doi.org/10.1002/1522-2594(200010)44:4<625::AID-MRM17>3.0.CO;2-O).
- 68 Yeh FC, Wedeen VJ, Tseng WYI. Generalized q-sampling imaging. *IEEE Trans Med Imaging* 2010;**29**:1626–35. <https://doi.org/10.1109/TMI.2010.2045126>.
- 69 Verstynen TD, Badre D, Jarbo K, Schneider W. Microstructural organizational patterns in the human corticostriatal system. *J Neurophysiol* 2012;**107**:2984–95.
<https://doi.org/10.1152/jn.00995.2011>.
- 70 Karlsgodt KH, John M, Ikuta T, Rigoard P, Peters BD, Derosse P, *et al.* The accumbofrontal tract: Diffusion tensor imaging characterization and developmental change from childhood to adulthood. *Hum Brain Mapp* 2015;**36**:4954–63. <https://doi.org/10.1002/hbm.22989>.
- 71 Skudlarski P, Jagannathan K, Calhoun VD, Hampson M, Skudlarska BA, Pearlson G. Measuring brain connectivity: Diffusion tensor imaging validates resting state temporal correlations. *Neuroimage* 2008;**43**:554–61.
<https://doi.org/10.1016/j.neuroimage.2008.07.063>.

- 72 Honey CJ, Honey CJ, Sporns O, Sporns O, Cammoun L, Cammoun L, *et al.* Predicting human resting-state functional connectivity from structural connectivity. *Proc Natl Acad Sci U S A* 2009;**106**:2035–40. <https://doi.org/10.1073/pnas.0811168106>.
- 73 Pol HEH. Functionally Linked Resting-State Networks Reflect the Underlying Structural Connectivity Architecture of the Human Brain. *Hum Brain Mapp* 2009;**0**:. <https://doi.org/10.1002/hbm.20737>.
- 74 Bowman FDB, Zhang L, Derado G, Chen S. Determining functional connectivity using fMRI data with diffusion-based anatomical weighting. *Neuroimage* 2012;**62**:1769–79. <https://doi.org/10.1016/j.neuroimage.2012.05.032>.
- 75 Alexander AL, Hasan KM, Lazar M, Tsuruda JS, Parker DL. Analysis of partial volume effects in diffusion-tensor MRI. *Magn Reson Med* 2001;**45**:770–80. <https://doi.org/10.1002/mrm.1105>.
- 76 Jeurissen B, Leemans A, Tournier JD, Jones DK, Sijbers J. Investigating the prevalence of complex fiber configurations in white matter tissue with diffusion magnetic resonance imaging. *Hum Brain Mapp* 2013;**34**:2747–66. <https://doi.org/10.1002/hbm.22099>.
- 77 Costa Dias TG, Wilson VB, Bathula DR, Iyer SP, Mills KL, Thurlow BL, *et al.* Reward circuit connectivity relates to delay discounting in children with attention-deficit/hyperactivity disorder. *Eur Neuropsychopharmacol* 2013;**23**:33–45. <https://doi.org/10.1016/j.euroneuro.2012.10.015>.
- 78 Juckel G, Schlagenhauf F, Koslowski M, Wüstenberg T, Villringer A, Knutson B, *et al.* Dysfunction of ventral striatal reward prediction in schizophrenia.

- Neuroimage* 2006;**29**:409–16. <https://doi.org/10.1016/j.neuroimage.2005.07.051>.
- 79 Keller J, Young CB, Kelley E, Prater K, Levitin DJ, Menon V. Trait anhedonia is associated with reduced reactivity and connectivity of mesolimbic and paralimbic reward pathways. *J Psychiatr Res* 2013;**47**:1319–28. <https://doi.org/10.1016/j.jpsychires.2013.05.015>.
- 80 Belmonte MK, Allen G, Beckel-Mitchener A, Boulanger LM, Carper R a, Webb SJ. Autism and abnormal development of brain connectivity. *J Neurosci* 2004;**24**:9228–31. <https://doi.org/10.1523/JNEUROSCI.3340-04.2004>.
- 81 Just MA, Cherkassky VL, Keller TA, Minshew NJ. Cortical activation and synchronization during sentence comprehension in high-functioning autism: Evidence of underconnectivity. *Brain* 2004;**127**:1811–21. <https://doi.org/10.1093/brain/awh199>.
- 82 Maximo JO, Cadena EJ, Kana RK. The implications of brain connectivity in the neuropsychology of autism. *Neuropsychol Rev* 2014:16–31. <https://doi.org/10.1007/s11065-014-9250-0>.
- 83 Keown CL, Datko MC, Chen CP, Maximo JO, Jahedi A, Müller R-A, *et al*. Network Organization Is Globally Atypical in Autism: A Graph Theory Study of Intrinsic Functional Connectivity. *Biol Psychiatry Cogn Neurosci Neuroimaging* 2016;**0**:1–20. <https://doi.org/10.1016/j.bpsc.2016.07.008>.
- 84 Tsiaras V, Simos PG, Rezaie R, Sheth BR, Garyfallidis E, Castillo EM, *et al*. Extracting biomarkers of autism from MEG resting-state functional connectivity networks. *Comput Biol Med* 2011;**41**:1166–77. <https://doi.org/10.1016/j.combiomed.2011.04.004>.

- 85 Domínguez LG, Velázquez JLP, Galán RF. A model of functional brain connectivity and background noise as a biomarker for cognitive phenotypes: application to autism. *PLoS One* 2013;**8**:e61493.
- 86 Nielsen JA, Zielinski BA, Fletcher PT, Alexander AL, Lange N, Bigler ED, *et al.* Multisite functional connectivity MRI classification of autism: ABIDE results 2013.
- 87 Chen H, Duan X, Liu F, Lu F, Ma X, Zhang Y, *et al.* Multivariate classification of autism spectrum disorder using frequency-specific resting-state functional connectivity-A multi-center study. *Prog Neuro-Psychopharmacology Biol Psychiatry* 2016;**64**:1–9. <https://doi.org/10.1016/j.pnpbp.2015.06.014>.
- 88 Ingalhalikar M, Parker D, Bloy L, Roberts TPL, Verma R. Diffusion based abnormality markers of pathology: Toward learned diagnostic prediction of ASD. *Neuroimage* 2011;**57**:918–27. <https://doi.org/10.1016/j.neuroimage.2011.05.023>.
- 89 Lange N, Dubray MB, Lee JE, Froimowitz MP, Froehlich A, Adluru N, *et al.* Atypical diffusion tensor hemispheric asymmetry in autism. *Autism Res* 2010;**3**:350–8. <https://doi.org/10.1002/aur.162>.
- 90 Sabbagh MA. Understanding orbitofrontal contributions to theory-of-mind reasoning: Implications for autism. *Brain Cogn* 2004:209–19. <https://doi.org/10.1016/j.bandc.2003.04.002>.
- 91 Gallagher HL, Frith CD. Functional imaging of ‘theory of mind’. *Trends Cogn Sci* 2003:77–83. [https://doi.org/10.1016/S1364-6613\(02\)00025-6](https://doi.org/10.1016/S1364-6613(02)00025-6).
- 92 Völlm BA, Taylor ANW, Richardson P, Corcoran R, Stirling J, McKie S, *et al.* Neuronal correlates of theory of mind and empathy: A functional magnetic

- resonance imaging study in a nonverbal task. *Neuroimage* 2006;**29**:90–8. <https://doi.org/10.1016/j.neuroimage.2005.07.022>.
- 93 Kana RK, Keller TA, Cherkassky VL, Minshew NJ, Just MA. Sentence comprehension in autism: Thinking in pictures with decreased functional connectivity. *Brain* 2006;**129**:2484–93. <https://doi.org/10.1093/brain/awl164>.
- 94 Schmitz N, Rubia K, Daly E, Smith A, Williams S, Murphy DGM. Neural correlates of executive function in autistic spectrum disorders. *Biol Psychiatry* 2006;**59**:7–16. <https://doi.org/10.1016/j.biopsych.2005.06.007>.
- 95 Gilbert SJ, Bird G, Brindley R, Frith CD, Burgess PW. Atypical recruitment of medial prefrontal cortex in autism spectrum disorders: An fMRI study of two executive function tasks. *Neuropsychologia* 2008;**46**:2281–91. <https://doi.org/10.1016/j.neuropsychologia.2008.03.025>.
- 96 Harms MB, Martin A, Wallace GL. Facial emotion recognition in autism spectrum disorders: A review of behavioral and neuroimaging studies. *Neuropsychol Rev* 2010;**20**:290–322. <https://doi.org/10.1007/s11065-010-9138-6>.
- 97 Schultz RT, Gauthier I, Klin A, Fulbright RK, Anderson AW, Volkmar F, *et al.* Abnormal ventral temporal cortical activity during face discrimination among individuals with autism and Asperger syndrome. *Arch Gen Psychiatry* 2000;**57**:331–40.
- 98 Kleinhans NM, Richards T, Sterling L, Stegbauer KC, Mahurin R, Johnson LC, *et al.* Abnormal functional connectivity in autism spectrum disorders during face processing. *Brain* 2008;**131**:1000–12. <https://doi.org/10.1093/brain/awm334>.
- 99 Luman M, Van Meel CS, Oosterlaan J, Geurts HM. Reward and punishment

- sensitivity in children with ADHD: Validating the sensitivity to punishment and sensitivity to reward questionnaire for children (SPSRQ-C). *J Abnorm Child Psychol* 2012;**40**:145–57. <https://doi.org/10.1007/s10802-011-9547-x>.
- 100 von dem Hagen EAH, Stoyanova RS, Rowe JB, Baron-Cohen S, Calder AJ. Direct gaze elicits atypical activation of the theory-of-mind network in autism spectrum conditions. *Cereb Cortex* 2013:bht003.
- 101 Murphy ER, Foss-Feig J, Kenworthy L, Gaillard WD, Vaidya CJ. Atypical Functional Connectivity of the Amygdala in Childhood Autism Spectrum Disorders during Spontaneous Attention to Eye-Gaze. *Autism Res Treat* 2012;**2012**:652408. <https://doi.org/10.1155/2012/652408>.
- 102 Dawson G, Webb SJ, Wijsman E, Schellenberg G, Estes A, Munson J, *et al.* Neurocognitive and electrophysiological evidence of altered face processing in parents of children with autism: implications for a model of abnormal development of social brain circuitry in autism. *Dev Psychopathol* 2005;**17**:679–97. <https://doi.org/10.1017/S0954579405050327>.
- 103 Schultz RT, Gauthier I, Klin A, Fulbright RK, Anderson AW, Volkmar F, *et al.* Abnormal ventral temporal cortical activity during face discrimination among individuals with autism and Asperger syndrome. *Arch Gen Psychiatry* 2000;**57**:331–40. <https://doi.org/10.1001/archpsyc.57.4.331>.
- 104 Scott-Van Zeeland AA, Dapretto M, Ghahremani DG, Poldrack RA, Bookheimer SY. Reward processing in autism. *Autism Res* 2010;**3**:53–67. <https://doi.org/10.1002/aur.122>.
- 105 Kohls G, Schulte-Rüther M, Nehr Korn B, Müller K, Fink GR, Kamp-Becker I, *et*

- al.* Reward system dysfunction in autism spectrum disorders. *Soc Cogn Affect Neurosci* 2013;**8**:565–72. <https://doi.org/10.1093/scan/nss033>.
- 106 Hollander E, Anagnostou E, Chaplin W, Esposito K, Haznedar MM, Licalzi E, *et al.* Striatal volume on magnetic resonance imaging and repetitive behaviors in autism. *Biol Psychiatry* 2005;**58**:226–32. <https://doi.org/10.1016/j.biopsych.2005.03.040>.
- 107 Langen M, Leemans A, Johnston P, Ecker C, Daly E, Murphy CM, *et al.* Fronto-striatal circuitry and inhibitory control in autism: Findings from diffusion tensor imaging tractography. *Cortex* 2012;**48**:183–93. <https://doi.org/10.1016/j.cortex.2011.05.018>.
- 108 Larson MJ, South M, Krauskopf E, Clawson A, Crowley MJ. Feedback and reward processing in high-functioning autism. *Psychiatry Res* 2011;**187**:198–203. <https://doi.org/10.1016/j.psychres.2010.11.006>.
- 109 Neuhaus E, Beauchaine TP, Bernier R. Neurobiological correlates of social functioning in autism. *Clin Psychol Rev* 2010:733–48. <https://doi.org/10.1016/j.cpr.2010.05.007>.
- 110 Allman JM, Watson KK, Tetreault NA, Hakeem AY. Intuition and autism: A possible role for Von Economo neurons. *Trends Cogn Sci* 2005;**9**:367–73. <https://doi.org/10.1016/j.tics.2005.06.008>.
- 111 Sears LL, Vest C, Mohamed S, Bailey J, Ranson BJ, Piven J. An MRI study of the basal ganglia in autism. *Prog Neuropsychopharmacol Biol Psychiatry* 1999;**23**:613–24.
- 112 Langen M, Durston S, Staal WG, Palmen SJMC, van Engeland H. Caudate

- Nucleus Is Enlarged in High-Functioning Medication-Naive Subjects with Autism. *Biol Psychiatry* 2007;**62**:262–6. <https://doi.org/10.1016/j.biopsych.2006.09.040>.
- 113 Wegiel J, Flory M, Kuchna I, Nowicki K, Ma SY, Imaki H, *et al*. Stereological study of the neuronal number and volume of 38 brain subdivisions of subjects diagnosed with autism reveals significant alterations restricted to the striatum, amygdala and cerebellum. *Acta Neuropathol Commun* 2014;**2**:141. <https://doi.org/10.1186/s40478-014-0141-7>.
- 114 Deramus TP, Kana RK. Anatomical likelihood estimation meta-analysis of grey and white matter anomalies in autism spectrum disorders. *NeuroImage Clin* 2015;**7**:525–36. <https://doi.org/10.1016/j.nicl.2014.11.004>.
- 115 Aylward EH, Minshew NJ, Goldstein G, Honeycutt N a, Augustine a M, Yates KO, *et al*. MRI volumes of amygdala and hippocampus in non-mentally retarded autistic adolescents and adults. *Neurology* 1999;**53**:2145–50. <https://doi.org/10.1212/WNL.53.9.2145>.
- 116 Schumann CM, Hamstra J, Goodlin-Jones BL, Lotspeich LJ, Kwon H, Buonocore MH, *et al*. The amygdala is enlarged in children but not adolescents with autism; the hippocampus is enlarged at all ages. *J Neurosci* 2004;**24**:6392–401. <https://doi.org/10.1523/JNEUROSCI.1297-04.2004>.
- 117 Hardan AY, Girgis RR, Lacerda ALT, Yorbik O, Kilpatrick M, Keshavan MS, *et al*. Magnetic Resonance Imaging Study of the Orbitofrontal Cortex in Autism. *J Child Neurol* 2006;**21**:866–71. <https://doi.org/10.1177/08830738060210100701>.
- 118 Girgis RR, Minshew NJ, Melhem NM, Nutche JJ, Keshavan MS, Hardan AY. Volumetric alterations of the orbitofrontal cortex in autism. *Prog Neuro-*

Psychopharmacology Biol Psychiatry 2007;**31**:41–5.

<https://doi.org/10.1016/j.pnpbp.2006.06.007>.

- 119 Cascio CJ, Foss-Feig JH, Heacock JL, Newsom CR, Cowan RL, Benningfield MM, *et al.* Response of neural reward regions to food cues in autism spectrum disorders. *J Neurodev Disord* 2012;**4**:9. <https://doi.org/10.1186/1866-1955-4-9>.
- 120 Richey JA, Rittenberg A, Hughes L, Damiano CR, Sabatino A, Miller S, *et al.* Common and distinct neural features of social and non-social reward processing in autism and social anxiety disorder. *Soc Cogn Affect Neurosci* 2014;**9**:367–77. <https://doi.org/10.1093/scan/nss146>.
- 121 Padmanabhan A, Lynn A, Foran W, Luna B, O’Hearn K. Age related changes in striatal resting state functional connectivity in autism. *Front Hum Neurosci* 2013;**7**:814. <https://doi.org/10.3389/fnhum.2013.00814>.
- 122 South M, Dana J, White SE, Crowley MJ. Failure is not an option: Risk-taking is moderated by anxiety and also by cognitive ability in children and adolescents diagnosed with an autism spectrum disorder. *J Autism Dev Disord* 2011;**41**:55–65. <https://doi.org/10.1007/s10803-010-1021-z>.
- 123 Murray MJ. Attention-deficit/hyperactivity disorder in the context of autism spectrum disorders. *Curr Psychiatry Rep* 2010:382–8. <https://doi.org/10.1007/s11920-010-0145-3>.
- 124 Mayes SD, Calhoun SL, Murray MJ, Ahuja M, Smith LA. Anxiety, depression, and irritability in children with autism relative to other neuropsychiatric disorders and typical development. *Res Autism Spectr Disord* 2011;**5**:474–85. <https://doi.org/10.1016/j.rasd.2010.06.012>.

- 125 Joshi G, Wozniak J, Petty C, Martelon MK, Fried R, Bolfek A, *et al.* Psychiatric comorbidity and functioning in a clinically referred population of adults with autism spectrum disorders: A comparative study. *J Autism Dev Disord* 2013;**43**:1314–25. <https://doi.org/10.1007/s10803-012-1679-5>.
- 126 Strang JF, Kenworthy L, Daniolos P, Case L, Wills MC, Martin A, *et al.* Depression and anxiety symptoms in children and adolescents with autism spectrum disorders without intellectual disability. *Res Autism Spectr Disord* 2012;**6**:406–12. <https://doi.org/10.1016/j.rasd.2011.06.015>.
- 127 Cath DC, Ran N, Smit JH, van Balkom AJLM, Comijs HC. Symptom overlap between autism spectrum disorder, generalized social anxiety disorder and obsessive-compulsive disorder in adults: a preliminary case-controlled study. *Psychopathology* 2008;**41**:101–10. <https://doi.org/10.1159/000111555>.
- 128 Ivarsson T, Melin K. Autism spectrum traits in children and adolescents with obsessive-compulsive disorder (OCD). *J Anxiety Disord* 2008;**22**:969–78. <https://doi.org/10.1016/j.janxdis.2007.10.003>.
- 129 Mattila M-L, Hurtig T, Haapsamo H, Jussila K, Kuusikko-Gauffin S, Kielinen M, *et al.* Comorbid Psychiatric Disorders Associated with Asperger Syndrome/High-functioning Autism: A Community- and Clinic-based Study. *J Autism Dev Disord* 2010;**40**:1080–93. <https://doi.org/10.1007/s10803-010-0958-2>.
- 130 Anholt GE, Cath DC, van Oppen P, Eikelenboom M, Smit JH, van Megen H, *et al.* Autism and ADHD Symptoms in Patients with OCD: Are They Associated with Specific OC Symptom Dimensions or OC Symptom Severity? *J Autism Dev Disord* 2010;**40**:580–9. <https://doi.org/10.1007/s10803-009-0922-1>.

- 131 Canitano R, Vivanti G. Tics and Tourette syndrome in autism spectrum disorders. *Autism* 2007;**11**:19–28. <https://doi.org/10.1177/1362361307070992>.
- 132 Stahlberg O, Soderstrom H, Rastam M, Gillberg C. Bipolar disorder, schizophrenia, and other psychotic disorders in adults with childhood onset AD/HD and/or autism spectrum disorders. *J Neural Transm* 2004;**111**:891–902. <https://doi.org/10.1007/s00702-004-0115-1>.
- 133 Baron-Cohen S, Mortimore C, Moriarty J, Izaguirre J, Robertson M. The Prevalence of Gilles de la Tourette’s Syndrome in Children and Adolescents with Autism. *J Child Psychol Psychiatry* 1999;**40**:213–8. <https://doi.org/10.1111/1469-7610.00434>.
- 134 Zandt F, Prior M, Kyrios M. Repetitive Behaviour in Children with High Functioning Autism and Obsessive Compulsive Disorder. *J Autism Dev Disord* 2007;**37**:251–9. <https://doi.org/10.1007/s10803-006-0158-2>.
- 135 Simonoff E, Pickles A, Charman T, Chandler S, Loucas T, Baird G. Psychiatric Disorders in Children With Autism Spectrum Disorders: Prevalence, Comorbidity, and Associated Factors in a Population-Derived Sample. *J Am Acad Child Adolesc Psychiatry* 2008;**47**:921–9. <https://doi.org/10.1097/CHI.0b013e318179964f>.
- 136 Matson JL, Nebel-Schwalm MS. Comorbid psychopathology with autism spectrum disorder in children: An overview. *Res Dev Disabil* 2007;**28**:341–52. <https://doi.org/10.1016/j.ridd.2005.12.004>.
- 137 van Steensel FJA, Bögels SM, Perrin S. Anxiety Disorders in Children and Adolescents with Autistic Spectrum Disorders: A Meta-Analysis. *Clin Child Fam Psychol Rev* 2011:302–17. <https://doi.org/10.1007/s10567-011-0097-0>.

- 138 Sprooten E, Rasgon A, Goodman M, Carlin A, Leibu E, Lee WH, *et al.* Addressing reverse inference in psychiatric neuroimaging: Meta-analyses of task-related brain activation in common mental disorders. *Hum Brain Mapp* 2016. <https://doi.org/10.1002/hbm.23486>.
- 139 Ströhle A, Stoy M, Wrase J, Schwarzer S, Schlagenhauf F, Huss M, *et al.* Reward anticipation and outcomes in adult males with attention-deficit/hyperactivity disorder. *Neuroimage* 2008;**39**:966–72. <https://doi.org/10.1016/j.neuroimage.2007.09.044>.
- 140 Plichta MM, Vasic N, Wolf RC, Lesch KP, Brummer D, Jacob C, *et al.* Neural Hyporesponsiveness and Hyperresponsiveness During Immediate and Delayed Reward Processing in Adult Attention-Deficit/Hyperactivity Disorder. *Biol Psychiatry* 2009;**65**:7–14. <https://doi.org/10.1016/j.biopsych.2008.07.008>.
- 141 Carmona S, Hoekzema E, Ramos-Quiroga JA, Richarte V, Canals C, Bosch R, *et al.* Response inhibition and reward anticipation in medication-naïve adults with attention-deficit/hyperactivity disorder: A within-subject case-control neuroimaging study. *Hum Brain Mapp* 2012;**33**:2350–61. <https://doi.org/10.1002/hbm.21368>.
- 142 Stark R, Bauer E, Merz CJ, Zimmermann M, Reuter M, Plichta MM, *et al.* ADHD related behaviors are associated with brain activation in the reward system. *Neuropsychologia* 2011;**49**:426–34. <https://doi.org/10.1016/j.neuropsychologia.2010.12.012>.
- 143 Hoogman M, Aarts E, Zwiers M, Slaats-Willemsse D, Naber M, Onnink M, *et al.* Nitric oxide synthase genotype modulation of impulsivity and ventral striatal

- activity in adult ADHD patients and healthy comparison subjects. *Am J Psychiatry* 2011;**168**:1099–106. <https://doi.org/10.1176/appi.ajp.2011.10101446>.
- 144 Edel M-A, Enzi B, Witthaus H, Tegenthoff M, Peters S, Juckel G, *et al.* Differential reward processing in subtypes of adult attention deficit hyperactivity disorder. *J Psychiatr Res* 2013;**47**:350–6. <https://doi.org/10.1016/j.jpsychires.2012.09.026>.
- 145 Hoogman M, Onnink M, Cools R, Aarts E, Kan C, Arias Vasquez A, *et al.* The dopamine transporter haplotype and reward-related striatal responses in adult ADHD. *Eur Neuropsychopharmacol* 2013;**23**:469–78. <https://doi.org/10.1016/j.euroneuro.2012.05.011>.
- 146 Wilbertz G, Tebartz van Elst L, Delgado MR, Maier S, Feige B, Philippsen A, *et al.* Orbitofrontal reward sensitivity and impulsivity in adult attention deficit hyperactivity disorder. *Neuroimage* 2012;**60**:353–61. <https://doi.org/10.1016/j.neuroimage.2011.12.011>.
- 147 Scheres A, Milham MP, Knutson B, Castellanos FX. Ventral Striatal Hyporesponsiveness During Reward Anticipation in Attention-Deficit/Hyperactivity Disorder. *Biol Psychiatry* 2007;**61**:720–4. <https://doi.org/10.1016/j.biopsych.2006.04.042>.
- 148 Guyer AE, Choate VR, Detloff A, Benson B, Nelson EE, Perez-Edgar K, *et al.* Striatal functional alteration during incentive anticipation in pediatric anxiety disorders. *Am J Psychiatry* 2012;**169**:205–12. <https://doi.org/10.1176/appi.ajp.2011.11010006>.
- 149 Tromp DPM, Grupe DW, Oathes DJ, McFarlin DR, Hernandez PJ, Kral TRA, *et*

- al.* Reduced structural connectivity of a major frontolimbic pathway in generalized anxiety disorder. *Arch Gen Psychiatry* 2012;**69**:925.
<https://doi.org/10.1001/archgenpsychiatry.2011.2178>.
- 150 McFarland BR, Klein DN. Emotional reactivity in depression: Diminished responsiveness to anticipated reward but not to anticipated punishment or to nonreward or avoidance. *Depress Anxiety* 2009;**26**:117–22.
<https://doi.org/10.1002/da.20513>.
- 151 Knutson B, Bhanji JP, Cooney RE, Atlas LY, Gotlib IH. Neural Responses to Monetary Incentives in Major Depression. *Biol Psychiatry* 2008;**63**:686–92.
<https://doi.org/10.1016/j.biopsych.2007.07.023>.
- 152 Pizzagalli DA, Holmes AJ, Dillon DG, Goetz EL, Birk JL, Bogdan R, *et al.* Reduced caudate and nucleus accumbens response to rewards in unmedicated subjects with major depressive disorder. *Am J Psychiatry* 2009;**166**:702–10.
<https://doi.org/10.1176/appi.ajp.2008.08081201.Reduced>.
- 153 Epstein J, Pan H, Kocsis JH, Yang Y, Butler T, Chusid J, *et al.* Lack of ventral striatal response to positive stimuli in depressed versus normal subjects. *Am J Psychiatry* 2006;**163**:1784–90. <https://doi.org/10.1176/appi.ajp.163.10.1784>.
- 154 Heller A, Johnstone T, Shackman A, Light S, Peterson M, Kolden G, *et al.* Reduced capacity to sustain positive emotion in major depression reflects diminished maintenance of fronto-striatal brain activation. *Proc Natl Acad Sci U S A* 2009;**106**:22445–50. <https://doi.org/10.1073/pnas.0910651106>.
- 155 Lui S, Wu Q, Qiu L, Yang X, Kuang W, Chan RCK, *et al.* Resting-state functional connectivity in treatment-resistant depression. *Am J Psychiatry* 2011;**168**:642–8.

- <https://doi.org/10.1176/appi.ajp.2010.10101419>.
- 156 Furman DJ, Hamilton JP, Gotlib IH. Frontostriatal functional connectivity in major depressive disorder. *Biol Mood Anxiety Disord* 2011;**1**:11.
<https://doi.org/10.1186/2045-5380-1-11>.
- 157 Tang Y, Kong L, Wu F, Womer F, Jiang W, Cao Y, *et al*. Decreased functional connectivity between the amygdala and the left ventral prefrontal cortex in treatment-naive patients with major depressive disorder: a resting-state functional magnetic resonance imaging study. *Psychol Med* 2013;**43**:1921–7.
<https://doi.org/10.1017/S0033291712002759>.
- 158 Vissers ME, X Cohen M, Geurts HM. Brain connectivity and high functioning autism: A promising path of research that needs refined models, methodological convergence, and stronger behavioral links. *Neurosci Biobehav Rev* 2012:604–25.
<https://doi.org/10.1016/j.neubiorev.2011.09.003>.
- 159 Poldrack RA. Can cognitive processes be inferred from neuroimaging data? *Trends Cogn Sci* 2006;**10**:59–63.
- 160 Vul E, Harris C, Winkielman P, Pashler H. Puzzlingly High Correlations in fMRI Studies of Emotion, Personality, and Social Cognition. *Psychol Sci* 2009;**4**:274–90. <https://doi.org/10.1111/j.1745-6924.2009.01132.x>.
- 161 Lieberman MD, Berkman ET, Wager TD. Correlations in Social Neuroscience Aren't Voodoo: Commentary on Vul et al. (2009). *Perspect Psychol Sci* 2009;**4**:299–307. <https://doi.org/10.1111/j.1745-6924.2009.01128.x>.
- 162 Nichols TE, Poline J-B. Commentary on Vul et al.'s (2009)'Puzzlingly High Correlations in fMRI Studies of Emotion, Personality, and Social Cognition'.

- Perspect Psychol Sci* 2009;**4**:291–3. <https://doi.org/10.1111/j.1745-6924.2009.01126.x>.
- 163 Mueller S, Keeser D, Samson AC, Kirsch V, Blautzik J, Grothe M, *et al*. Convergent Findings of Altered Functional and Structural Brain Connectivity in Individuals with High Functioning Autism: A Multimodal MRI Study. *PLoS One* 2013;**8**:. <https://doi.org/10.1371/journal.pone.0067329>.
- 164 Damoiseaux JS, Greicius MD. Greater than the sum of its parts: a review of studies combining structural connectivity and resting-state functional connectivity. *Brain Struct Funct* 2009;**213**:525–33. <https://doi.org/10.1007/s00429-009-0208-6>.
- 165 Horn A, Ostwald D, Reisert M, Blankenburg F. The structural-functional connectome and the default mode network of the human brain. *Neuroimage* 2014;**102**:142–51. <https://doi.org/10.1016/j.neuroimage.2013.09.069>.
- 166 Warbrick T, Rosenberg J, Shah NJ. The relationship between {BOLD} fMRI response and the underlying white matter as measured by fractional anisotropy (FA): a systematic review. *Neuroimage* 2017. <https://doi.org/http://dx.doi.org/10.1016/j.neuroimage.2016.12.075>.
- 167 Vasa RA, Mostofsky SH, Ewen JB. The Disrupted Connectivity Hypothesis of Autism Spectrum Disorders: Time for the Next Phase in Research. *Biol Psychiatry Cogn Neurosci Neuroimaging* 2016;**1**:245–52. <https://doi.org/10.1016/j.bpsc.2016.02.003>.
- 168 Kern JK. Purkinje cell vulnerability and autism: a possible etiological connection. *Brain Dev* 2003;**25**:377–82.
- 169 Lazar N. Discussion of puzzlingly high correlations in fMRI studies of\remotion,

- personality, and social cognition" by Vul., et al. (2009). *Perspect Psychol Sci* 2009;**4**:308–9. <https://doi.org/10.1111/j.1745-6924.2009.01129.x>.
- 170 Yarkoni T. Big Correlations in Little Studies: Inflated fMRI Correlations Reflect Low Statistical Power-Commentary on Vul et al. (2009). *Perspect Psychol Sci* 2009;**4**:294–8. <https://doi.org/10.1111/j.1745-6924.2009.01127.x>.
- 171 Finn ES, Shen X, Scheinost D, Rosenberg MD, Huang J, Chun MM, *et al.* Functional connectome fingerprinting: identifying individuals using patterns of brain connectivity. *Nat Neurosci* 2015;**18**:1–11. <https://doi.org/10.1038/nn.4135>.
- 172 Biswal BB, Mennes M, Zuo XN, Gohel S, Kelly C, Smith SM, *et al.* Toward discovery science of human brain function. *Proc Natl Acad Sci USA* 2010;**107**:4734–9. <https://doi.org/0911855107> [pii];10.1073/pnas.0911855107 [doi].
- 173 Yeo BTT, Krienen FM, Sepulcre J, Sabuncu MR, Lashkari D, Hollinshead M, *et al.* The organization of the human cerebral cortex estimated by intrinsic functional connectivity. *J Neurophysiol* 2011;**106**:1125–65. <https://doi.org/10.1152/jn.00338.2011>.
- 174 Hagmann P, Kurant M, Gigandet X, Thiran P, Wedeen VJ, Meuli R, *et al.* Mapping human whole-brain structural networks with diffusion MRI. *PLoS One* 2007;**2**:. <https://doi.org/10.1371/journal.pone.0000597>.
- 175 Yeh FC, Vettel JM, Singh A, Poczos B, Grafton ST, Erickson KI, *et al.* Quantifying Differences and Similarities in Whole-Brain White Matter Architecture Using Local Connectome Fingerprints. *PLoS Comput Biol* 2016;**12**:. <https://doi.org/10.1371/journal.pcbi.1005203>.
- 176 Yeh FC, Badre D, Verstynen T. Connectometry: A statistical approach harnessing

- the analytical potential of the local connectome. *Neuroimage* 2016;**125**:162–71.
<https://doi.org/10.1016/j.neuroimage.2015.10.053>.
- 177 Hermundstad AM, Bassett DS, Brown KS, Aminoff EM, Clewett D, Freeman S, *et al*. Structural foundations of resting-state and task-based functional connectivity in the human brain. *PNAS*. 2013. <https://doi.org/10.1073/pnas.1219562110>.
- 178 Tomasi D, Volkow ND. Abnormal functional connectivity in children with attention-deficit/hyperactivity disorder. *Biol Psychiatry* 2012;**71**:443–50.
<https://doi.org/10.1016/j.biopsych.2011.11.003>.
- 179 Plichta MM, Scheres A. Ventral-striatal responsiveness during reward anticipation in ADHD and its relation to trait impulsivity in the healthy population: A meta-analytic review of the fMRI literature. *Neurosci Biobehav Rev* 2014:125–34.
<https://doi.org/10.1016/j.neubiorev.2013.07.012>.
- 180 Cremers HR, Veer IM, Spinhoven P, Rombouts S a RB, Roelofs K. Neural sensitivity to social reward and punishment anticipation in social anxiety disorder. *Front Behav Neurosci* 2014;**8**:439. <https://doi.org/10.3389/fnbeh.2014.00439>.
- 181 Cha J, Carlson JM, Dedora DJ, Greenberg T, Proudfit GH, Mujica-Parodi LR. Hyper-reactive human ventral tegmental area and aberrant mesocorticolimbic connectivity in overgeneralization of fear in generalized anxiety disorder. *J Neurosci* 2014;**34**:5855–60. <https://doi.org/10.1523/JNEUROSCI.4868-13.2014>.
- 182 Konrad K, Eickhoff SB. Is the ADHD brain wired differently? A review on structural and functional connectivity in attention deficit hyperactivity disorder. *Hum Brain Mapp* 2010:904–16. <https://doi.org/10.1002/hbm.21058>.
- 183 Christakou A, Murphy CM, Chantiluke K, Cubillo AI, Smith AB, Giampietro V, *et*

- al.* Disorder-specific functional abnormalities during sustained attention in youth with Attention Deficit Hyperactivity Disorder (ADHD) and with autism. *Mol Psychiatry* 2013;**18**:236–44. <https://doi.org/10.1038/mp.2011.185>.
- 184 Yeh FC, Tseng WYI. NTU-90: A high angular resolution brain atlas constructed by q-space diffeomorphic reconstruction. *Neuroimage* 2011;**58**:91–9. <https://doi.org/10.1016/j.neuroimage.2011.06.021>.
- 185 Tuch DS. Q-ball imaging. *Magn Reson Med* 2004;**52**:1358–72. <https://doi.org/10.1002/mrm.20279>.
- 186 Yeh FC, Verstynen TD, Wang Y, Fernández-Miranda JC, Tseng WYI. Deterministic diffusion fiber tracking improved by quantitative anisotropy. *PLoS One* 2013;**8**:e80713. <https://doi.org/10.1371/journal.pone.0080713>.
- 187 Wechsler D. *Wechsler abbreviated scale of intelligence : WASI*. San Antonio [u.a.]: Psychological Corp., Harcourt Brace; 1999.
- 188 Wechsler D, Hsiao-pin C. *WASI-II: Wechsler abbreviated scale of intelligence*. Pearson; 2011.
- 189 Roalf DR, Quarmley M, Elliott MA, Satterthwaite TD, Vandekar SN, Ruparel K, *et al.* The impact of quality assurance assessment on diffusion tensor imaging outcomes in a large-scale population-based cohort. *Neuroimage* 2016;**125**:903–19. <https://doi.org/10.1016/j.neuroimage.2015.10.068>.
- 190 Whitfield-Gabrieli S, Nieto-Castanon A. Conn: a functional connectivity toolbox for correlated and anticorrelated brain networks. *Brain Connect* 2012;**2**:125–41.
- 191 Wilcoxon F. Individual comparisons by ranking methods. *Biometrics Bull* 1945;**1**:80–3.

- 192 With S. Wilcoxon – Mann – Whitney. *Stat Surv* 1945;**4**:1–3.
<https://doi.org/10.1214/09-SS051>.
- 193 Anderson T, Darling D. A test of goodness-of-fit. *J Am Stat Assoc* 1954;**49**:765–9.
<https://doi.org/10.1080/01621459.1954.10501232>.
- 194 Inc. TM. MATLAB (R2016a). *MathWorks Inc* 2016.
<https://doi.org/10.1007/s10766-008-0082-5>.
- 195 Wilke M, Schmithorst VJ, Holland SK. Normative pediatric brain data for spatial normalization and segmentation differs from standard adult data. *Magn Reson Med* 2003;**50**:749–57. <https://doi.org/10.1002/mrm.10606>.
- 196 Muzik O, Chugani DC, Juhász C, Shen C, Chugani HT. Statistical parametric mapping: assessment of application in children. *Neuroimage* 2000;**12**:538–49.
<https://doi.org/10.1006/nimg.2000.0651>.
- 197 Byars AW, Holland SK, Strawsburg RH, Bommer W, Dunn RS, Schmithorst VJ, *et al*. Practical Aspects of Conducting Large-Scale Functional Magnetic Resonance Imaging Studies in Children. *J Child Neurol* 2002;**17**:885–9.
<https://doi.org/10.1177/08830738020170122201>.
- 198 Hoeksma MR, Kenemans JL, Kemner C, Van Engeland H. Variability in spatial normalization of pediatric and adult brain images. *Clin Neurophysiol* 2005;**116**:1188–94. <https://doi.org/10.1016/j.clinph.2004.12.021>.
- 199 Machilsen B, d’Agostino E, Maes F, Vandermeulen D, Hahn HK, Lagae L, *et al*. Linear normalization of MR brain images in pediatric patients with periventricular leukomalacia. *Neuroimage* 2007;**35**:686–97.
<https://doi.org/10.1016/j.neuroimage.2006.12.037>.

- 200 Wilke M, Altaye M, Holland SK, Consortium CA, others. CerebroMatic: a versatile toolbox for spline-based MRI template creation. *Front Comput Neurosci* 2017;**11**:
- 201 Fox MD, Corbetta M, Snyder AZ, Vincent JL, Raichle ME. Spontaneous neuronal activity distinguishes human dorsal and ventral attention systems. *Proc Natl Acad Sci* 2006;**103**:10046–51. <https://doi.org/10.1073/pnas.0604187103>.
- 202 Vincent JL, Patel GH, Fox MD, Snyder AZ, Baker JT, Van Essen DC, *et al*. Intrinsic functional architecture in the anaesthetized monkey brain. *Nature* 2007;**447**:83–6. <https://doi.org/10.1038/nature05758>.
- 203 Saleem KS, Kondo H, Price JL. Complementary circuits connecting the orbital and medial prefrontal networks with the temporal, insular, and opercular cortex in the macaque monkey. *J Comp Neurol* 2008;**506**:659–93. <https://doi.org/10.1002/cne.21577>.
- 204 Fischl B, Sereno MI, Dale AM. Cortical surface-based analysis. II: Inflation, flattening, and a surface-based coordinate system. *Neuroimage* 1999;**9**:195–207. <https://doi.org/10.1006/nimg.1998.0396>.
- 205 Fischl B, Salat DH, Busa E, Albert M, Dieterich M, Haselgrove C, *et al*. Whole brain segmentation: automated labeling of neuroanatomical structures in the human brain. *Neuron* 2002;**33**:341–55.
- 206 Fischl B, van der Kouwe A, Destrieux C, Halgren E, Segonne F, Salat DH, *et al*. Automatically parcellating the human cerebral cortex. *Cereb Cortex* 2004;**14**:11–22.
- 207 Dale AM, Fischl B, Sereno MI. Cortical surface-based analysis. I. Segmentation

- and surface reconstruction. *Neuroimage* 1999;**9**:179–94.
<https://doi.org/10.1006/nimg.1998.0395>.
- 208 Fischl B, Liu A, Dale AM. Automated manifold surgery: constructing geometrically accurate and topologically correct models of the human cerebral cortex. *IEEE Trans Med Imaging* 2001;**20**:70–80.
<https://doi.org/10.1109/42.906426>.
- 209 Jenkinson M, Beckmann CF, Behrens TEJ, Woolrich MW, Smith SM. FSL. *Neuroimage* 2012:782–90. <https://doi.org/10.1016/j.neuroimage.2011.09.015>.
- 210 Cox RW. AFNI: software for analysis and visualization of functional magnetic resonance neuroimages. *Comput Biomed Res* 1996;**29**:162–73.
<https://doi.org/10.1006/cbmr.1996.0014>.
- 211 MATLAB and Statistics Toolbox Release 2012b, The MathWorks, Inc., Natick, Massachusetts, United States. n.d.
- 212 Tustison NJ, Avants BB, Cook PA, Zheng Y, Egan A, Yushkevich PA, *et al*. N4ITK: Improved N3 bias correction. *IEEE Trans Med Imaging* 2010;**29**:1310–20. <https://doi.org/10.1109/TMI.2010.2046908>.
- 213 Avants BB, Epstein CL, Grossman M, Gee JC. Symmetric diffeomorphic image registration with cross-correlation: Evaluating automated labeling of elderly and neurodegenerative brain. *Med Image Anal* 2008;**12**:26–41.
<https://doi.org/10.1016/j.media.2007.06.004>.
- 214 Worsley KJ, Friston KJ. Analysis of fMRI Time-Series Revisited—Again. *Neuroimage* 1995;**2**:173–81. <https://doi.org/10.1006/nimg.1995.1023>.
- 215 Stelzer J, Lohmann G, Mueller K, Buschmann T, Turner R. Deficient approaches

- to human neuroimaging. *Front Hum Neurosci* 2014;**8**:462.
<https://doi.org/10.3389/fnhum.2014.00462>.
- 216 Behzadi Y, Restom K, Liao J, Liu TT. A component based noise correction method (CompCor) for BOLD and perfusion based fMRI. *Neuroimage* 2007;**37**:90–101. <https://doi.org/10.1016/j.neuroimage.2007.04.042>.
- 217 Satterthwaite TD, Elliott MA, Gerraty RT, Ruparel K, Loughead J, Calkins ME, *et al.* An improved framework for confound regression and filtering for control of motion artifact in the preprocessing of resting-state functional connectivity data. *Neuroimage* 2013;**64**:240–56. <https://doi.org/10.1016/j.neuroimage.2012.08.052>.
- 218 Mann HB, Whitney DR. On a test of whether one of two random variables is stochastically larger than the other. *Ann Math Stat* 1947:50–60.
- 219 Benjamini Y, Hochberg Y. Controlling the false discovery rate: a practical and powerful approach to multiple testing. *J R Stat Soc B* 1995:289–300.
<https://doi.org/10.2307/2346101>.
- 220 Hedges L V. Distribution Theory for Glass's Estimator of Effect size and Related Estimators. *J Educ Behav Stat* 1981;**6**:107–28.
<https://doi.org/10.3102/10769986006002107>.
- 221 Kerby DS. The Simple Difference Formula: An Approach to Teaching Nonparametric Correlation. *Compr Psychol* 2014;**3**:11.IT.3.1.
<https://doi.org/10.2466/11.IT.3.1>.
- 222 Giannelli M, Diciotti S, Tessa C, Mascalchi M. Characterization of Nyquist ghost in EPI-fMRI acquisition sequences implemented on two clinical 1.5 T MR scanner systems: Effect of readout bandwidth and echo spacing. *J Appl Clin Med Phys*

- 2010;**11**:170–80. <https://doi.org/10.1118/1.3271130>.
- 223 Ciric R, Wolf DH, Power JD, Roalf DR, Baum GL, Ruparel K, *et al.* Benchmarking of participant-level confound regression strategies for the control of motion artifact in studies of functional connectivity. *Neuroimage* 2017;**154**:174–87. <https://doi.org/10.1016/j.neuroimage.2017.03.020>.
- 224 Parkes L, Fulcher BD, Yucel M, Fornito A. An evaluation of the efficacy, reliability, and sensitivity of motion correction strategies for resting-state functional MRI. *bioRxiv* 2017:156380.
- 225 Power JD, Schlaggar BL, Petersen SE. Recent progress and outstanding issues in motion correction in resting state fMRI. *Neuroimage* 2015:536–51. <https://doi.org/10.1016/j.neuroimage.2014.10.044>.
- 226 van Dijk KRA, Sabuncu MR, Buckner RL. The influence of head motion on intrinsic functional connectivity MRI. *Neuroimage* 2012;**59**:431–8. <https://doi.org/10.1016/j.neuroimage.2011.07.044>.
- 227 Power JD, Barnes KA, Snyder AZ, Schlaggar BL, Petersen SE. Spurious but systematic correlations in functional connectivity MRI networks arise from subject motion. *Neuroimage* 2012;**59**:2142–54. <https://doi.org/10.1016/j.neuroimage.2011.10.018>.
- 228 Satterthwaite TD, Wolf DH, Loughead J, Ruparel K, Elliott MA, Hakonarson H, *et al.* Impact of in-scanner head motion on multiple measures of functional connectivity: Relevance for studies of neurodevelopment in youth. *Neuroimage* 2012;**60**:623–32. <https://doi.org/10.1016/j.neuroimage.2011.12.063>.
- 229 Liang X, Wang J, Yan C, Shu N, Xu K, Gong G, *et al.* Effects of different

- correlation metrics and preprocessing factors on small-world brain functional networks: A resting-state functional MRI study. *PLoS One* 2012;**7**:. <https://doi.org/10.1371/journal.pone.0032766>.
- 230 Courchesne E, Pierce K. Why the frontal cortex in autism might be talking only to itself: local over-connectivity but long-distance disconnection. *Curr Opin Neurobiol* 2005;**15**:225–30. <https://doi.org/10.1016/j.conb.2005.03.001>.
- 231 Wass S. Distortions and disconnections: Disrupted brain connectivity in autism. *Brain Cogn* 2011;**75**:18–28. <https://doi.org/10.1016/j.bandc.2010.10.005>.
- 232 Spearman C. Spearman's rank correlation coefficient. *Amer J Psychol* 1904;**15**:72–101. <https://doi.org/10.1136/bmj.g7327>.
- 233 Lam KSL, Aman MG. The repetitive behavior scale-revised: Independent validation in individuals with autism spectrum disorders. *J Autism Dev Disord* 2007;**37**:855–66. <https://doi.org/10.1007/s10803-006-0213-z>.
- 234 Association AP, Association AP, others. DSM-IV-TR: Diagnostic and statistical manual of mental disorders, text revision. *Washington, DC Am Psychiatr Assoc* 2000;**75**:.
- 235 Dosenbach NUF, Fair DA, Miezin FM, Cohen AL, Wenger KK, Dosenbach RAT, *et al*. Distinct brain networks for adaptive and stable task control in humans. *Proc Natl Acad Sci* 2007;**104**:11073–8. <https://doi.org/10.1073/pnas.0704320104>.
- 236 Fair DA, Dosenbach NU, Church JA, Cohen AL, Brahmbhatt S, Miezin FM, *et al*. Development of distinct control networks through segregation and integration. *Proc Natl Acad Sci U S A* 2007;**104**:13507–12. <https://doi.org/10.1073/pnas.0705843104>.

- 237 Constantino JN, Przybeck T, Friesen D, Todd RD. Reciprocal social behavior in children with and without pervasive developmental disorders. *J Dev Behav Pediatr* 2000;**21**:2–11.
- 238 Grzadzinski R, Di Martino A, Brady E, Mairena MA, O’Neale M, Petkova E, *et al.* Examining autistic traits in children with ADHD: Does the Autism Spectrum Extend to ADHD? *J Autism Dev Disord* 2011;**41**:1178–91.
<https://doi.org/10.1007/s10803-010-1135-3>.
- 239 Hus V, Bishop S, Gotham K, Huerta M, Lord C. Factors influencing scores on the social responsiveness scale. *J Child Psychol Psychiatry Allied Discip* 2013;**54**:216–24. <https://doi.org/10.1111/j.1469-7610.2012.02589.x>.
- 240 Aldridge FJ, Gibbs VM, Schmidhofer K, Williams M. Investigating the clinical usefulness of the Social Responsiveness Scale (SRS) in a tertiary level, autism spectrum disorder specific assessment clinic. *J Autism Dev Disord* 2012;**42**:294–300. <https://doi.org/10.1007/s10803-011-1242-9>.
- 241 Figley TD, Bhullar N, Courtney SM, Figley CR. Probabilistic atlases of default mode, executive control and salience network white matter tracts: an fMRI-guided diffusion tensor imaging and tractography study. *Front Hum Neurosci* 2015;**9**:.
<https://doi.org/10.3389/fnhum.2015.00585>.
- 242 Aron AR, Behrens TE, Smith S, Frank MJ, Poldrack RA. Triangulating a cognitive control network using diffusion-weighted magnetic resonance imaging (MRI) and functional MRI. *J Neurosci* 2007;**27**:3743–52.
<https://doi.org/10.1523/jneurosci.0519-07.2007>.
- 243 Whitfield-Gabrieli S, Nieto-Castanon A. Conn: A Functional Connectivity

- Toolbox for Correlated and Anticorrelated Brain Networks. *Brain Connect* 2012;**2**:125–41. <https://doi.org/10.1089/brain.2012.0073>.
- 244 Siegel JS, Mitra A, Laumann TO, Seitzman BA, Raichle M, Corbetta M, *et al.* Data Quality Influences Observed Links Between Functional Connectivity and Behavior. *Cereb Cortex* 2016:1–11. <https://doi.org/10.1093/cercor/bhw253>.
- 245 Duan F, Zhao T, He Y, Shu N. Test-retest reliability of diffusion measures in cerebral white matter: A multiband diffusion MRI study. *J Magn Reson Imaging* 2015;**42**:1106–16. <https://doi.org/10.1002/jmri.24859>.
- 246 Ioannidis JPA. Why most published research findings are false. *PLoS Med* 2005;0696–701. <https://doi.org/10.1371/journal.pmed.0020124>.
- 247 Ebrahim S, Sohani ZN, Montoya L, Agarwal A, Thorlund K, Mills EJ, *et al.* Reanalyses of randomized clinical trial data. *Jama* 2014;**312**:1024–32. <https://doi.org/10.1001/jama.2014.9646>.
- 248 Button KS, Ioannidis JP a, Mokrysz C, Nosek B a, Flint J, Robinson ESJ, *et al.* Power failure: why small sample size undermines the reliability of neuroscience. *Nat Rev Neurosci* 2013;**14**:365–76. <https://doi.org/10.1038/nrn3475>.
- 249 Nosek BA, Alter G, Banks GC, Borsboom D, Bowman SD, Breckler SJ, *et al.* Promoting an open research culture. *Science (80-)* 2015;**348**:1422–5. <https://doi.org/10.1126/science.aab2374>.
- 250 Nichols TE, Das S, Eickhoff SB, Evans AC, Glatard T, Hanke M, *et al.* *Best Practices in Data Analysis and Sharing in Neuroimaging using MRI*. 2016.
- 251 Sui J, Adali T, Yu Q, Chen J, Calhoun VD. A review of multivariate methods for multimodal fusion of brain imaging data. *J Neurosci Methods* 2012:68–81.

- <https://doi.org/10.1016/j.jneumeth.2011.10.031>.
- 252 Chung MK, Hanson JL, Adluru N, Alexander AL, Davidson RJ, Pollak SD. Integrative Structural Brain Network Analysis In Diffusion Tensor Imaging. *bioRxiv* 2017:129015.
- 253 Maier-Hein K, Neher P, Houde J-C, Cote M-A, Garyfallidis E, Zhong J, *et al*. Tractography-based connectomes are dominated by false-positive connections. *bioRxiv* 2016:1–23. <https://doi.org/10.1101/084137>.
- 254 Conturo TE, Williams DL, Smith CD, Gultepe E, Akbudak E, Minshew NJ. Neuronal fiber pathway abnormalities in autism: an initial MRI diffusion tensor tracking study of hippocampo-fusiform and amygdalo-fusiform pathways. *J Int Neuropsychol Soc* 2008;**14**:933–46. <https://doi.org/10.1017/S1355617708081381>.
- 255 Baron-Cohen S, Ring HA, Bullmore ET, Wheelwright S, Ashwin C, Williams SCR. The amygdala theory of autism. *Neurosci Biobehav Rev* 2000:355–64. [https://doi.org/10.1016/S0149-7634\(00\)00011-7](https://doi.org/10.1016/S0149-7634(00)00011-7).
- 256 Weisberg J, Milleville SC, Kenworthy L, Wallace GL, Gotts SJ, Beauchamp MS, *et al*. Social perception in autism spectrum disorders: Impaired category selectivity for dynamic but not static images in ventral temporal cortex. *Cereb Cortex* 2014;**24**:37–48. <https://doi.org/10.1093/cercor/bhs276>.
- 257 Di Martino A, Zuo XN, Kelly C, Grzadzinski R, Mennes M, Schvarcz A, *et al*. Shared and distinct intrinsic functional network centrality in autism and attention-deficit/hyperactivity disorder. *Biol Psychiatry* 2013;**74**:623–32. <https://doi.org/10.1016/j.biopsych.2013.02.011>.
- 258 Delmonte S, Balsters JH, Mcgrath J, Fitzgerald J, Brennan S, Fagan AJ, *et al*.

- Social and monetary reward processing in autism spectrum disorders. *Mol Autism* 2012;**3**:7. <https://doi.org/10.1186/2040-2392-3-7>.
- 259 Delmonte S, Gallagher L, O’Hanlon E, McGrath J, Balsters JH. Functional and structural connectivity of frontostriatal circuitry in Autism Spectrum Disorder. *Front Hum Neurosci* 2013;**7**:430. <https://doi.org/10.3389/fnhum.2013.00430>.
- 260 Damiano CR, Cockrell DC, Dunlap K, Hanna EK, Miller S, Bizzell J, *et al.* Neural mechanisms of negative reinforcement in children and adolescents with autism spectrum disorders. *J Neurodev Disord* 2015;**7**:12. <https://doi.org/10.1186/s11689-015-9107-8>.
- 261 Power JD, Mitra A, Laumann TO, Snyder AZ, Schlaggar BL, Petersen SE. Methods to detect, characterize, and remove motion artifact in resting state fMRI. *Neuroimage* 2014;**84**:320–41. <https://doi.org/10.1016/j.neuroimage.2013.08.048>.
- 262 Vasa RA, Mostofsky SH, Ewen JB. The Disrupted Connectivity Hypothesis of Autism Spectrum Disorders: Time for the Next Phase in Research. *Biol Psychiatry Cogn Neurosci Neuroimaging* 2016:245–52. <https://doi.org/10.1016/j.bpsc.2016.02.003>.
- 263 Pierce K, Redcay E. Fusiform function in children with an autism spectrum disorder is a matter of ‘who’. *Biol Psychiatry* 2008;**64**:552–60. <https://doi.org/10.1016/j.biopsych.2008.05.013>.
- 264 Sharda M, Midha R, Malik S, Mukerji S, Singh NC. Fronto-Temporal connectivity is preserved during sung but not spoken word listening, across the autism spectrum. *Autism Res* 2015;**8**:174–86. <https://doi.org/10.1002/aur.1437>.
- 265 Radulescu E, Minati L, Ganeshan B, Harrison NA, Gray MA, Beacher FDCC, *et*

- al.* Abnormalities in fronto-striatal connectivity within language networks relate to differences in grey-matter heterogeneity in Asperger syndrome. *NeuroImage Clin* 2013;2:716–26. <https://doi.org/10.1016/j.nicl.2013.05.010>.
- 266 Zhang W, Groen W, Mennes M, Greven C, Buitelaar J, Rommelse N. Revisiting subcortical brain volume correlates of autism in the ABIDE dataset: effects of age and sex. *Psychol Med* 2017. <https://doi.org/10.1017/S003329171700201X>.
- 267 Larsen B, Verstynen TD, Yeh F-C, Luna B. Developmental Changes in the Integration of Affective and Cognitive Corticostriatal Pathways are Associated with Reward-Driven Behavior. *Cereb Cortex* 2017:1–12. <https://doi.org/10.1093/cercor/bhx162>.
- 268 Fan L, Li H, Zhuo J, Zhang Y, Wang J, Chen L, *et al.* The Human Brainnetome Atlas: A New Brain Atlas Based on Connectional Architecture. *Cereb Cortex* 2016;26:3508–26. <https://doi.org/10.1093/cercor/bhw157>.
- 269 Sporns O. Graph Theory Methods for the Analysis of Neural Connectivity Patterns. *Neurosci. Databases*. 2003. p. 171–85.
- 270 Lee H, Kang H, Chung MK, Lim S, Kim B-N, Lee DS. Integrated multimodal network approach to PET and MRI based on multidimensional persistent homology. *Hum Brain Mapp* 2016. <https://doi.org/10.1002/hbm.23461>.
- 271 Corbetta M, Shulman GL. CONTROL OF GOAL-DIRECTED AND STIMULUS-DRIVEN ATTENTION IN THE BRAIN. *Nat Rev Neurosci* 2002;3:215–29. <https://doi.org/10.1038/nrn755>.
- 272 Faul F, Erdfelder E, Lang A-G, Buchner A. G*Power 3: a flexible statistical power analysis program for the social, behavioral, and biomedical sciences. *Behav Res*

- Methods* 2007;**39**:175–91. <https://doi.org/10.3758/BF03193146>.
- 273 Faul F, Erdfelder E, Buchner A, Lang A-G. Statistical power analyses using G*Power 3.1: tests for correlation and regression analyses. *Behav Res Methods* 2009;**41**:1149–60. <https://doi.org/10.3758/BRM.41.4.1149>.
- 274 Yoon U, Fonov VS, Perusse D, Evans AC. The effect of template choice on morphometric analysis of pediatric brain data. *Neuroimage* 2009;**45**:769–77. <https://doi.org/10.1016/j.neuroimage.2008.12.046>.
- 275 Wilke M, Schmithorst VJ, Holland SK. Assessment of spatial normalization of whole-brain magnetic resonance images in children. *Hum Brain Mapp* 2002;**17**:48–60. <https://doi.org/10.1002/hbm.10053>.
- 276 Greicius MD, Supekar K, Menon V, Dougherty RF. Resting-state functional connectivity reflects structural connectivity in the default mode network. *Cereb Cortex* 2009;**19**:72–8. <https://doi.org/10.1093/cercor/bhn059>.
- 277 Wang J, Xie S, Guo X, Becker B, Fox PT, Eickhoff SB, *et al*. Correspondent Functional Topography of the Human Left Inferior Parietal Lobule at Rest and Under Task Revealed Using Resting-State fMRI and Coactivation Based Parcellation. *Hum Brain Mapp* 2017;**38**:1659–75. <https://doi.org/10.1002/hbm.23488>.
- 278 Coury DL, Anagnostou E, Manning-Courtney P, Reynolds A, Cole L, McCoy R, *et al*. Use of psychotropic medication in children and adolescents with autism spectrum disorders. *Pediatrics* 2012;**130 Suppl**:S69-76. <https://doi.org/10.1542/peds.2012-0900D>.
- 279 Linke AC, Olson L, Gao Y, Fishman I, Müller R-A. Psychotropic medication use

- in autism spectrum disorders may affect functional brain connectivity. *Biol Psychiatry Cogn Neurosci Neuroimaging* 2017.
- 280 Di Martino A, O'Connor D, Chen B, Alaerts K, Anderson JS, Assaf M, *et al.* Enhancing studies of the connectome in autism using the autism brain imaging data exchange II. *Sci Data* 2017;**4**:170010.
- 281 Plitt M, Barnes KA, Martin A. Functional connectivity classification of autism identifies highly predictive brain features but falls short of biomarker standards. *NeuroImage Clin* 2015;**7**:359–66. <https://doi.org/10.1016/j.nicl.2014.12.013>.
- 282 Smith SM, Beckmann CF, Ramnani N, Woolrich MW, Bannister PR, Jenkinson M, *et al.* Variability in fMRI: A re-examination of inter-session differences. *Hum Brain Mapp* 2005;**24**:248–57. <https://doi.org/10.1002/hbm.20080>.
- 283 Pua EPK, Bowden SC, Seal ML. Autism spectrum disorders: Neuroimaging findings from systematic reviews. *Res Autism Spectr Disord* 2017;**34**:28–33.
- 284 Uddin LQ, Supekar K, Menon V. Reconceptualizing functional brain connectivity in autism from a developmental perspective. *Front Hum Neurosci* 2013;**7**:458. <https://doi.org/10.3389/fnhum.2013.00458>.
- 285 Friedman L, Glover GH, The FBIRN Consortium. Reducing interscanner variability of activation in a multicenter fMRI study: Controlling for signal-to-fluctuation-noise-ratio (SFNR) differences. *Neuroimage* 2006;**33**:471–81. <https://doi.org/10.1016/j.neuroimage.2006.07.012>.
- 286 Gradin V, Gountouna VE, Waiter G, Ahearn TS, Brennan D, Condon B, *et al.* Between- and within-scanner variability in the CaliBrain study n-back cognitive task. *Psychiatry Res - Neuroimaging* 2010;**184**:86–95.

<https://doi.org/10.1016/j.psychresns.2010.08.010>.

- 287 Friedman L, Stern H, Brown GG, Mathalon DH, Turner J, Glover GH, *et al*. Test-retest and between-site reliability in a multicenter fMRI study. *Hum Brain Mapp* 2008;**29**:958–72. <https://doi.org/10.1002/hbm.20440>.
- 288 Song J, Desphande AS, Meier TB, Tudorascu DL, Vergun S, Nair VA, *et al*. Age-Related Differences in Test-Retest Reliability in Resting-State Brain Functional Connectivity. *PLoS One* 2012;**7**:. <https://doi.org/10.1371/journal.pone.0049847>.
- 289 Ferreira LK, Busatto GF. Resting-state functional connectivity in normal brain aging. *Neurosci Biobehav Rev* 2013:384–400. <https://doi.org/10.1016/j.neubiorev.2013.01.017>.

APPENDIX A

tSNR by ROI and Correlations with Age, FSIQ, and QC metrics

Appendix Table 1. Tests for group differences in temporal signal-to-noise ratio in subcortical and ventromedial pre-frontal brain regions

Region of Interest	Mean TD	Median TD	StdDevTD	Mean ASD	Median ASD	StdDevTD	r-value	Z-value	df	ranksum	Hedges' g	r _b	P-value	95% Confidence Interval
Choi Left Network 10 NAcc	116.50		25.27	103.48		21.38	1.72	0.58	35.04		0.54	0.10	0.10	[-2.39,28.44]
Choi Left Network 12 Putamen tail		121.35	21.70		126.07	34.75				391.00		0.10	0.56	[-0.42,0.23]
Choi Left Network 13 Caudate body	130.54		24.67	122.94		19.52	1.05		34.20		0.33	0.30	0.30	[-7.06,22.27]
Choi Left Network 16 Caudate head	128.94		24.56	112.51		21.13	2.21		35.22		0.70	*0.03	*0.03	[1.34,31.52]
Choi Left Network 17 Caudate	137.69		28.62	130.23		25.49	0.85		35.53		0.27	0.40	0.40	[-10.37,25.30]
Choi Left Network 17 Putamen body	131.62		22.03	127.17		21.52	0.63		35.98		0.20	0.53	0.53	[-9.87,18.79]
Choi Left Network 17 Putamen tail		126.75	37.09		102.34	34.46		1.39		418.50		0.23	0.17	[-0.53,0.09]
Choi Left Network 3 Putamen tail	133.90		20.94	129.85		23.95	0.55		35.37		0.18	0.58	0.58	[-10.77,18.86]
Choi Left Network 4 Putamen tail	130.12		22.10	125.26		14.85	0.79		31.50		0.25	0.43	0.43	[-7.60,17.30]
Choi Left Network 7 Putamen body	147.57		20.43	145.21		19.23	0.37		35.87		0.12	0.72	0.72	[-10.70,15.41]
Choi Left Network 8 Caudate	141.53		24.80	127.67		21.58	1.84		35.33		0.58	0.07	0.07	[-1.44,29.16]
Choi Left Network 8 Putamen body	138.43		19.82	132.71		19.60	0.89		36.00		0.28	0.38	0.38	[-7.25,18.69]
Choi Left Network 8 Putamen tail		115.44	63.46		126.12	54.48		-0.45		354.50		0.08	0.65	[-0.25,0.40]
Choi Right Network 10 NAcc	111.09		24.59	96.94		22.30	1.86		35.66		0.59	0.07	0.07	[-1.29,29.60]
Choi Right Network 12 Putamen tail	125.41		20.70	110.54		24.63	2.02		34.97		0.64	>0.05	>0.05	[-0.11,29.86]
Choi Right Network 13 Caudate body	117.21		21.28	107.77		20.40	1.40		35.94		0.44	0.17	0.17	[-4.28,23.16]
Choi Right Network 16 Caudate head	118.03		27.42	104.95		24.47	1.55		35.54		0.49	0.13	0.13	[-4.03,30.19]
Choi Right Network 3 Putamen tail	125.96		23.59	119.38		17.36	0.98		33.08		0.31	0.33	0.33	[-7.09,20.25]
Choi Right Network 4 Putamen tail	126.25		18.76	116.44		17.64	1.66		35.86		0.53	0.11	0.11	[-2.17,21.79]
Choi Right Network 7 Putamen body	134.16		22.18	131.09		11.92	0.53		27.60		0.17	0.60	0.60	[-8.77,14.92]
Choi Right Network 8 Caudate	125.15		20.71	116.82		20.79	1.24		36.00		0.39	0.22	0.22	[-5.32,21.98]
Choi Right Network 8 Putamen	126.21		27.13	117.29		17.98	1.19		31.25		0.38	0.24	0.24	[-6.31,24.15]
Yeo Left Network 10 OFC	79.51		19.47	69.91		22.19	1.42		35.40		0.45	0.17	0.17	[-4.15,23.34]
Yeo Right Network 10 OFC	72.69		17.49	64.49		20.87	1.31		34.93		0.42	0.20	0.20	[-4.48,20.89]

* $p < 0.05$

Appendix Table 2. Significant correlations between FC, Age, and WASI Full Scale IQ.

Age at Scan	Connection	r	p	PValue	FDR-Pvalue	
	Yeo Right 8 ACC SFG	Yeo Left 8 Paracingulatelabel		-0.35	0.03	0.71
	Yeo Right 12 ACC	Yeo Left 12 FP Precen MFG		-0.43	0.01	0.43
	Yeo Right 12 ACC	Yeo Right 12 SFG Paracing		-0.35	0.03	0.71
	Yeo Right 13 IPL	Yeo Left 13 SFG MFG		-0.35	0.03	0.71
	Yeo Right 16 FP MFG	Yeo Right 16 LOC IPL		-0.41	0.01	0.44
	Yeo Left 16 FP ACC	Yeo Right 16 PCC Precuneous		-0.33	0.04	0.73
	Yeo Right 16 PCC Precuneous	Yeo Left 16 LOC		-0.35	0.03	0.71
	Yeo Right 16 PCC Precuneous	Yeo Left 16 SFG		-0.43	0.01	0.43
	Yeo Right 17 IPL	Yeo Left 17 IPL		-0.32	0.05	0.73
	Yeo Right 17 IPL	Yeo Left 17 SFG MFG		-0.47	<0.003	0.43
	Yeo Right 17 IPL	Yeo Left 17 TP MTG		-0.32	0.05	0.73
	Yeo Right 17 TP STG ITG	Yeo Left 17 IPL		-0.38	0.02	0.55
WASI FSIQ						
	Choi Left 3 Putamen tail	Yeo Right 3 SMA Precen SPL	-0.38		0.02	1.00
	Choi Left 4 Putamen tail	Yeo Left 4 Oper	-0.35		0.03	1.00
	Choi Right 7 Putamen body	Choi Left 7 Putamen body	0.40		0.01	1.00
	Choi Right 7 Putamen body	Yeo Right 7 Insula Oper	-0.34		0.04	1.00
	Choi Left 7 Putamen body	Yeo Left 7 Precen	-0.32		0.05	1.00
	Yeo Right 7 ACC SMA Para	Yeo Left 7 Insula	0.32		0.05	1.00
	Yeo Right 7 Insula Oper	Yeo Right 7 MTG LOC	0.34		0.04	1.00
	Yeo Right 7 Insula Oper	Yeo Right 7 Oper IPL	0.32		0.05	1.00
	Yeo Right 7 Insula Oper	Yeo Left 7 MTG	0.37		0.02	1.00
	Yeo Right 7 MTG LOC	Yeo Left 7 Insula	0.35		0.03	1.00
	Yeo Left 7 Insula	Yeo Left 7 SMA Cingulate	0.35		0.03	1.00
	Choi Left 8 Caudate	Yeo Left 8 IPL	-0.33		0.04	1.00
	Choi Left 8 Putamen Body	Yeo Right 8 Precentral	-0.32		0.05	1.00
	Yeo Right 8 PCC ACC	Yeo Right 8 Precen	0.34		0.04	1.00
	Yeo Right 8 Precen	Yeo Left 8 IPLlabel	0.34		0.04	1.00
	Yeo Right 12 ACC	Yeo Right 12 SFG Paracing	-0.44		0.01	1.00
	Yeo Left 12 ITG LOC	Yeo Left 12 SFG	-0.35		0.03	1.00
	Yeo Right 13 SFG MFG	Yeo Right 13 SFG Paracingulate	0.38		0.02	1.00
	Choi Left 14 Putamen body	Yeo Right 14 IFG	-0.36		0.03	1.00
	Choi Right 16 Caudate head	Yeo Right 16 FP OFC	-0.32		0.05	1.00
	Yeo Right 16 FP ACC	Yeo Right 16 LOC IPL		0.38	0.02	1.00
	Yeo Right 16 FP MFG	Yeo Right 16 LOC IPL	0.38		0.02	1.00
	Yeo Right 17 FP SFG	Yeo Right 17 IPL	0.33		0.05	1.00
	Yeo Right 17 FP SFG	Yeo Left 17 Cingulate	0.46		<0.004	1.00
	Yeo Right 17 FP SFG	Yeo Left 17 IPL	0.35		0.03	1.00
	Yeo Right 17 IPL	Yeo Left 17 Cingulate	0.36		0.03	1.00
	Yeo Left 17 FP	Yeo Left 17 FP OFC	-0.54		<0.0005	0.27
	Yeo Left 17 FP	Yeo Left 17 MFG	-0.33		0.04	1.00
	Yeo Left 17 FP	Yeo Left 17 TP MTG	-0.36		0.02	1.00

Appendix Table 3. Partial Correlations of GFA values in which demographic and MRI quality variables were found to highly correlate with FC or GFA.

Nuisance Variables	Connection	Motion Correction	partial-ρ	% of Participants below threshold	PValue
Age, WASI FSIQ	Yeo Right 13 FP	Yeo Right 13 SFG MFG	No	2.63	*0.02
Age	Choi Left 16 Caudate head	Yeo Left 16 SFG	DWI	0.00	*0.02
Age, DWI Registration Accuracy	Yeo Left 17 FP OFC	Yeo Left 17 MFG	No	0.00	0.07
DWI Registration Accuracy	Yeo Right 13 IFG	Yeo Right 13 IPL	No	13.16	0.06
DWI Registration Accuracy	Yeo Right 16 FP MFG	Yeo Left 16 SFG	BOLD	2.63	0.11
Age	Yeo Right 16 PCC Precuneous	Yeo Left 16 SFG	BOLD	23.68	*0.03

Data describes the adjusted ρ correlation and p-value when including the nuisance variable in the partial- ρ correlation.

* $p < 0.05$

APPENDIX B

UAB IRB Exemption Form



Exemption Designation
 Identification and Certification of Research
 Projects Involving Human Subjects

UAB's Institutional Review Boards for Human Use (IRBs) have an approved Federalwide Assurance with the Office for Human Research Protections (OHRP). The Assurance number is FWA00005960 and it expires on November 8, 2021. The UAB IRBs are also in compliance with 21 CFR Parts 50 and 56.

Principal Investigator: DeRamus, Thomas P

Co-Investigator(s):

Protocol Number: **E170309007**

Protocol Title: *Connectivity of Striatal Resting-State Networks in Autism Spectrum Disorder*

The above project was reviewed on 3/22/17 The review was conducted in accordance with UAB's Assurance of Compliance approved by the Department of Health and Human Services. This project qualifies as an exemption as defined in 45CFR46.101(b), paragraph 4.

This project received EXEMPT review.

Date IRB Designation Issued: March 22, 2017

Jessy Blake Headley, CIP

Expedited Reviewer
 Member - Institutional Review Board
 for Human Use (IRB)

Investigators please note:

Any modifications in the study methodology, protocol and/or consent form/information sheet must be submitted for review to the IRB prior to implementation.

470 Administration Building
 701 20th Street South
 205.934.3789
 Fax 205.934.1301
 irb@uab.edu

The University of
 Alabama at Birmingham
 Mailing Address:
 AB 470
 1720 2ND AVE S
 BIRMINGHAM AL 35294-0104